The role of $CD8^+$ T cell phenotype and cytotoxicity on cancer immunotherapy

Felicity Christana Stark

Thesis submitted to the
Faculty of Graduate and Postdoctoral Studies
In partial fulfillment of the requirements
For the PhD degree in Microbiology and Immunology

Department of Biochemistry, Microbiology and Immunology
Faculty of Medicine
University of Ottawa

ABSTRACT

Cancer vaccines can fail despite the induction of large numbers of $CD8^+$ T cells. Two categories of memory $CD8^+$ T cells have been defined; central memory (T_{CM}, IL-$7R\alpha^{high}CD44^{high}$**$CD62L^{high}$**) and effector memory (T_{EM}, IL-$7R\alpha^{high}CD44^{high}$**$CD62L^{low}$**). It is clear that the memory phenotype of $CD8^+$ T cells can affect vaccine potential; however methods to augment a beneficial phenotype are not clear. I have compared three vaccine delivery systems: *Listeria monocytogenes*, *Salmonella enterica* serovar Typhimurium and the particulate liposomal adjuvant, archaeosomes, for their efficacy to protect against murine melanoma. My study revealed that the anti-tumour response is strongly influenced by the kinetics, phenotype, and lymph node homing potential of $CD8^+$ T cells.

Listeria monocytogenes-ovalbumin (LM-OVA) induced T_{CM} cells were adept at long lasting protection against B16-OVA melanoma due to their increased homeostatic and antigen-induced proliferation, interleukin-2 production, and ability to extravasate into tumour draining lymph nodes. Conversely, although *Salmonella* Typhimurium-ovalbumin (ST-OVA) induced $T_{EM,}$ produced IFN-γ, and killed target cells, this was insufficient for long-term tumour protection.

Selectin-ligand engagements of T_{CM} cells influenced their homing potential and efficacy against murine melanoma. Fucosyltransferase deficient (FtDKO) mice, lacking functional selectin ligands, were vaccinated with LM-OVA; despite the activation of cytotoxic $CD8^+$ T cells, there was a reduced protection against murine melanoma compared to wild-type. FtDKO $CD8^+$ T cells exhibited reduced extravasation into FtDKO lymph nodes compared to wild-type. Additionally, fewer FtDKO $CD8^+$ T cells compared to wild-type migrated into tumour sites.

Archaeosome vaccination was used to compare the influence of $CD8^+$ T cell quantity versus phenotype. Single or multiple therapeutic vaccinations with archaeosome-OVA yielded transient melanoma tumour protection, despite an increased frequency of circulating and tumour infiltrating $CD8^+$ T cells. This correlated with increased expression of Program death receptor-1 (PD-1) on $CD8^+$ T cells and induction of regulatory T cells. Prophylactic archaeosome-OVA vaccination resulted in a maximal frequency of antigen-specific $CD8^+$ T cells of ~50-60 % with just three injections, and ~50 % of the mice were of mice were afforded long-term tumour protection (> 90 days).

Overall, my study shows that the choice of vaccine adjuvant and/or vector can profoundly influence $CD8^+$ T cell quality and cancer vaccine efficacy.

ACKNOWLEDGEMENTS

First of all I would like to thank my supervisor, Dr. Lakshmi Krishnan. I feel very fortunate to have had the opportunity to study in your lab, I have learned so much and I am truly grateful for your continued encouragement, support and guidance. I have much appreciation and gratitude to my co-supervisor Dr. Lionel Filion, my first exposure to Immunology in my last year of undergraduate studies was in your classroom; thank you very much for introducing immunology to me in such an inspiring way. I would also like to thank my thesis advisory committee members Dr. Subash Sad and Dr. Christina Addison for their encouragement to view my project from many angles. I was very fortunate to have had the technical support and friendship of Komal Gurnani, thank you very much for everything. And to all my labmates thank you very much for pitching in during those large experiments and for all the brainstorming sessions.

To Isabelle, I am forever grateful for your love and support. To my friend Dietwald, thank you for all the wonderfully engaging and thought-provoking conversations. Lastly, thank you to Paula, Brittany, Mum and Dad, your constant love, support and encouragement has kept me focused and helped me to realize my dreams.

This research was supported by a grant from the Ontario Institute for Cancer Research Network. Scholarships were provided by the Ontario Graduate Scholarship Program and the Ontario Graduate Scholarship in Science and Technology program.

TABLE OF CONTENTS

LIST OF FIGURES

LIST OF ABBRIEVIATIONS:

α4β7:	Lymphocyte integrins; involved in T lymphocyte homing to the gut
Ag:	Antigen
APC:	**A**ntigen **P**resentation **C**ell
ACT:	**A**doptive T **C**ell **T**herapy
B16-OVA:	Mouse melanoma cell line producing plasmid derived ovalbumin
B6129F1:	129SvJ x C57BL/6
B7.1:	CD80; Co-stimulatory molecule expressed on activated APCs, binds to CD28 or CTLA-4.
B7.2:	CD86; Co-stimulatory molecule expressed on activated APCs, binds to CD28 or CTLA-4.
BGC:	**B**acillus **C**almette-**G**uérin
BHI:	**B**rain **H**eart **I**nfusion agar
CCR4:	Chemokine Receptor type 4: CD194; T cell receptor for thymus and activation-regulated chemokine (TARC) and macrophage derived chemokine (MDC)
CCR7:	Chemokine Receptor type 7: CD197; T cell receptor for CCL21
CCR9:	Chemokine Receptor type 9: CD199; T cell receptor for thymus expressed chemokine. Involved in thymocyte development and trafficking to the gut.
CTLA-4:	**C**ytotoxic **T** **L**ymphocyte **A**ntigen – **4**; Co-stimulatory molecule expressed on activated T cells. Supports T cell negative regulation
CD3:	**C**luster of **D**ifferentiation 3; used to identify T cells
CD4:	**C**luster of **D**ifferentiation 4; used to identify helper $CD3^+$ T cells
CD8:	**C**luster of **D**ifferentiation 8; used to identify cytotoxic $CD3^+$ T cells
CD25:	**C**luster of **D**ifferentiation 25: IL-2Rα; expressed on effector T cells
CD27:	**C**luster of **D**ifferentiation 27; TNF receptor, co-stimulator for T and B cells
CD28:	**C**luster of **D**ifferentiation 28; Co-stimulatory molecule expressed constitutively on T cells; supports T cell activation
CD40:	**C**luster of **D**ifferentiation 40; TNF receptor, promotes B cell activation and cytokine production by Macrophages and Dendritic Cells.
CD43:	**C**luster of **D**ifferentiation 43; Mucin, Leukosialin; the 130 kDa glycoform is associated with T cell activation and involved in cell adhesion.
CD44:	**C**luster of **D**ifferentiation 44; Receptor for hyaluronic acid expressed on activated T cells
CD62L:	**C**luster of **D**ifferentiation 62L; L-selectin. Leukocyte selectin.
CD95:	**C**luster of **D**ifferentiation 95; Fas Receptor
CFSE:	**C**arboxy**F**luorescein **S**uccinimidyl **E**ster
CpG:	**C**ytosine-**P**hosphate-**G**uanine; unmethylated CpG di-nucleotides activate TLR9
CTL:	**C**ytotoxic **T** **L**ymphocyte
DC:	**D**endritic **C**ell
DISC:	**D**eath **I**nducing **S**ignaling **C**omplex
ER:	**E**ndoplasmic **R**eticulum
FtDKO:	α(1,3) **Fucosyl**transferase IV & VII **D**eficient **K**nock **O**ut mouse
FasL:	**Fas** **L**igand
GlyCAM-1:	**Gly**cosylation-dependent **C**ell **A**dhesion **M**olecule-1

IFN-γ:	**I**nter**F**ero**N** – γ
JAK-STAT:	**Ja**nus-family tyrosine **k**inase - **S**ignal **T**ransducer and **A**ctivator of **T**ranscription
IL-2:	**I**nter**L**eukin 2; Growth factor for effector T cells
IL-2Rα:	**I**nter**L**eukin 2 receptor alpha; expressed on effector T cells
IL-4:	**I**nter**L**eukin 4; Induces T_H2 and M2 differentiation
IL-7:	**I**nter**L**eukin 7; Growth factor for naïve and memory T cells
IL-7Rα:	**I**nter**L**eukin 7 **R**eceptor alpha; expressed on naïve and memory T cells
IL-10:	**I**nter**L**eukin 10; suppressant of macrophages
IL-13:	**I**nter**L**eukin 13; suppressant of macrophages and T_H1 cells
IL-15:	**I**nter**L**eukin 15; Growth factor for naïve and memory T cells
ITIM:	**I**mmunoreceptor **T**yrosine-based **I**nhibition **M**otif
ITSM:	**I**mmunoreceptor **T**yrosine-based **S**witch **M**otif
LM-OVA:	***L**isteria **M**onocytogenes* – **OVA**lbumin
LN:	**L**ymph **N**ode
LPS:	**L**ipo**P**oly**S**accharide
TIL:	**T**umour **I**nfiltrating **L**ymphocytes
TPL:	**T**otal **P**olar **L**ipids
M1:	**M**acrophage subset **1**; present antigen in defense against infections
M2:	**M**acrophage subset **2**; poor antigen presentation but contribute to wound healing
MAdCAM-1:	**M**ucosal **Ad**dressin **C**ell **A**dhesion **M**olecule-1; L-selectin Ligand
MDSC:	**M**yeloid-**D**erived **S**uppressor **C**ells
MHC-I:	**M**ajor **H**istocompatibility **C**omplex I
MHC-II:	**M**ajor **H**istocompatibility **C**omplex II
MS	**M**ethanobrevibacter **S**mithii
MS-OVA:	**M**ethanobrevibacter **S**mithii - **OVA**lbumin
NLR:	**N**ucleotide-binding domain, **L**eucine-rich **R**epeat containing protein
NRAMP:	**N**atural **R**esistance-**A**ssociated **M**acrophage **P**rotein
OT.1:	TCR transgenic mouse with >95 % of all $CD8^+$ T cells expressing a TCR specific for $OVA_{257-264}$
OVA:	**OVA**lbumin
PDGF:	**P**latelet **D**erived **G**rowth **F**actor
PD-1:	**P**rogram **D**eath **R**eceptor**-1**
PD-L1/L2:	**P**rogram **D**eath receptor **L**igand**-1** and **-2**
PPR:	**P**attern **R**ecognition **R**eceptor
PSGL-1:	**P**-**S**electin **G**lycoprotein **L**igand–**1**
$RAG^{-/-}$:	**R**ecombination **A**ctivation **G**ene knockout mice; produce no mature T and B cells
RLR:	**R**etinoic acid inducible gene-1 **L**ike **R**eceptor
sLe^x:	**S**ialyl **Le**wis **X**
Sgp200:	**S**ulfated **g**lyco**p**rotein – 200kDa. L-selectin Ligand expressed in peripheral and mesenteric lymph nodes
SPI-1:	***S**almonella* **P**athogenicity **I**sland**-1**
SPI-2:	***S**almonella* **P**athogenicity **I**sland**-2**
ST-OVA:	***S**almonella enterica* serovar **T**yphimurium – **OVA**lbumin
TAM:	**T**umour **A**ssociated **M**acrophage

TAP-1/2:	**T**ransporters associated with **A**ntigen **P**rocessing-1 and -2
TDLN:	**T**umour **D**raining **L**ymph **N**ode
T_{CM}:	$CD8^+$ **T** cell, **C**entral **M**emory
T_{EM}:	$CD8^+$ **T** cell, **E**ffector **M**emory
T_E:	$CD8^+$ **T** cell, **E**ffector
T_N:	$CD8^+$ **T** cell, **N**aïve
TCR:	**T C**ell **R**eceptor
TLR:	**T**oll **L**ike **R**eceptor
TNF:	**T**umour **N**ecrosis **F**actor
T_{reg}:	**T reg**ulatory cell
VEGF:	**V**ascular **E**ndothelial **G**rowth **F**actor
VLA-1/-2:	**V**ery **L**ate **A**ctivation antigen -1 and -2

1.0 CHAPTER 1: LITERATURE REVIEW

1.1 Initiation of an immune response

Mammalian immune responses can be broken down in to two broad categories, the innate and adaptive immune responses. Innate immune responses constitute a fast acting first line response to combat infection. Innate immune cell types such as macrophages recognize pathogen-associated molecular patterns (PAMPs) via their pathogen recognition receptors (PRRs) [1]. Activated macrophages produce a cascade of soluble functional proteins; chemokines and cytokines that can effectively curtail infection and also activate other innate immune cells such as Natural Killer cells (NKs) [2]. In contrast, adaptive immunity is mediated by antigen-specific lymphocytes namely, B and T cells which gain antigen specificity during germline differentiation via a process of genetic recombination of their cell surface receptors. Clonal expansion of the lymphocyte occurs when it comes into contact with its cognate antigen. For T cells, this process is further refined as the T cell receptor (TCR) recognizes antigen that is complexed with a major histocompatibility complex (MHC) on the cell surface of an adjacent cell. $CD4^+$ and $CD8^+$ T cells are activated by engaging antigen that is bound to the cell surface binding groove of MHC-class II or MHC-class I, respectively [3]. For proper activation of T cells two signals are required; signal one is provided by the MHC-TCR complex, whereas signal two is provided by the interaction of co-stimulatory molecules on antigen presenting cells (APCs) with their ligands on T cells. A key differentiating feature of adaptive immunity is the ability to generate "immune memory". Thus collectively, innate and adaptive immunity ensure that the host is rapidly protected from pathogen attack as well as able to retain memory to combat a second pathogen attack [4].

B cell activation, leads to the production of antibodies which can neutralize extracellular pathogens often by targeting their effector and/or functional proteins. This kind of immunity confers protection against a number of invading pathogens [5,6] and can also provide early protective immunity when transferred from mother to newborn infant [7]. Strong B cell immunity requires help of $CD4^+$ T cells, which are potent cytokine producers that alter isotype class switching and B cell proliferation [8].

Many infections are caused by intracellular bacteria, viruses, and parasites where the foreign antigen is sequestered away from extracellular niches where antibody detection occurs. Similarly, in case of cancer, the immune response is tasked with having to eliminate transformed "self" cells. In such cases, direct killing of the invaded or transformed cell is required. This capability is uniquely attributed to $CD8^+$ T cells which are hence also called cytotoxic T lymphocytes (CTLs). NKs are also capable of exerting direct cytolytic killing of infected and transformed cells; while their activation is not known to be antigen dependant, their cytotoxic activity and cytokine production can facilitate tumour elimination [9]. Since $CD8^+$ T cells can be expanded by vaccination and is thought to be the primary immune cell type that eliminates most tumours [10,11], this review focuses on their activation and the factors that promote or inhibit their function.

The immunological processes discussed in this thesis concern immunological responses in the mouse model. While many extrapolations can be made from discoveries in mouse immunity to humans, it is important to note that the mechanisms and phenotypes are not identical [12].

1.1-01 Antigen presenting cell activation

The activation of $CD8^+$ T cells begins with its encounter with an APC. Professional APCs such as macrophages and dendritic cells (DCs) are the most efficient at antigen presentation and T cell activation because they are highly phagocytic and express co-stimulatory molecules and cytokines necessary for T cell activation. B cells are also capable of antigen presentation and likely play an important role in activating $CD4^+$ T cells that provide help to B cells [13]. Non-professional APCs, including tumour cells and fibroblasts, can activate T cells however they do not reliably express the co-factors, such as upregulated co-stimulatory marker expression, that support T cell activation.

Macrophages are mainly found within body cavities and connective and lymphoid tissue. They are highly phagocytic innate immune cells capable of engulfing and killing pathogens, producing proinflammatory cytokines that draw other cells to the infected area. Macrophages are also capable of antigen presentation; however, they are not thought to be the most potent activators of naïve cells [14]. It is widely agreed upon that DCs are the most potent activators of naïve T cells. Immature professional DCs are highly phagocytic and reside ubiquitously throughout the body where they can easily come into contact with an invading pathogen [15]. When DCs become activated in the presence of pathogen components, they become less phagocytic, and increase the expression of chemokine receptor type 7 (CCR7) which directs their migration towards lymphoid tissues where they can come into contact with naïve $CD8^+$ T cells. The pathogen components that initiate APC activation are recognized by PRRs such as Toll-like receptors (TLRs), nucleotide-binding domain, leucine-rich repeat containing protein (NLRs), and the retinoic acid inducible gene-1 like receptor (RLRs). TLRs recognize a variety of extracellular and phagosomal resident microbial structures (flagellin, lipopolysaccharide (LPS) and unmethylated **c**ytosine-phosphate-guanine

(CpG)) [16]. NLRs and RLRs are known to detect cytosolic bacterial and viral components respectively [17–19]. Sufficient activation of PPRs results in the activation of the APC, upregulation of co-stimulatory molecules and the secretion of cytokines that support T cell activation. Activation of APCs induces their maturation and increases their expression of MHC and co-stimulatory molecules as well as their migration towards lymphoid sites where they can come into contact with, and activate, naïve or memory T cells.

1.1-02 MHC and TCR engagement

The activation of T cells occurs via the engagement of its TCR with the antigen complexed histocompatibility antigen (MHC/HLA) of an adjacent APC. There are two types of MHC/HLA molecules, namely class I and class II. In mice, all nucleated cells express MHC-class I whereas MHC-Class II is expressed almost exclusively on mouse monocytes/macrophages, B cells and dendritic cells. MHC molecules act as a scaffold to present a wide variety of short peptides to the TCR of T cells. In order to maintain the tertiary structure of the MHC-class I molecules, peptide must be bound at all times; these are peptides of self origin and are constitutively bound in the MHC binding groove but can become dislodged by foreign peptides that have a greater affinity. In contrast, an invariant chain is bound within the binding groove of MHC-class II molecules during synthesis. The invariant chain is later broken down by accessory proteins prior to the MHC-Class II molecule reaching the cell surface. The binding site of the MHC-class I molecule limits peptide length to 10 amino acids whereas the binding site of MHC-class II molecules are more open and can support a longer peptide usually around 13-17 amino acids in length [20]. MHC-class I molecules will present antigen to the TCR of $CD8^+$ T cells whereas MHC-class II molecules present peptide antigen to $CD4^+$ T cells. This selective recognition begins a

cascade of immune reactions that directs host immunity to deal with extracellular and intracellular infections differently. As extracellular protein becomes endocytosed and digested they gain access to MHC-Class II molecules that cause the activation of $CD4^+$ T cells that in turn can promote B cell class switching. Thus, a predominant antibody mediated immune response eliminates extracellular infections. Conversely, intracellular pathogens proliferate within a host cell, thus cytosolic foreign protein can become targeted for proteosomal degradation. Host machinery will direct cytosolic peptides towards MHC-class I molecules that initiate the activation of $CD8^+$ T cells which in turn exert direct cytolytic killing of infected cells that display the exact same antigen complexed with MHC-class I. Thus, the differential mechanisms of MHC presentation efficiently guide immune responses to deal with extracellular and intracellular infections [21].

1.1-03 MHC-Class I and -Class II presentation

MHC-Class I is a transmembrane protein composed of two polypeptide chains, α and β2-microglobulin linked non-covalently. With the assistance of a number of accessory proteins such as (tapasin and calreticulin), the assembly of the MHC-Class I molecule occurs in the endoplasmic reticulum (ER), where the α and β polypeptide chains and the variable peptide come together to form a stable membrane bound complex capable of transportation through the Golgi complex to the cell surface via secretory vesicles. MHC-Class I must be bound by peptide within the ER prior to exiting, therefore mechanisms exist to transport cytosolic foreign peptide into the ER. When a cell becomes infected with cytosolic resident bacteria or virus, cytosolic foreign protein can be processed by proteosomal degradation. The resulting short peptide fragments (8-40 amino acids) are transported by Transporters associated with Antigen Processing-1 and -2 (TAP1 and TAP2) to gain access to the ER.

The binding groove of MHC-Class I molecules limits the length of a bound peptide, therefore peptides are generally 8 to 10 amino acids in length. Peptide is loaded on to MHC-Class I molecules and subsequently transferred to the cell surface for $CD8^+$ T cell recognition [22].

MHC-Class II is a transmembrane protein composed of two homologous peptides, an α and β chain. MHC-Class II is synthesized in the ER and is complexed with a polypeptide called the invariant chain that occupies the peptide binding groove. The invariant chain prevents foreign peptides from loading on to MHC-Class II molecules in the ER that are destined for MHC-Class I. Instead, MHC-Class II molecules will engage foreign peptides in transit, when the MHC-Class II containing endosomal vesicles become fused with phagosomal vesicles. During vesicular transport to the cell membrane, accessory proteins sequentially remove the invariant chain from the MHC-Class II molecule leaving it free to bind to phagosomal derived high affinity foreign peptides. Lastly, the foreign peptide bound MHC-Class II molecule is shuttled to the cell membrane where it can come into contact with the TCR of $CD4^+$ T cells causing $CD4^+$ T cell activation [23].

1.2 $CD8^+$ T cells

The mechanism of $CD8^+$ T cell activation and differentiation into memory T cells will be discussed in detail below with an emphasis on the role of selectin/selectin-ligand interactions.

1.2-01 $CD8^+$ T cell activation

The activation of a naïve $CD8^+$ T cell requires the formation of an immune synapse with a professional APC. In addition to TCR-MHC-Class I engagement, co-stimulatory

molecule engagement must also occur to provide sufficient T cell stimulation to avoid T cell anergy [24]. With the engagement of co-stimulatory molecules B7.1 (CD80) and B7.2 (CD86) of the APC with CD28 of the T cell, the activated T cell begins to synthesize interleukin-2 receptor α (IL-2Rα - which forms the IL-2 receptor in complex with the β and γ chains) as well as the cytokine IL-2. Stimulation through the high-affinity IL-2 receptor induces $CD8^+$ T cell proliferation and within 4 to 5 days, armed effector $CD8^+$ T cells are in circulation. Activated effector $CD8^+$ T cells, also known as cytotoxic T lymphocytes (CTLs), differ from naïve $CD8^+$ T cells as they upregulate the cell adhesion molecule CD44, downregulate the selectin molecule CD62L, which would otherwise initiate tethering interactions in lymphoid compartments [25,26]. Activated $CD8^+$ T cells also upregulate adhesion molecules P-selectin glycoprotein ligand – 1 (PSGL-1) and very late activation antigen -1 and -2 (VLA-1 and -2) that enable tethering and firm adhesions in peripheral sites of inflammation [27,28]. Activated $CD8^+$ T cells undergo rapid proliferation and exert immediate cytolytic killing of target cells that express their cognate antigen-MHC-Class I receptor with little or no co-stimulatory signals. It was initially thought that CTL responses require $CD4^+$ T cell help during priming via "licensing" of DCs through CD40L-CD40 engagement to promote co-stimulation of $CD8^+$ T cells [29–31]. However, later studies showed that CD40 co-stimulation could occur in the absence of DCs; this indicated a direct helping role of $CD4^+$ T cells on $CD8^+$ T cell co-stimulation [32]. Studies have shown that $CD8^+$ T cell priming can occur in the absence of $CD4^+$ T cell help however the maintenance of memory $CD8^+$ T cells and secondary expansion are impaired as a result [33–37]. The early engagement of CD40 on $CD8^+$ T cells by CD40L on $CD4^+$ T cells is thought to be important for memory $CD8^+$ T cell persistence [33]. Thus, the continued presence of $CD4^+$ T cells also supports the maintenance of memory $CD8^+$ T cells [34].

$CD8^+$ T cell activation traditionally occurs within lymphoid compartments where activated professional APCs such as DCs carry foreign antigen in from the periphery. Sequestration of $CD8^+$ T cell activation within lymphoid compartments increases the rate at which a specific $CD8^+$ T cell clone will encounter its cognate antigen. $CD8^+$ T cell activation, expansion and contraction differ depending on the type of intracellular infection and the speed at which the host immune response sequesters the pathogen. Studies with viral infections have shown that the $CD8^+$ T cell response peaks at day 7 followed by a massive contraction where >90 % of CTLs perish [38]. Upon resolution of infection or latency, the remaining antigen experienced $CD8^+$ T cells reduce expression of IL-2Rα and IL-2, and upregulate the expression of interleukin-7 receptor α (IL-7Rα) and interleukin-15 receptor α (IL-15Rα) and use IL-7 and IL-15 to maintain proliferation and survival homeostasis [39–41].

1.2-02 Heterogeneity of memory $CD8^+$ T cells

Memory $CD8^+$ T cells are heterogeneous in phenotype, function and proliferative potential and have been classified broadly into two general groups, namely the effector memory T cells (T_{EM}) and central memory T cells (T_{CM}) [42] (Figure 1). While both subtypes are antigen experienced, T_{CM} cells have an upregulated expression of CCR7 and CD62L, which enable their recruitment and attachment to high endothelial venules and subsequent extravasation into lymphoid compartments. T_{EM} have a decreased expression of CD62L that allows them to take up residence in peripheral tissues such as sites of inflammation, the liver or the lungs where they are able to exert cytolytic functions quickly [43–45]. Additional phenotypic markers such as CD27 (TNF receptor involved in co-stimulation) and CD43 (involved in T cell activation and cell adhesion) have recently been suggested to define 3 subpopulations of

memory $CD8^+$ T cells: $CD27^{high}/CD43^{low}$, $CD27^{high}/CD43^{high}$, and $CD27^{low}/CD43^{low}$ with $CD27^{high}CD43^{low}$ cells exhibiting the strongest recall response to Sendai virus infection [46].

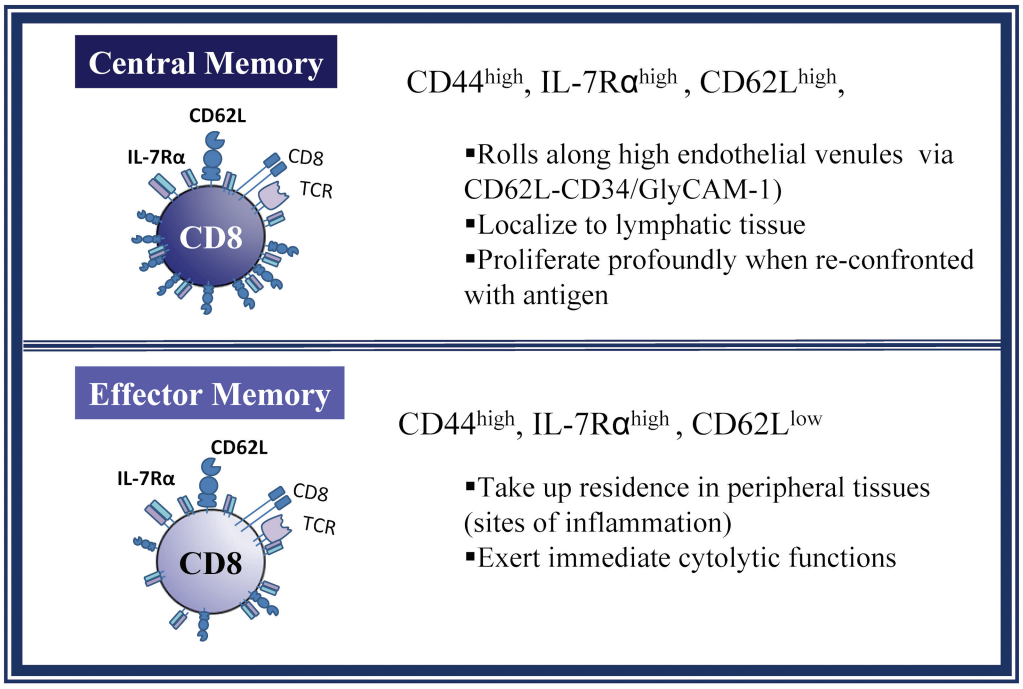

FIGURE 1: Central and Effector memory CD8$^+$ T cells.
A general classification of memory CD8$^+$ T cells was proposed in 1999 by Sallusto et al., to distinguish between memory CD8$^+$ T cells that resided in lymph nodes or those that persisted in the periphery [42].

Additionally, memory $CD8^+$ T cells residing in different tissues are known to harbor tissue-specific phenotypes such as α4β7 and chemokine receptor type 9 (CCR9) in the small intestine or CCR4 and E-selectin in the skin [47]. It is important to note that the sole expression of these markers does not confer pan-superiority of one type to mount a recall response; rather each subpopulation likely plays a role to control different infection types in differing locations. It has been shown that T_{EM} confer better protection against a peripheral vaccinia virus infection while T_{CM} provide better protection from systemic LCMV infection and many tumours [44,48,49]. A clearer understanding of the factors that drive memory formation and the differentiation pathways of each subtype will aid in the development of better cancer vaccines and treatment regimes.

1.2-03 Memory $CD8^+$ T cell differentiation

Two possible models for $CD8^+$ T cell differentiation have been suggested; linear and parallel differentiation. The linear model predicts that naïve $CD8^+$ T cells give rise to effectors of which 90 % are eliminated and <5 % go onto develop into memory $CD8^+$ T cells. This model is supported by adoptive transfer studies whereby transferred effector $CD8^+$ T cells develop into memory cells [50,51]. The second model of parallel differentiation proposes that memory $CD8^+$ T cells arise in parallel with effector differentiation, and indeed are two distinct lineages derived from a common naïve pre-cursor. This model is supported by recent studies that show a weak immunizing stimulus (DNA vaccine or peptide loaded DCs) can activate naïve $CD8^+$ T cells to form a small population of memory $CD8^+$ T cells capable of early expansion as early as day 4; this suggests that an early memory cell can arise from a naïve cell. These early responders differ from a typical CTL response because they retain CD127 expression and do not transiently express negative regulators like PD-1 [52–54].

Similarly, infection with an attenuated pathogen such as *Bacillus Calmette-Guérin* (BCG) induces a low level of antigen presentation and inflammatory stimuli and can induce an early T_{CM} response [55]. This parallel differentiation model implies that strong inflammatory stimuli associated with priming aids in the formation of effector cells; conversely, minimizing inflammation can generate memory $CD8^+$ T cells without a prior CTL phase. Figuring out when memory T cells develop and whether they are descendents of effectors is important when developing vaccination strategies to generate potent and efficacious memory $CD8^+$ T cell responses capable of controlling tumour or infection. New evidence suggests that T cells with a greater proliferative capacity provide superior protection from tumour. $CD8^+$ T cells with a proliferative advantage include T_{CM} and naïve $CD8^+$ T cells. Since naïve $CD8^+$ T cells of certain specificity are so few, and require much co-stimulation to become activated it was initially thought their usefulness in tumour protection was limited. However, recent evidence suggests that transforming this subset of cells to express a TCR specific to a tumour antigen yields very strong anti-tumour protection [56]. As of yet, when comparing the usefulness of $CD8^+$ T cells for immunotherapy, the adoptive transfer of cultured anti-tumour $CD8^+$ T cells for immunotherapy has been shown to be most beneficial when they are of a T_{CM} rather than a T_{EM} phenotype [49].

While it was initially thought that T_{EM} cells are well suited to mediate tumour protection [57] as they can quickly exert cytolytic functions, more evidence suggests that T_{CM} cells, due to their ability to proliferate and kill infected targets, mediated better protection against tumours. *In vitro* generated T_{CM} compared to T_{EM} cells in combination with a tumour antigen vaccine were better able to respond to and abolish an established tumour [49,58,59]. Furthermore, clinical trials involving adoptive T cell transfer of *in vitro* expanded tumour infiltrating lymphocytes to lymphodepleted cancer patients yields ~50 % response rates [60].

Therefore, it appears that if the appropriate phenotype of endogenously acquired tumour specific $CD8^+$ T cells is allowed to expand, efficient cancer elimination may follow.

1.2-04 Selectins and $CD8^+$ T cells

T_{CM} are distinguished from T_{EM} by their re-expression of CD62L (L-selectin); whether this molecule has functional significance for T_{CM} anti-tumour immunity is currently not known. Selectins are type I transmembrane glycoproteins that bind to sialylated carbohydrate antigens. Three selectins are known, P-, E- and L-selectin, and they bind with low affinity to carbohydrate sialyl $Lewis^x$ (sLe^x) on glycoprotein scaffolds. L-selectin (CD62L) is a cell surface adhesion molecule found to be upregulated on naïve and T_{CM} lymphocytes. It transiently interacts with selectin ligands on adjacent cells which initiate the tethering and rolling of lymphocytes along high endothelial venules, later leading to other firm adhesions with integrins that mediate entry of the lymphocyte into lymphoid tissue [61]. Selectin ligands present the carbohydrate antigen, sLe^x, to their cognate receptors, L, P and E-selectins [62,63]. Some L-selectin ligands found on high-endothelial venules such as P-selectin glycoprotein ligand-1 (PSGL-1), CD34, mucosal addressin cell adhesion molecule-1 (MAdCAM-1) and sulphated glycoprotein 200 (Sgp200) are transmembrane glycoproteins that mediate tethering whereas glycosylated cell adhesion molecule-1 (GlyCAM-1) is a secreted protein and is thought to induce signaling responses in leukocytes that lead to firm adhesions and diapedesis. L-selectin signaling is also thought to play a co-stimulatory role in T cell activation [62,64,65].

The synthesis of functional selectin ligands requires many post-translational modifications including a terminal fucosylation mediated by α(1,3) fucosyltransferase IV and VII [28,66]. Selectin-ligand/selectin interactions play a role at many stages during an immune

response from the interaction of naïve and memory T cells with high endothelial venules of lymph nodes to later interactions of activated T cells with activated epithelium at a site of inflammation. In the absence of CD62L a redistribution of naïve $CD8^+$ T cells towards non-lymphoid organs occurs, thus naïve T cells are thought to be dependent on CD62L to gain access to lymphoid compartments [67–69]. Since T_{CM} cells have a higher level of CD62L and are thought to mediate better anti-tumour responses compared to their T_{EM} $CD62L^{low}$ counterparts, the presence of CD62L might play a functional role in augmenting anti-tumour immunity. A recent study has postulated that CD62L mediated trafficking of $CD8^+$ T cells to lymph nodes may not be necessary for T_{CM} formation [69], therefore it raises the interesting question of whether selectin ligand interactions are necessary for the maintenance of an anti-tumour $CD8^+$ T cell response as they may impact their infiltration within tumor sites.

1.3 $CD8^+$ T cell cytotoxicity

$CD8^+$ T cells mediate target cell killing, and they are capable of releasing cytokines such as interferon-γ (IFN-γ) and tumour necrosis factor-α (TNF-α) that contribute to host immunity. $CD8^+$ T cell mechanisms of cytotoxicity are discussed in detail below.

1.3-01 Lytic granules

Activated $CD8^+$ T cells are capable of exerting direct cell killing upon engagement of its TCR with its cognate antigen in the context of MHC-class I. CTLs contain lytic granules that are expelled towards an engaged target cell by calcium dependent processes [70]. Granules are a type of lysosome containing two types of effector proteins, granzymes and perforin. Once expelled into the interstitial space between the CTL and its target, perforin polymerizes to form transmembrane pores in the target cell membrane. Granzymes, which are serine

proteases, are thought to initiate target cell apoptosis. However, because granzymes have been shown to cleave hundreds of intracellular proteins the mechanism is still debated [71,72]. Direct enzymatic cleavage of procaspases can drive apoptosis [73], yet others have suggested that it occurs by alterations of the outer mitochondrial membrane [74,75].

1.3-02 Fas/FasL

Another mechanism of killing mediated by CTLs is the engagement of its Fas-ligand/CD178 (FasL) with Fas receptor/CD95 (also called death receptor) on target cells. Engagement triggers the formation of death-inducing signaling complexes (DISCs) that contain pro-caspases-8 and/or -10 that cleave procaspase-3 and -7 leading to target cell apoptosis [71,76]. CD95 is widely expressed on a number of cell types including T cells [77], whereas FasL is found on T cells, immune privileged sites such as the eye [78] or testis [79] as well as many tumour sites [80,81]. Expression of FasL on tumour cells can activate CD95 on infiltrating T cells, initiating apoptosis of the T cells; this is thought to be a mechanism of tumour immune evasion [82].

1.3-03 $CD8^+$ T cell cytokines

$CD8^+$ T cells also produce effector cytokines such as IFN-γ and TNF-α. However, relative to $CD4^+$ T cells that produce an abundance of cytokines, $CD8^+$ T cells produce lower amounts as their cytotoxic activities dampen cytokine production [83].

IFN-γ is predominantly produced by NKs but is also produced by activated $CD4^+$ and $CD8^+$ T cell. It is known to mediate potent protection from pathogens and is sometimes used for the treatment of invasive fungal infections [84]. The binding of IFN-γ to its receptor initiates the JAK-STAT signaling pathway which activates several genes. For example, it is known to amplify transcription of TLRs and increase signaling through TLRs during

bacterial or viral infection thereby enhancing co-stimulation and activation of T cells [85,86]. As mentioned earlier, IFN-γ maintains the presence of Th1 type $CD4^+$ T cells which in turn promotes macrophage activation to kill intracellular bacteria. Mice and humans deficient in IFN-γ or its receptor are more susceptible to intracellular infections [87] as well as metastatic tumour development [88]. IFN-γ enhances the immunogenicity of tumours by upregulating the cellular expression of MHC-Class I and is additionally attributed with direct anti-proliferative properties by reducing cell growth and survival in a number of tumour cell types [89,90].

TNF-α is produced by macrophages, NKs and CTLs and is a strong inducer of inflammation which triggers early local containment of infecting pathogens [91]. Early studies identified TNFα as a factor that could kill tumour cells however its administration to humans systemically resulted in severe toxicity [92]. Later on it was identified as an important mediator of host defense against intracellular infections. However, it's over production was associated with destructive autoimmune induced inflammation [93]. Anti-TNF-α therapy has been met with success in the treatment of Crohn's disease [94] and rheumatoid arthritis [95]. However, in some cases latent chronic infections like *Mycobacterium tuberculosis* may become reactivated [92]. While the targeted delivery of TNF-α towards tumour sites has been correlated with slowing tumour growth [96], recent studies have attributed anti-TNF-α therapy with relieving harmful tumour induced immunosuppression by TNFR2 expressing regulatory T cells (T_{regs}) [97].

1.4 Tumour Specific $CD8^+$ T cells and Mechanisms of Immune Evasion

Immunodominant self-reactive $CD8^+$ T cells are mostly depleted in the thymus during development relieving the host of unwanted destructive autoimmune responses.

However, some self-reactive cells survive depletion and linger in the periphery giving rise to a ready population of potential tumour specific $CD8^+$ T cells. The mechanism by which these self-reactive $CD8^+$ T cells avoid their cognate antigen in the thymus may be attributable to sequestration of antigen in other locations or the temporal regulation of antigen expression. Nevertheless, peripheral tolerance mechanisms limit the activation of self-reactive $CD8^+$ T cells that escape thymic selection [98]. The mechanisms of tolerance and how it impacts tumour vaccine therapeutics is discussed below.

1.4-01 Tolerance and survival of tumour reactive T cells

T cell precursors originate in the bone marrow like all blood cells, but they mature and undergo positive and negative selection in the thymus. Upon the genetic rearrangement of the αβ TCR, double positive $CD4^+$ $CD8^+$ T cells, that interact weakly with self-peptide bound to self MHC, become 'positively selected' and develop into mature singly $CD4^+$ or $CD8^+$ T cells. 'negative selection' occurs to those T cells that bind self-peptide too strongly; as a result they are deleted by apoptosis. Thus, thymic selection of T cells during development selects for T cells restricted to self MHC but eliminates self-reactive T cells leaving a varied population of T cells with an affinity for non-self-peptide-MHC complexes. The process of Negative selection is known as 'central tolerance'. When low affinity self-reactive T cells (such as tumour specific T cells) escape thymic deletion but are found to be impaired and unable to exert cytolytic functions 'peripheral tolerance' mechanisms are thought to be at play. T_{regs} are thought to play a role in peripheral tolerance by limiting cytotoxicity of self/tumour reactive T cells [99]. When considering methods to turn otherwise quiescent self/tumour specific T cells into efficacious CTLs, it is important to understand the regulatory mechanisms that keep them at bay. The removal of T_{regs} prior to vaccination has

been shown to augment $CD8^+$ T cell priming and promote tumour clearance in a number of studies [100–103]. Another mechanism of peripheral tolerance is the removal of co-stimulation during TCR signaling. This form of peripheral tolerance can be circumvented by introducing the self antigen along with strong inflammatory stimuli resulting in the generation of robust $CD8^+$ T cell responses capable of delaying the onset of tumour burden [104,105]. Pathogen-associated molecular patterns such as LPS or flagellin can activate PRRs of APCs, causing activation and down-stream co-stimulation of T cells. Such an example of non-antigen dependent circumvention of peripheral tolerance was observed as early as 1891 when killed bacteria were injected into malignant tumour sites and caused substantial regressions with a 10 % success rate [106,107]. Additionally, cancer patients were shown to undergo a brief period of remission following infection with influenza [108–110]. While these methods are not antigen-specific in nature, danger signals associated with infection can play a role in disrupting cell or tissue barriers of the tumour to release sequestered self antigen. Lastly, some pathogens contain molecules similar to self; the infecting molecular mimic can result in the production of cross-reactive T cells that aid in the destruction of tumour [111]. While infection related inflammation can sometime correlate with short-term tumour regression, tumours can return. Host immune evasive mechanisms intended to protect a host from deadly autoimmune reactions can be hijacked by a tumour to prevent its destruction by CTLs [112–115].

1.4-02 Regulatory T cells (T_{regs})

While T_{regs} are important for immune homeostasis, as they downregulate harmful autoimmune responses, they can also be involved in the immunosuppression of anti-tumour T cell responses. T_{regs} are diverse in their developmental origins as they can arise from the thymus (natural T_{regs}) or the periphery in an antigen dependent manner (induced or adaptive

T_{regs}). The peripheral activation of naïve $CD4^+$ T cells by APCs in the presence of interleukin-10 (IL-10) can cause the activation of suppressor functions. While most natural T_{regs} are specific for self molecules, inducible T_{regs} can be generated against self and non-self antigens. The expression of the transcription factor FoxP3 is necessary for T_{reg} development and suppressive function; therefore it is a deterministic marker for the identification of T_{regs} [116]. T_{regs} also express a high amount of the cell surface receptor CD25 making it a good target for antibody mediated depletions of T_{regs}. Nevertheless, it is important to consider the timing of αCD25 depletion to avoid elimination of activated T cells, as CD25 is the IL-2 receptor α-chain that becomes upregulated during T cell activation. T_{regs} have been associated with a poor prognosis for a number of tumour types in both mice and humans and their removal by antibody depletions without further manipulation can cause the reduction of tumour burden [101,117]. Notably, T_{regs} can be actively recruited to the tumour by chemokines such as CCL22 that are produced by tumour associated macrophages (TAMs) [112,118]. Activation of T_{regs} can occur in the tumour tissue as well as draining lymph nodes and are known to exert suppressive action on tumour specific $CD8^+$ T cells. Furthermore, it has been suggested that effector T cells are not only suppressed by T_{regs} but are active participants in the continued survival of T_{regs} by producing the growth cytokine IL-2 as well as other unknown mechanisms from direct cell-cell contact [112,119]. Therefore, inducing anti-tumour CTL responses with immunotherapy might also support the formation of T_{regs}; this presents an opportunity to explore the potential of immunotherapeutic treatments in the absence of T_{regs} by α-CD25 depletion. The removal of T_{regs} can potentially lift $CD8^+$ T cell suppression and restore anti-tumour immunity. However, as described below, other immune cells such as macrophages are also recruited to generate an immunosuppressive environment.

1.4-03 Tumour-associated macrophages and myeloid-derived suppressor cells

Tumour-associated macrophages (TAMs) have recently been identified as having immunosuppressive mechanisms and are thought to play an important role in tumour immune escape as they can constitute up to 50 % of the total tumour mass [120]. Their infiltration into tumour sites usually is associated with a negative prognosis and has been shown to increase tumour growth and metastatis [121,122]. Macrophages can be broadly classified into two subsets, M1 and M2. M1 macrophages develop in the presence of IFN-γ and bacterial danger signals, like LPS; they are known to contribute in defense against bacterial infections and tumours. M2 macrophages develop in the presence of interleukin-4 (IL-4), interleukin-13 (IL-13) and IL-10 and are attributed with wound healing properties and a poor-ability to present antigen. TAMs are considered to be of the M2 phenotype and known to exert strong immunosuppression by producing IL-10 which attracts T_{regs}. Additionally TAMs are associated with an increase in tumour vasculature and are thought to directly enhance angiogenesis by releasing growth factors such as vascular endothelial growth factor (VEGF) and platelet derived growth factor (PDGF) [120].

Myeloid-derived suppressor cells (MDSC) are found in most cancer patients and are known to cause T cell suppression. MDSCs do not terminally differentiate into mature macrophages and are heterogenous in phenotype with two major subclasses, namely granulocytic and monocytic [123]. They mediate immunosuppression by many mechanisms; however, two recently described mechanisms highlight their mode of action on T cells. T cells require exogenous sources of cysteine for activation. MDSCs which can be induced in tumour sites are thought to sequester cysteine thereby inhibiting T cell activation [123,124]. Another mechanism of MDSC immunosuppression is the down-regulation of L-selectin on T cells [125]. MDSCs are known to constitutively express the proteolytic molecule ADAM17

that is typically involved in activation induced CD62L down-regulation on T cells [125]. Decreasing CD62L on naïve T cells impairs their extravasation towards lymph node sites where they could otherwise become activated and generate an anti-tumour CTL response. Additional studies provide evidence that MDSCs support the growth and activation of T_{regs} that are known to further suppress tumour reactive T cell responses [126,127]. In addition to immune cell mediated suppression of $CD8^+$ T cells, tumour cells are capable of downregulating $CD8^+$ T cell cytotoxicity by engaging regulatory molecules such as PD-1.

1.4-04 Inhibitory checkpoint proteins

A number of T cell surface receptors have been identified as having suppressive roles on T cell cytotoxicity[114,128]. Upon ligand engagement, these receptors initiate the downregulation of many intracellular signaling events involved in TCR signaling, cell proliferation and cytokine production. Well characterized inhibitory receptors currently targeted with antibody therapy in cancer pre-clinical and clinical trials include CTLA-4, program death receptor -1 (PD-1), lymphocyte activation gene -3 (LAG-3), and mucin domain containing molecule -3 (Tim-3) [129–132]. While their mechanisms of suppression differ, each has been attributed with contributing to the persistence of tolerogenic or anergic T cell responses in the tumour environment [115,128,133]. PD-1 expression on $CD8^+$ T cells was investigated in this study; therefore, the mechanism of inhibition by PD-1 receptor engagement is elaborated.

PD-1 belongs to the immunoglobulin (Ig) superfamily and is related to co-stimulatory molecules expressed on activated T cells, CTLA-4 and CD28; however, it differs as it exists in a monomeric state. The cytoplasmic domain of PD-1 has two tyrosine based motifs including an immunoreceptor tyrosine-based inhibition motif (ITIM) and an immunoreceptor

tyrosine based switch motif (ITSM). Upon engagement of PD-1 by its ligand, ITIM and ITSM become phosphorylated and become docking sites for SHP-1 and/or SHP-2 effectively inhibiting signaling events involved in both TCR signaling and IL-2 production of activated T and B cells [134]. PD-1 ligands, including program death receptor ligand -1 or -2 (PD-L1 or PD-L2), are selectively expressed on a variety of cells types. PD-L1 is most diversely expressed on nonhematopoietic cells including endothelial cells, muscle fibres and myoblasts [135] as well as cells of the pancreas, thymus, cardiac and placenta [136–138] in addition to a variety of lymphoid cell types including activated B, T, myeloid and DCs [136]. PD-L2 is more restrictively expressed only on macrophages and DCs [139]. The wide variety of cell types that express PD-1 ligands may indicate a control of T cell responses could be localized to specific sites. Since PD-1 is highly expressed on tumour infiltrating lymphocytes (TILs), the inducible expression of PD-L1 negatively regulates $CD8^+$ T cells as they pass through tumour sites. Interestingly, the PD-1 blocking antibody heightened CTL proliferation and was associated with anti-tumour immunity in a Phase I clinical trial with metastatic melanoma [140].

1.5 Role of $CD8^+$ T cell responses in combating intracellular infections and tumours

$CD8^+$ T cells are uniquely skilled at controlling intracellular infections due to their method of killing which does not include sequestration of the whole pathogen; rather they sense and exert targeted killing of infected host cells that are presenting foreign antigen complexed with MHC-class I. Interestingly, the timing and extent of $CD8^+$ T cell responses can vary greatly between acute and chronic infections [141]. Specifically, while many acute intracellular infections elicit $CD8^+$ T cell responses that peak in proliferation by day 7, some chronic infections evoke delayed $CD8^+$ T cell responses [142].

Intracellular pathogens induce a number of inflammatory pathways that attract $CD8^+$ T cells. Many viruses and intracellular bacteria will infect macrophages and DCs directly and they are capable of activating naïve $CD8^+$ T cells. However, in some cases APCs take up exogenous pathogen protein debris excluded from other infected cell types, and cross-present them to initiate $CD8^+$ T cell activation. An activated $CD8^+$ T cell is constantly sensing MHC-class I molecules present on all nucleated cells. Once a firm adhesion is made on an infected target cell, the CTL releases cytotoxic granules inducing host cell apoptosis and destruction of the intracellular pathogen. The activation of $CD8^+$ T cells is under tight regulatory control requiring engagement of co-stimulatory molecules for full activation; this ensures that cytotoxic $CD8^+$ T cell responses inflict minimal collateral damage. However, once a $CD8^+$ T cell becomes activated, continued co-stimulation is not required for them to perform their cytolytic functions on target cells [143]. Thus, $CD8^+$ T cell responses are critical for the detection and killing of pathogens within host cells.

$CD8^+$ T cell responses can also exert potent anti-tumour immunity. Since the identification of tumour specific $CD8^+$ T cells, the search for potent $CD8^+$ T cell stimulating vaccines was initiated. Importantly, because tumour cells lack the danger signals required for $CD8^+$ T cell co-stimulation, adjuvants that trigger macrophage activation, MHC expression and co-stimulatory molecule expression are required to induce activation of $CD8^+$ T cells following vaccination.

The administration of soluble foreign protein, even when targeted towards DCs (fused with antibodies that bind to DC), induces tolerance, not $CD8^+$ T cell activation [144–146]. However, $CD8^+$ T cell responses can be initiated against tumour antigens when they are delivered along with or by viruses or intracellular bacteria [147,148]. Live viral vectors currently under investigation for use in $CD8^+$ T cell immunotherapy include vaccinia virus [149],

poxviruses [150,151], Semliki Forest virus [152] adenovirus [153], herpes virus, measles virus and vesicular stomatitis virus [151]. Intracellular bacterial vectors such as *Listeria monocytogenes* (LM), BCG as well as *Salmonella enterica* serovar Typhimurium (ST) are also being investigated for use in tumour-specific-$CD8^+$ T cell activation [106,147,154–157]. The ability of facultative intracellular bacteria to exist extracellularly confers an advantage over viral vectors as these bacteria can induce both humoral and cellular T helper immune responses which can help $CD8^+$ T cell responses [158].

In addition to bacterial vectors for cancer immunotherapy, particulate immunotherapeutics such as liposomes are also under investigation for their potential to carry tumour antigen to APCs and provide adjuvanting signals. Liposomes are typically composed of natural eubacterial or synthetic ester phospholipids and have been used in vaccination against hepatitis A [159]. While many conventional liposomes deliver cargo antigen to MHC-class I processing machinery, they do so inefficiently and fail to provide strong co-stimulation. Thus, strategies have been developed to include immuno-stimulants such as Lipid A [160], CpG [161] or other PAMPS [162]. In contrast, liposomes composed of Archaeal lipids (Archaeosomes) represent a novel method for inducing tumour protective CTL responses as they can recruit and activate DCs *in vivo* and direct antigen towards MHC-class I processing machinery. Upon Archaeosome vaccination, activation of CTLs occurs rapidly with the peak of proliferation at 7 days post vaccination, followed by a steep contraction phase similar to what can be observed following acute infection with LM-OVA [163–165].

1.6 Immunotherapeutic vectors

The three immunotherapeutics used throughout this study (LM, ST and Archaeosomes) have been extensively characterized with respect to their pattern of $CD8^+$ T cell activation [141,142,163,165–168]. Thus, they form convenient model systems to address the tenets of $CD8^+$ T cell immunity to tumours. Utilizing these diverse vectors, I have addressed the influence of quality and quantity of $CD8^+$ T cells on anti-tumour immunity.

1.6-01 Listeria monocytogenes – OVA (LM-OVA)

L. monocytogenes (LM) is a rod-shaped Gram-positive, facultative anaerobe, non-spore forming bacterium. LM is a food-borne pathogen that can cause listeriosis in humans and mice and is popularly used to study host-pathogen interactions and activation of $CD8^+$ T cell responses during an acute infection [169–171]. The invasion of non-phagocytic cells by LM is mediated by the "zipper" mechanism, whereby it manipulates host actin rearrangement to extend the host cell membrane around the bacterium [172,173]. LM also invades phagocytic cells; following internalization, LM escapes from the vacuoles prior to lysosome fusion and enters the cytosol. Subsequent cell to cell spreading can occur via actin rearrangement that propels the bacteria, pushing the host cell membrane into adjacent cells where it is taken up to reside within a double membrane vacuole. A similar mechanism of vacuole escape occurs in the adjacent cell. The LM strain used in this thesis (10403S) is a streptomycin resistant strain first isolated in 1987 at Montana State University from a human skin lesion [174]. Truncated OVA (including the $CD8^+$ T cell epitope SIINFEKL), was previously introduced into the chromosomal DNA by plasmid electroporation to recombinant LM-OVA [157]. The infection of C57BL/6J and B6129F1 mice with LM-OVA has been well characterized [141,157,175,176]. Additionally, LM is currently under investigation for its potential use as an anti-

cancer vector by a number of research groups [105,106,147,155,177,178]. Its nature to enter the host cell cytosol provides an opportunity to deliver tumour antigens to the MHC-Class I presenting machinery while providing PRR stimulating danger signals associated with infection related inflammation that can co-stimulate T cell responses [147,155,177].

1.6-02 Salmonella enterica serovar Typhimurium – *OVA (ST-OVA)*

Salmonella enterica serovar Typhimurium (ST) is a rod-shaped, aerobic, Gram-negative bacterium responsible for many gastroenteric fevers in humans. However, *Salmonella enterica enterica,* serovar Typhi is much more virulent in humans causing typhoid fever which is listed as a serious public health problem by the World Health Organization. Recently, *Salmonella enterica* serovar Typhimurium has been attributed with causing approximately 3 million deaths worldwide, [179,180] thus a renewed interest to study host-pathogen relationships with this chronic pathogen is underway [141,142,168,181,182]. Infection of B6129F1 with ST is considered to closely parallel the chronic ST pathogenicity of systemic typhoid infection in humans. ST (strain SL1344) delivered systemically in C57BL/6J mice causes a lethal infection with as few as 100 bacteria [168]. In contrast, mice that express the natural resistance-associated macrophage protein (NRAMP) such as 129SvJ or B6.129F1 mice, develop a chronic infection that clears by day 60 to 90 [183,184]. ST invasion of eukaryotic cells is well characterized and is mediated by its type III secretion system encoded within the *Salmonella* pathogenicity island 1 (SPI-1). SPI-1 proteins assemble a secretion apparatus at the host cell membrane and deliver effector proteins into the cytosol inducing the rearrangement of actin to induce membrane ruffling and macropinocytosis of the bacterium into the cell [185–188]. Upon containment of ST within a host vacuole, ST uses *Salmonella* pathogenicity island 2 (SPI-2) proteins to prevent phago-

lysosome formation that promotes ST survival. SPI-II effectors also enhance ST replication by altering a number of host cell properties including signal transduction pathways and cytoskeletal structure [189,190]. ST can infect a wide variety of cells [191]; interestingly some strains of ST have been shown to have direct oncolytic effects on cancer [192–195]. ST has a unique ability to replicate within harsh anaerobic tumour sites, preferentially infecting tumour sites over spleen and liver [192]. Therefore, it has been evaluated as a vector candidate to carry anti-cancer agents including IL-2 [196], tumour antigen bound to type-III secretion protein fused to heat shock protein 70 [148] or shRNA specific to tumour mRNA [197] and mediate tumour regression. Notably, recombinant ST constructs that redirect tumour antigen to the cytosol for MHC-Class I presentation are capable of inducing potent $CD8^+$ T cell responses as early as can be seen with acute infections such as LM [148,198]. However, the ST-OVA construct used in this study does not secrete tumour antigen (OVA), and induces delayed $CD8^+$ T cell priming consistent with what occurs during chronic wild type infection [142], thus providing a reasonable model for the study of a $CD8^+$ T cell response to a chronic infection.

1.6-03 Archaeosomes – OVA (MS-OVA)

Archaeosomes are liposome vesicles composed of the polar lipids unique to the domain *Archaea*. Archaeal lipids bear unique structural signatures with phytanyl fully saturated core lipid tails, ether linked to the glycerol back-bone, unlike ester linked fatty acyl chains of eubacteria [199].

Archaeosomes were initially discovered and patented by NRC researchers Sprott et al., (US Patent: 6403117/ European Patent: EP1223978) [164,200–202] who found that when compared to conventional liposomes, archeaosomes elicited superior humoral responses

towards entrapped cargo (BSA or cholera toxin B subunit). Notably, the antibody titres rivaled antibody titres achieved with Complete Freunds adjuvant. Many different archaeosomes composed of total polar lipids (TPL) of various genera were characterized and archaeosomes composed of lipids from *Methanobrevibacter smithii* (MS) was selected as the optimum composition that elicited profound $CD8^+$ T cell effector and memory responses [163,164]. MS lipids uniquely comprise of a mixture of archaeols and caldarchaeols (3:2) and are high in phosphoserine head groups [200]. Caldarchaeols impart membrane rigidity due to their membrane spanning C-40 backbone leading to stable liposomes that can impart prolonged antigen presentation and immune memory [203]. MS liposomes also have an abundance of phosphatidyl serine (PS) head groups which mediate DC uptake via engagement of PS receptor; blocking this receptor significantly impairs MHC-class I presentation and $CD8^+$ T cell activation [167]. Following PS-receptor mediated endocytosis of MS archaeosomes, acidification of the phagosome facilitates fusion of the archaeosomes with the phagosomal membrane and expulsion of antigen into the cytosol. Subsequent TAP mediated processing results in efficient MHC-class I antigen presentation [167]. However, some degradation of the archaeosomes appears to occur in the endosome as well, allowing release of antigenic material for loading onto MHC-II molecules (Figure 2) that causes the induction of antibody and T helper responses [164]. Directing antigenic presentation towards MHC-class I facilitates a strong $CD8^+$ T lymphocyte response by archaeosomes and favours strong anti-tumour responses [201]. Additionally, antigen-free archaeosomes activate APCs upregulating co-stimulation and proinflammatory cytokine production [164]. *In vivo* injection of MS archaeosomes facilitates recruitment of professional APCs towards the injection site supporting potent cell mediated immunity to entrapped antigen. A model is proposed in

Figure 2 for the possible ways in which archaeosome-entrapped antigen may enter the cytoplasm of the APC for presentation on MHC-class I.

A

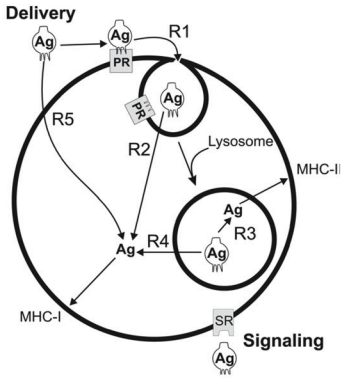

Sprott GD., et.al. Archaea. 2003 Oct;1(3):151-64..

B

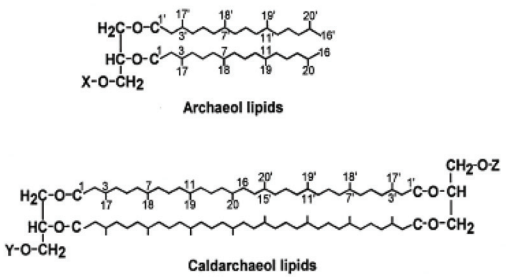

Sprott GD., et.al. Biochim. Biophys. Acta. 1999. Sept;1440(2-3):275-88

FIGURE 2: Model for archaeosome directed antigen presentation and the structure of common archaeol lipids.

(A) A phagocytosis receptor (PR) is shown interacting with an archaeosome vesicle to promote endocytosis (R1). Fusion with lysosomes is shown to be followed by release of antigen (Ag) (R3) for processing and presentation of peptides by MHC-II. Ag delivery to the cytosol for MHC-I presentation may occur in theory by direct fusion of archaeosomes with the plasma membrane (R5), or fusion with the endosome (R2) or phagolysosome (R4) membranes. Cell signaling receptors may be activated by archaeosomes either before or after endocytosis [200]. (B) Two classes of lipids found in Archaea. X, Y and Z are head group moieties which are often sugars [201]. Figures provided by Drs. Dennis Sprott and Lakshmi Krishnan [200].

Archaea are non-pathogenic; and methanogens such as MS are found to exist as commensals in the human gut [204]. Archaeosomes have been demonstrated to be non-toxic *in vivo* and *in vivo* even after repeated injections [164,202]. Additionally, archaeosomes do not evoke anti-lipid immunity, an advantage for repeated boosting. Archaeosome vaccines have been shown to effectively break tolerance to self antigens in murine cancer models [104]. Overall archaeosomes contribute convenient particulate vaccine model systems for the study of $CD8^+$ T cell responses.

1.7 Immunotherapy for melanoma

Metastatic melanoma is a deadly form of cancer due to its highly invasive nature and limited treatment options. While localized non-melanoma skin cancers can be easily cured by surgical removal with little risk of relapse, metastatic melanoma has an estimated survival rate of 6-8 months and an estimated 5 year survival rate of less than 5 % [205]. Recent advances attribute surgical metastasectomy with increasing the 5 year survival rates to 20 % [206,207]. However, there is a need for treatment options to improve survival rates. Currently, very few treatment options are available for the treatment of metastatic melanoma. The widely used Dacarbazine, can only provide complete remission in 3 % of people [205]. The addition of IFN-γ or IL-2 therapy for multidrug combination therapy has not been beneficial [208]. Interestingly, incidences of spontaneous metastatic melanoma remission have been recorded in humans [209,209,210] and are thought to be mediated by TILs. In the early 1990's the first tumour associated antigens were identified in melanoma [211]; since then, melanoma has remained a popular tumour model for testing $CD8^+$ T cell cancer vaccines [145,148,212].

Despite the infiltration of a large number of tumour specific effector $CD8^+$ T cells, tumour progression can persist. Therefore, many of the current immunotherapeutic strategies

aim to not only activate melanoma specific T cells but also inhibit regulatory receptors such as CTLA-4 or PD-1 that are responsible for immunosuppression. Clinical trials with antibodies targeting the blockade of CTLA-4, which rescues T cells from suppression, have shown a benefit in overall patient survival, but arguably only in a small subset of people [130,213]. Other pre-clinical studies have shown that a simultaneous depletion of T_{regs} with anti-CTLA-4 therapy further prolongs survival [102,214]. This brings attention to a promising tactic of immunotherapy which is to combine therapies that induce T cell activity with those that lessen the affect of tumour suppressive mechanisms.

While advancements have been made in the last decade with respects to identifying tumour suppressive mechanisms and various correlates of tumour protection, the greatest advancement so far has been met in the adoptive T cell transfer therapy (ACT) in lymphodepleted metastatic melanoma patients. ACT involves the isolation of TILs from a melanoma lesion followed by culturing in *in vitro*. The host is treated with total body irradiation to maximize lymphodepletion and the cultured TILs are delivered back to the host. This treatment regime has been met with objective response rates between 49 and 72 % [215]. Whole body radiation (lymphodepletion) achieves the removal of T_{regs} from the periphery but also frees up cytokines that would otherwise be consumed by neighbouring cells (removes the 'cytokine sink') thereby enhancing the effector functions of the transferred T cells [216].

Since melanoma has many identified immunogenic $CD8^+$ T cell antigenic epitopes from tumour antigen such as GP100, MART-1 and TRP-2 (many conserved between mice and humans) there lies a unique opportunity to attempt to break tolerance and induce potent anti-tumour T cell responses. Prostate cancer is another tumour with clearly identified tumour specific antigens, and hence has been a target for immunotherapy [149,156,217]. The first

approved cellular immunotherapy for cancer in humans was Sipuleucel-T, a recombinant DC vaccine expressing granulocyte-macrophage colony-stimulating factor (GM-CSF) and a prostate self tumour antigen used to treat patients with hormone refractory prostate cancer [218–221]. DC based vaccines aim to stimulate potent $CD8^+$ T cell responses by the adoptive transfer of DCs incubated with tumour peptide and PAMPs. While the overall survival of people treated with Sipuleucel-T is significantly increased, the majority of patients eventually succumb quickly to tumour burden [222]. Complementary therapies that reduce tumour induced attenuation of DCs might also help to promote DC activation that leads to potent anti-tumour $CD8^+$ T cell responses [223].

Unraveling the unique attributes of a $CD8^+$ T cell that confer success in combating tumour is an important step in designing optimal immunotherapeutics. While ATC therapy has currently raised the bar of what we can expect from immunotherapeutics, they highlight the importance of supplying tumour reactive T cells with an environment capable of supporting their activation and maintenance. This includes removing T_{regs}, myeloid suppressor cells, blocking PD-1 and CTLA-4. There are two avenues to explore when considering using adjuvants to induce anti-tumour $CD8^+$ T cells; these include therapeutic strategies, whereby $CD8^+$ T cells must be induced in the presence of tumour as well as preventative strategies of prophylactic vaccination to prevent initial tumour occurrence. The obstacles for each avenue likely differ as do the treatment options; for example the removal of the bystander cells that act as a 'cytokine sink' by lymphoablation is a viable option during the therapeutic treatment of cancer. However, the resulting severely weakened immune state renders this treatment too risky when considering prophylactic vaccination. The continued identification of key features of anti-tumour $CD8^+$ T cells that confer superiority in combating tumour sheds light on what is required of anti-tumour vaccines.

Recombinant viral and bacterial vectors or liposomes vaccines that can induce potent $CD8^+$ T cell responses *in vivo*, eliminate the need to culture TILs *ex vivo*. Additionally, these vaccinations can be used to generate protective immune responses that could potentially prevent cancer in healthy individuals. In pre-clinical studies it has been shown that the transfer of T cells with a T_{CM} phenotype is better able to confer tumour protection compared to the transfer of T cells with a T_{EM} phenotype.[59] Conversely, others report that the use of naïve transgenic tumour specific $CD8^+$ confer the best protection due to their high replicative potential [56]. Yet others suggest that a mixed population of T_{CM} and T_{EM} is ideal for adoptive T-cell therapy [224]. Most adoptive T cell studies agree that the transfer of effector $CD8^+$ T cells is least effective at mediating objective tumour responses even though they are the most potent cytotoxic killers [225]. This is because CTL have a decreased proliferative potential which can limit their usefulness in combating cancer. Additionally, their decreased expression of CD62L limits their residence within lymphoid compartments where they could encounter their cognate antigen presented by APCs. The selectin molecule CD62L is highly expressed on naïve $CD8^+$ T cells as well as T_{CM}; however, its expression is minimal on CTL and T_{EM}. Additionally, whether the expression of CD62L has functional importance to sustain anti-tumour immunity is currently not known. While T_{CM} are thought to be more potent mediators of anti-tumour immunity compared to T_{EM}, as has been shown in adoptive T cell transfer assays, a comparison of their tumour protective affects have not been characterized in bacterial vector vaccines. Since many different attenuated pathogens are being developed as cancer vaccines [147,150,194,226], it is important to determine whether the tumour protective attributes of adoptively transferred T_{CM} cells can be replicated *in vivo*.

2.0 CHAPTER 2

2.1 SUMMARY:

The idea of immunotherapy for cancer has challenged researchers for more than a decade and is based on the premise that one's own immune system can be triggered to eliminate tumour cells. Generating a $CD8^+$ T cell response against tumour antigen is possible with current technologies but the response does not control tumour burden in the long-run. In many cancer models, following treatment of the tumour with immunotherapy, a brief period of remission follows. However, subsequently, the tumour returns. Further, some studies have reported that tumour recurrence occurs despite the presence of tumour infiltrating lymphocytes and continued antigen expression by the tumour.

The focus of tumour cellular immunotherapy has long been the induction of large quantities of $CD8^+$ T cells. However, as described in the previous chapter, $CD8^+$ T cells are heterogeneous in their phenotype and can be classified into distinct subsets based on the expression of CD62L. The factors that prevent the long-term protective effect of T cells in a cancer setting are not fully understood. A number of tumour environment and host-specific factors probably modulate the $CD8^+$ T cell response to tumours. In order to critically evaluate the role of T cell quantity versus phenotype on efficacious anti-tumour $CD8^+$ T cell responses, I have utilized distinct vaccine delivery systems that differentially modulate the kinetics, magnitude and phenotype of the $CD8^+$ T cell response. The model antigen OVA was expressed in live bacterial vectors *Listeria monocytogenes* (LM-OVA) and *Salmonella enterica* serovar Typhimurium (ST-OVA) or entrapped within a liposome composed of archaeal lipids (archaeosomes) from *Methanobrevibacter smithii* (MS-OVA). Additionally I used α(1,3) fucosyltransferase IV&VII knockout mice (lacking functional selectin-ligands) to

characterize the anti-tumour capabilities of $CD8^+$ T cells in the absence of selectin/selectin-ligand interactions. The particulate archaeosome adjuvant also provided a convenient model system to evaluate benefits of multiple vaccinations in both a prophylactic and therapeutic setting.

Overall, I utilized archaeosomes and live bacterial vectors as candidate therapeutic vaccine delivery vehicles to address host immunomodulation to cancer, and aim to identify potential ways of improving the functionality and efficacy of T cells to control tumour burden.

2.2 HYPOTHESIS:

$CD8^+$ T cell responses generated in a tumour bearing mouse are qualitatively different and fail to provide protective anti-tumour immunity. The generation of a T_{CM} memory phenotype of $CD8^+$ T cells rather than a large quantity may provide long-term tumour protection and repeated frequent vaccination may negatively affect the quality of the memory response detrimentally impacting tumour immunity.

2.3 AIMS:

1. To characterize the $CD8^+$ T cell memory phenotype, kinetics and the anti-tumour properties following infection of mice with LM-OVA or ST-OVA.
2. To determine the role of selectin ligands in modulating $CD8^+$ T cell phenotype homing and anti-tumour immunity.
3. To evaluate benefits of repeated dose vaccination and modulation by immune regulatory mechanisms on tumour immunity, utilizing the particulate archaeosome adjuvant system.

3.00 CHAPTER 3: MATERIALS AND METHODS

3.01 Mouse strains

C57BL/6, 129x1SvJ, B6.129S7-*Rag1*^{tm1Mom}/J (homozygous for the *Rag1*^{tm1Mom} mutation producing no mature T cells or B cells) and OT.1 TCR transgenic mice (CD45.2^{+} Thy1.2^{+} with >95 % of the CD8^{+} T cells expressing the $OVA_{257–264}$ TCR) were obtained from The Jackson Laboratory (Bar Harbor, Maine, US). B6129F1 mice were generated in house in our experimental animal facility by mating 129x1SvJ female mice with C57BL/6J male mice. The B6129F1 strain was used as they were able to survive an ST-OVA infection and receive transgenic OT.1 cells or B16-OVA tumour cells both of which are of C57BL/6J origin. FtDKO mice on a C57BL/6J genetic background were generated by Dr. John Lowe [227] and obtained through the Consortium for Functional Glycomics, and bred in-house by homozygote matings. Mice were maintained at the Institute for Biological Sciences (IBS) at the National Research Council Canada (NRC) in accordance with the guidelines of the Canadian Council on Animal Care. All animals use protocols were approved annually by the NRC-IBS Animal Care Committee.

3.02 Tumour model (B16-OVA, Melanoma)

B16-OVA (expressing plasmid derived full length OVA) cells were obtained from Dr. Edith Lord (University of Rochester, Rochester, New York) [228]. B16-OVA cells were cultured in RPMI 1640 medium (Invitrogen, Life Technologies, Grand Island, New York) supplemented with 8 % fetal bovine serum (FBS) (HyClone Laboratories, Logan, Utah) (R8) containing 400 μg/ml G418 (for plasmid antibiotic selection) and 10 μg/ml gentamicin (Invitrogen, Life Technologies). B16-OVA cells (in PBS + 0.5 % normal mouse serum) were injected subcutaneously (s.c.) in the shaven lower dorsal region of mice. From day 5

onwards, detectable solid tumour was measured using calipers. Tumour size, expressed in mm^2, was obtained by multiplication of diametrically perpendicular measurements. In order to minimize pain and discomfort, mice were euthanized when tumours reached 300 mm^2. For the metastatic model, 5 x 10^5 B16-OVA cells were prepared in Hank's buffered salt solution (HBSS) (Invitrogen, Life Technologies) injected intravenously (i.v.) via the lateral tail vein. Mice were euthanized 15 days later for enumeration of black lung tumour foci. Conversely, to minimize pain and discomfort, survival was determined based on a 20 % loss in body weight or visible clinical signs of illness such as piloerection, hunched posture and lethargy.

3.03 Bacterial strains

Recombinant ST expressing the gene for OVA (ST-OVA) was previously generated by electroporating the plasmid pKK-OVA carrying the full-length OVA, into the virulent ST strain SL1344 [141]. Recombinant LM expressing the truncated gene for OVA (LM-OVA) was generated by electroporating the plasmid pJJD-OVA into the streptomycin resistant LM strain 10403S [229]. Chromosomal integration for LM-OVA was selected by several passages of culture in brain-heart infusion (BHI) (Difco, BD Biosciences, Franklin Lakes, New Jersey) agar with and without 5 μg/ml erythromycin (Sigma-Aldrich, Oakville, Ontario). Eventual loss of β-galactosidase activity was confirmed with blue-white screening. Bacteria were grown in liquid BHI medium containing 50 μg/ml streptomycin (Sigma-Aldrich) and harvested at mid-log phase (OD_{600} = 0.9). Bacteria were aliquoted and frozen at -80 °C in 20 % glycerol. Colony forming units (CFU) of the frozen stocks were enumerated by performing serial dilutions in 0.9 % NaCl, which were spread on BHI-streptomycin agar

plates (Difco, BD Biosciences). Expression of OVA by LM-OVA and ST-OVA was confirmed by Western blot analysis using an anti-OVA mAb [141].

3.04 Bacterial infection

Frozen LM-OVA or ST-OVA bacterial stocks were thawed and diluted in 0.9 % NaCl. Mice were infected i.v. (200 µl) via the lateral tail vein or s.c. (100 µl) in the mid dorsal flank. In some experiments, mice received 10^4, 10^5 or 10^6 OT.1 splenocytes i.v. before or after infection in order to increase the number of circulating $OVA_{257-264}$ specific $CD8^+$ T cells to enable later detection of T cell sub-populations by flow cytometry.

3.05 Archaeosome preparation

Archaea were grown in 250 l fermentors and archaeosomes comprising total polar lipids were prepared as described previously and provided by the group of Sprott et al. (NRC-IBS) [230,231].

3.05a Lipid extraction

Briefly, *Methanobrevibacter smithii* ALI (DSM 2375) was cultured anaerobically in pressurized sealed containers in a modified medium as described previously [232]. *Halobacterium salinarum* (ATCC 33170) and *Halococcus morrhuae* (NRCC strain 16008) were cultured aerobically in fermentors at 35 ^oC in HM2 medium with 25 % NaCl [200,230]. Cultures were harvested in late stationary phase and the biomass was frozen at -70 ^oC, and subjected to three freeze thaw cycles prior to total lipid extraction [230]. Lipids were extracted with methanol:chloroform:water (2:1:0.8, v/v) and total polar lipids (TPL) were precipitated with cold acetone and later dissolved in chloroform and stored at 4^oC.

3.05b Preparation of archaeosomes

The term archaeosomes was coined by Sprott et al., [202] and is ascribed to liposomes composed of archaeal polar lipids. In order to prepare archaeosomes, 30 mg of archaeal TPL in chloroform were dried with forced nitrogen in a 20 ml glass scintillation vial, until solvent was removed. Ovalbumin (OVA) type VI protein (Sigma-Aldrich) was diluted in PBS to 10 mg/ml and added to dried lipids at a ratio of 1:2 (5 mg protein to 10 mg lipid). To form liposomes, lipids were hydrated in the presence of 8-12 sterile glass beads (3mm diameter) at RT for 2 h with intermittent shaking/vortexing every 20-30 min. To reduce vesicle diameter to ~100 nm, the sample was sonicated for 2 min intervals and sample was intermittently visualized under oil immersion using an inverted microscope for formation of liposomes. The average diameter was assessed with a particle sizer (Nicomp 350, Santa Barbara, California). Non-entrapped OVA protein was removed from solution by ultracentrifugation at 327,000g. The supernatant was discarded and the pellet was resuspended in 1-2 ml of water by vortexing gently and filtered manually through a 0.45 μm, 25 mm diameter syringe-driven sterilizing filter. The filter was additionally washed with 0.5 ml PBS. An aliquot of archaeosomes was air dried overnight at 70 ^{o}C and lipid weight was determined. The amount of OVA encapsulated was determined by sodium dodecyl sulphate polyacrylamide gel electrophoresis (SDS-PAGE). Ovalbumin content (μg of OVA per mg of lipid) was estimated from band intensity compared to a standard curve of varying amounts of free protein loaded on the same gel. Approximately 30-70 μg of OVA protein was encapsulated per milligram of lipid. All glassware used throughout this procedure was rendered pyrogen-free by baking at 200^{o}C for 2 h. Water used for hydration was also pyrogen-free. All MS-

OVA immunizations were composed of 20 μg of OVA protein encapsulated in 0.3-0.7 mg of archaeal lipids.

3.06 Preparation of lymphocytes

Cell suspensions of lymphocytes were prepared from blood, spleen, lymph nodes, liver, lungs, bone marrow and tumour of infected or vaccinated mice at varying time-points. Cell suspensions were further manipulated for flow cytometry, culturing, purification or transfer to mice as described in detail in following sections.

3.06a Blood

Mice were bled by a small nick to the tail vein wherein 50-100 μl of blood was obtained. Alternatively, mice were bled via cardiac puncture under 4 % isofluorane, terminal anesthesia. Blood was collected in lithium heparin collection vials (BD Biosciences).

3.06b Spleen & lymph nodes

Organs were processed by mashing between the frosted ends of two glass slides in R8 medium. Cells were passed through a 45 μm Falcon cell strainers (BD Biosciences) and centrifuged at 400 g for 8 min at RT. Spleen cells were additionally subject to treatment with 500 μl of RBC lysing buffer (Sigma-Aldrich) for 1 min, and lysis was stopped with PBS. Cells were washed by centrifugation at 400 g for 8 min and finally re-suspended in 5-10 ml of R8 medium. Live cell number was enumerated by trypan blue exclusion using a haemocytometer.

3.06c Liver and lungs

Organs were collected in 10 ml PBS and homogenized with a drill mounted pestle and a round bottomed glass tube. Cell suspensions were passed through a 45 μm Falcon cell

strainer (BD Biosciences), centrifuged at 400 g for 8 min at RT and resuspended in PBS + 30 % Percoll™ (GE Healthcare Biosciences). Lymphocytes were isolated by Percoll™ density gradient centrifugation. Cell suspensions were overlaid on PBS + 70 % Percoll™ in 15 ml polystyrene tubes (Falcon, BD Biosciences) and centrifuged (in a swing bucket) at 800 g for 25 min at 4 ^{o}C with the breaking mechanism disabled to minimize disturbance of suspended cells. Lymphocytes were collected from the interphase in 50 ml polypropylene tubes (Falcon, BD Biosciences). Cells were thoroughly washed with a large amount of PBS (30 ml), centrifuged at 400 g for 8 min at RT, resuspended in R8 medium and enumerated.

3.06d Bone marrow

Femurs were dissected out from the mice by carefully cutting above and below the bone. The bone was thoroughly cleaned of tissue. Both ends of the femur bone were snipped and PBS was flushed through the marrow using a 26.5 gauge needle. Extracted progenitor cells were passed through a 45 μm Falcon cell strainer (BD Biosciences), centrifuged at 400 g for 8 min at RT and resuspended in R8 medium.

3.06e Tumour

Subcutaneous tumours were excised in R8 medium, cut into small pieces, and subject to digestion with sterile dissociation cocktail comprising a final concentration of 1 mg/ml of collagenase type 4 (Worthington Biochemical Corporation, Lakewood, New Jersey), and 0.1 mg/ml of Hyaluronidase (Sigma-Aldrich). Samples were incubated for 1 h in a 37 ^{o}C shaking incubator. Upon digestion, samples were vigorously pipetted and pushed through 45 μm Falcon cell strainers (BD Biosciences) with the hard end of a syringe plunger. Cells were centrifuged at 400 g for 8 min at RT and resuspended in 5 ml PBS + 1 % BSA. Cells were strained and washed repeatedly until there were no visible clumps. Lymphocytes were

isolated by Percoll^{TM} density gradient centrifugation. Briefly, a gradient was prepared by successively layering 40% and 70% percoll density solutions, and cells in PBS were loaded on top. Samples were centrifuged at 800 g for 25 min at 4 ^{o}C in a swing bucket with the breaking mechanism disabled. The lymphocytes that formed a band at the lower interphase were collected in a 50 ml polypropylene tube (Falcon, BD Biosciences) tube, thoroughly washed in PBS, centrifuged and resuspended in R8 medium. The low density tumour cells were found concentrated in the upper interphase.

3.07 Assessment of bacterial burden

Cell suspensions of various organs were prepared in PBS. 100 µl of serial 10-fold dilutions were plated on BHI agar plates (Difco, BD Biosciences). Plates were incubated at 37^{o}C for 24 h and bacterial colonies were enumerated.

3.08 Dendritic cell purification

DC purification was initially carried out with a kit from Miltenyi Biotech (Auburn, California) as described in the first subsection. Later on, a superior assay from STEMCELL technologies (Vancouver, BC) was used that does not require columns and was quicker, increasing both cell yield and purity.

3.08a Miltenyi method for purifying DCs

Spleens were excised at varying time-points after infection and mashed between the frosted ends of two glass slides and passed through a 45 µm Falcon cell strainer (BD Biosciences). Spleens were homogenized with 400 µl (per spleen) of PBS + 0.5 % BSA + 2 mM EDTA (Miltenyi DC cell buffer) containing 10 mg/ml collagenase type 4 (Worthington Biochemical Corporation) for 30 min at 37 ^{o}C to disperse DCs. Subsequently, cells were

washed with Miltenyi DC cell buffer, centrifuged at 400 g for 8 min and resuspended to a final concentration of 10^7 cells in 90 µl of Miltenyi cell buffer. Spleen cells samples were first depleted of T cells and B cells. For this purpose, cells were incubated with Miltenyi MicroBead bound antibodies anti-Thy1.2 (Catalog #: 130-049-101) and anti-B220 (Catalog #: 130-049-501); 10 µl of each antibody for 15 min at 4 ^oC (as per Miltenyi instructions). Cells (10^7) were then washed with 1-2 ml of Miltenyi DC cell buffer and centrifuged at 400 g for 10 min. Cell samples were resuspended in 500 µl of Miltenyi DC cell buffer and passed through a pre-washed MS column (Catalog #: 130-042-201) in a strong magnetic field. Unlabelled cells were eluted and the cell number was determined by trypan blue staining. The cell solution was centrifuged at 400 g for 10 min and resuspended in Miltenyi DC cell buffer to a final concentration of 10^8 cells per 400 µl buffer. Next, to positively select for DCs, 100 µl of anti-CD11c (Catalog #: 130-052-001) was added to the solution and incubated for 15 min at 4 ^oC. Cells were washed with 1-2 ml Miltenyi DC cell buffer and centrifuged at 200 g for 10 min and resuspended in 500 µl Miltenyi DC cell buffer. Cells were passed through a pre-washed MS column (Catalog #: 130-042-201) in a strong magnetic field. Labeled cells were eluted and cell number was determined. DC purity at 75-97 % was achieved. DCs were assayed for bacterial burden by serial dilutions on BHI agar plates (Difco, BD Biosciences); in addition their capacity to present antigen was also assayed as described in section 3.09.

3.08b STEMCELL method for purifying dendritic cells

Spleens were excised a varying time-points after infection and cut with razor blades on a sterile petri dish in 5 ml RPMI 1640 (Invitrogen, Life Technologies). DCs were dispersed by enzymatic digestion using spleen dissociation medium (Catalog #:7915.

STEMCELL technologies). DCs were purified using the positive selection DC purification kit (Cat#:18758, STEMCELL technologies). Briefly, cells were suspended at 10^8 cells/ml in PBS + 2 % FBS with 1 mM EDTA (STEMCELL medium) in 14 ml polystyrene round bottom tubes (Catalog #35207. BD Biosciences). Anti-CD16 antibody (Fc block) was added at 10 µl/ml of cells and mixed well followed by an incubation with 50 µl/ml CD11c PE antibody at RT for of 15 min. PE selection cocktail was added to a final concentration of 100 µl/ml for 15 min at RT followed by the addition of suspended magnetic nanoparticles (gentle mixing) at 50 µl/ml for 15 min at RT. The cell suspension was brought up to 5 ml with STEMCELL medium and placed into a Silver EasySep® magnet (Cat#: 18001, STEMCELL technologies) for 5 min at RT. In one continuous motion the tube and the magnet were tipped over to pour out the unwanted suspended cells and the remaining bound cells were washed in 5 ml of STEMCELL medium and incubated again in the magnet for 5 min with fresh wash buffer. The wash was repeated a total of 4 times and the magnetically bound cell fraction were isolated as positively selected DCs. DC purity of 85-90 % was achieved.

3.09 Antigen presentation

The ability of DCs from infected mice to present antigen was determined by co-culturing purified DCs with naïve OT.1 splenocytes. Splenic DCs were isolated as described in section 3.08. Spleens were excised from naïve OT.1 mice and mashed using the frosted end of two glass slides, thoroughly washed and suspended in PBS. 20 x 10^6 cells were stained with 0.125 µM CFSE for 8 min at RT with continual shaking in the dark. An equal volume FBS (HyClone Laboratories) was added to the cell suspension to stop the staining, and this was followed by centrifugation and re-suspension of the cells in R8 medium.

DCs were co-cultured for 4 days with CFSE stained OT.1 splenocytes, in 96-well microtiter plates, in R8 medium containing and 50 μg/ml of gentamicin. Antigen presentation was measured as loss of CFSE dye from OT.1 $OVA_{257-264}$ $CD8^+$ T cells indicating proliferation. Positive controls included DCs stimulated with 5 μg/ml of $OVA_{257-264}$ peptide that binds to cell surface MHC-Class I and causes OT.1 proliferation. Negative controls included CFSE stained OT.1 splenocytes alone or the co-culture of OT.1 splenocytes with DCs isolated from a mouse infected with LM, lacking the model antigen OVA. Proliferation of CFSE stained $OVA_{257-264}$ specific $CD8^+$ T cells was measured 4 days after co-culture with DCs by flow cytometric analysis.

3.10 $CD8^+$ T cell purification and enrichment

$CD8^+$ T cells can be isolated from whole spleens via positive selection or negative enrichment. Positive selection yields $CD8^+$ T cells that were bound to magnetic-bead conjugated antibody whereas negative enrichment yields untouched $CD8^+$ T cells with all other cells bound to magnetic-bead conjugated antibody. Untouched $CD8^+$ T cells are ideal for functional testing of the $CD8^+$ T cells such as adoptive transfer of the cells back into the host to mediate tumour protection. $CD8^+$ T cell positive purifications were conducted with Dynal Biotech products whereas $CD8^+$ T cell negative enrichments were carried out with Miltenyi products. In some experiments, $CD8^+$ T cell negative enrichments were also carried out with a STEMCELL technologies kit as the procedure does not require columns and was thus faster, increasing both cell yield and viability. The procedure used for various experiments is indicated in the following subsections.

3.10a Dynabead $CD8^+$ T cell positive selection purification

Cell suspensions of pooled spleen cells from infected mice in RPMI 1640 medium (Invitrogen, Life Technologies) were passed through a 45 μm Falcon cell strainer (BD Biosciences), centrifuged, and resuspended (20 x 10^6/ml) in 5 ml of R8 medium and 50 μg/ml gentamicin. $CD8^+$ T cells were positively selected for using the CELLection Biotin Binder Dynabeads as per manufacturer's instructions (Dynal Biotech, Lake Success, NY). Biotin-conjugated rat anti-mouse CD8β.2 mAb (Cat: 53.5.8; BD Biosciences), was added to the cells at a ratio of five beads to one cell, and incubated for 30 min at 4 °C on a shaking platform. $CD8\beta.2^+$ T cells were separated by magnetic isolation. Dynabeads were detached from the cells using the CELLection Biotin Binder kit releasing buffer (DNase; 188 U/10^8 Dynabeads) incubated at 37 °C for 15 min. This protocol resulted in >95 % pure $CD8^+$ T cells as determined by flow cytometric analysis.

3.10b Miltenyi $CD8^+$ T cell negative selection enrichment

$CD8^+$ T cells were negatively selected for using the $CD8a^+$ T Cell Isolation Kit (Cat: 130-090-859, Miltenyi Biotech, Auburn, CA) using mAb biotin-conjugated rat anti-mouse CD4, CD11b, CD45R, CD49b and Ter-119 (Miltenyi Biotech, Auburn, CA). $CD8^+$ T cells were isolated as per manufacturer's instructions described as follows. Cells were suspended in 40 μl of 0.5 % BSA, 2 mM EDTA in PBS (Miltenyi $CD8^+$ T cell buffer) per 10^7 total cells. 10 μl of Biotin-Antibody Cocktail was added to the cell suspension and incubated at 4 ^oC for 10 min. Anti-Biotin MicroBeads (20 μl) was added to the cell suspension and samples were incubated at 4 ^oC for 15 min. Cells were washed by adding 1−2 ml of Miltenyi $CD8^+$ T cell buffer per 10^7 cells and centrifuged at 300 g for 10 min. The pellet was resuspended in 500 μl of Miltenyi $CD8^+$ T cell buffer. LS columns were prepared by rinsing with 3 ml of Miltenyi $CD8^+$ T cell buffer and placed into a MACS Separator magnet. The cell suspension

was applied onto the column and the eluted unlabelled cells were collected as the enriched $CD8^+$ T cell fraction. The column was washed four times with 3 ml Miltenyi $CD8^+$ T cell buffer and the washes were combined with the cells. This protocol results in 85-95 % pure $CD8^+$ T cells as determined by flow cytometric analysis.

3.10c STEMCELL $CD8^+$ T cell negative selection enrichment

$CD8^+$ T cells were enriched using the STEMCELL mouse $CD8^+$ T cell enrichment kit (Cat# 19753, STEMCELL technologies) as per the protocol of the manufacturer. The following antibodies were provided in a master mix to remove non-$CD8^+$ T cells from cell suspension: anti-CD4, anti-CD11b, anti-CD19, anti-CD45R/B220, anti-CD49b, and anti-TER119. Cells were prepared at a concentration of 10^8 cells/ml in PBS + 2 % FBS containing 5 % normal rat serum (STEMCELL $CD8^+$ T cell buffer). Cells were placed in a 14 ml polystyrene tube (Catalog #35207,BD Biosciences Franklin Lakes, NJ) to properly fit into the Silver EasySep® magnet (Cat#: 18001, STEMCELL technologies). Mouse $CD8^+$ T Cell Enrichment Cocktail was added at a concentration of 50 µl/ml of cells. Samples were mixed and incubated at 4^oC for 15 min. Biotin Selection Cocktail was added at a concentration of 100 µl/ml cells. Samples were mixed well and incubated at 4 ^oC for 15 min. Magnetic nanoparticles were added at a concentration of 50 µl/ ml of cells, and the samples were mixed vigorously by pipetting 5 times (not vortexed). Samples were then incubated at 4^oC for 15 min. Cell suspensions were brought up to 5 ml (for $<10^8$ cells) or 10 ml (for 1 - 8.5 x 10^8 cells) by adding STEMCELL $CD8^+$ T cell buffer without rat serum and mixed by pipetting 2-3 times. The tube was then placed without cap into the EasySep® magnet and set aside for 10 min. The EasySep® Magnet was inverted in one continuous motion pouring off the desired fraction of $CD8^+$ T cells into a new 14 ml tube. The new tube containing the

desired enriched cells was placed inside the magnet to perform a second round of magnetic separation. This protocol resulted in 82-93 % pure $CD8^+$ T cells as determined by flow cytometric analysis with PE-conjugated rat anti-mouse CD8α (BD Biosciences Franklin Lakes, NJ).

3.11 Flow cytometric analysis for $CD8^+$ T cell phenotype

$CD8^+$ T cell phenotype was ascertained by flow-cytometric staining and analysis of cell surface expression of various activation markers. At various time intervals after infection, 50 µl of blood or 1-4 x 10^6 cells/50 µl were used for flow-cytometric staining. For spleen samples, red blood cells were first lysed with RBS lysing buffer (Sigma-Aldrich) prior to antibody staining. In contrast, blood samples were subject to RBC lysis after antibody staining. Cells were incubated with anti-Fc receptor antibody (anti-CD16) for 5 min at 4°C. Blocking of Fc receptors is not usually required for blood samples as endogenous anti-Fc antibodies present will block non-specific staining. Samples were incubated with 0.75 µl of PE-H-$2K^bOVA_{257–264}$ tetramer (Beckman Coulter, Mississauga, Ontario) for 10 min at RT. Fluorochrome conjugated anti-CD8 (catalog #: 551162, BD Biosciences) and anti-CD62L, anti-CD127, and anti-CD279 (catalog #: 25-0621, catalog #: 25-1271 and catalog #: 11-9985 respectively, eBioscience Inc., San Diego, California) antibodies were added and incubated at 4°C for 30 min. After antibody staining, blood was lysed with 1 ml of RBC lysing buffer (Sigma-Aldrich). After a few minutes, upon visual observation of lysis, cells were washed with 3.5 ml PBS + 1 % bovine serum albumin (BSA) followed by centrifugation at 400 g for 8 min at RT and fixed in PBS + 1 % formaldehyde for flow cytometric acquisition. All other cell samples were washed with 3.5 ml of PBS + 1

% BSA or FBS, centrifuged at 400 g for 8 min at RT and resuspended in 300 – 1000 µl of PBS + 1 % formaldehyde (fixing solution).

Samples were acquired on a BD FACS Canto analyzer (FACS) and voltages and compensation were optimized to ensure enumeration of positive and specific events. Unstained cell samples were used to set the gates for Forward Scatter (FSc) and Side Scatter (SSc) as well as 6 distinct emission channels. Single stained antibody controls were used to set compensation values between channels to prevent overlapping signals creating false-positives. Additionally, in some cases fluorescence minus one (FMO) controls (combining all stains in a tube minus one) were used to confirm that the combination of multiple antibodies did not create a false-positive on one channel. The concentration of cells in each sample and flow-rate was carefully adjusted to ensure acquisition of single events.

3.12 $CD8^+$ T cell ELISPOT

The frequency of IFN-γ producing $CD8^+$ T cells was determined by ELISPOT assays. 96-well ELISPOT plates (Millipore MultiScreen IP Plates Catalog #: MAIPS4510, Millipore, Danvers Massachusetts) were prepared by wetting each well with sterile 70 % MeOH for 1 min followed by 3 washes with 100 µl/well sterile fresh $NaHCO_3$ buffer for 5 min each time. The plate was coated with an in house prepared anti-IFN-γ-Ab (clone R46A2), 100 µl/well. Plates were covered with parafilm and incubated at RT for 18 h. Primary antibody was washed off with 3 separate 5 min washes of 100 µl/well RPMI medium. The plate was blocked with filtered (0.22µm) 1.5 % skim milk powder solution in RPMI medium + 10 µg/ml gentamicin for 3-4 h at 37 ^oC. Blocking buffer was aspirated and cells were suspended in R8 medium (to a final cell density of 5 x 10^5/well/100 µl) with or without $OVA_{257–264}$ (10 µg/ml), supplemented with IL-2 (0.1 ng/ml). Cultures were

incubated for 48 h at 37°C, 8 % CO_2. Often, cells were mixed with feeder splenocytes from a naïve mouse to decrease the number of cells in the assay while maintaining similar cell densities. After 48 h, cells were decanted from the wells and the plates washed with distilled H_2O to lyse the remaining cells. This was followed by thorough washing (6 times) with PBS + 0.01 % Tween for 5 min each. Plates were incubated with biotinylated secondary Ab (anti-mouse IgG) at 4 ^oC for 2 h. Plates were washed again thoroughly with PBS + 0.01 % Tween and developed using titrated amounts of avidin-peroxidase conjugate (Invitrogen) incubated at RT for 2 h. Conjugate solution was always prepared fresh in PBS + 0.05 % Tween. Finally, spots were revealed using AEC (3-amino-9-ethylcarbazole) peroxidase substrate solution kit (Cat: AEC101, Sigma-Aldrich). Spots were enumerated under a bright field dissection microscope.

3.13 Assessment of in vivo cytolytic activity

In vivo cytolytic activity of antigen-specific $CD8^+$ T cells was enumerated as described previously [233]. Briefly, cell suspensions were prepared from donor spleen. RBCs were lysed and cells were resuspended in R8 media and split into two populations, one was incubated with 10 μg/ml $OVA_{257-264}$ peptide (SIINFEKL) while the other was incubated in the same conditions without peptide. Both aliquots were stained with the cytoplasmic dye PKH26 (4 μM) for 8 min at RT with continuous agitation. Afterwards, the non-peptide aliquot was stained with a low concentration of CFSE (0.5 μM) and incubated in R8 medium while the peptide pulsed aliquot was stained with 10 X CFSE (5 μM) for 5 min at RT with continuous agitation. The two aliquots were mixed 1:1 and injected (20 x 10^6 cells/mouse) into recipient mice that were previously infected or vaccinated. At 24 h after the donor cell transfer, the relative numbers of peptide-pulsed versus control donor cells were enumerated

in the spleens of recipients by FACS, and percentage *in vivo* killing was calculated as follows:

100 - ([(% peptide pulsed in infected /% unpulsed in infected)/(% peptide pulsed in uninfected /% unpulsed in uninfected)] x 100). [233]

3.14 Staining for T_{reg} cells

T_{regs} from various tissues were identified using the mouse T_{reg} Staining Kit #3 (catalog #: 88-8115, eBioscience Inc.) using the manufacturer's protocol. Briefly, cells (10^7/ml) were incubated with anti-Fc-antibody for 5 min at 4°C and subsequently stained with 0.125 μg anti-CD4 and 0.06 μg of anti-CD25 antibodies at 4 °C for 30 min. Cells were washed in 1 to 2 ml of cold Flow Cytometry Staining Buffer and centrifuged at 400 g for 8 min. The pellet was resuspended and 1 ml of freshly prepared Fixation/Permeabilization working solution was added and vortexed. Samples were incubated at 4 °C for 30 min. After a wash with 2 ml Permeabilization Buffer samples were centrifuged at 400 g for 8 min at RT. The pellet was resuspended in 100 μl of permeabilization buffer containing 0.5 μg Fc block and incubated at 4 °C for 15 min. Samples were then stained with anti-mouse/rat Foxp3 (FJK-16s) antibody (0.5 μg) or isotype control for 30 min in the dark at 4°C. Cells were washed twice with 2 ml 1X Permeabilization Buffer and centrifuged at 400 g for 8 min at RT. The pellet was resuspended in Flow Cytometry Staining Buffer and analyzed with a BD Biosciences FACS Canto analyzer.

3.15 $CD8^+$ T cell proliferation assays

$CD8^+$ T cells were assayed for homeostatic proliferation both *in vitro* as well as *in vivo* in a lymphopenic host ($RAG^{-/-}$). Additionally for some experiments, $CD8^+$ T cells were

expanded in culture following *in vivo* and *in vitro* exposures to LM-OVA. These methods are described in detail below.

3.15a In vitro homeostatic proliferation of memory CD8$^+$ T cells

Spleens were excised after infection and cell suspensions were prepared at a concentration of 20 x 10^6 /ml in PBS. Cells were stained with CFSE (0.125 μM) and resuspended in 10 ml of R8 medium at 10 x 10^6 cells/ml. 60-70 x 10^6 cells were cultured at 37 ^oC in a humidified incubator with 8 % CO_2. IL-7 (1-10 ng/ml) and IL-15 (1-10 ng/ml) were added to each flask every 3 days. At varying time-points of culture, a sample of cultured cells was retrieved for flow cytometric analysis. Cells were first incubated with anti-Fc blocking antibody and stained with anti-CD8 antibody and $OVA_{257-264}$-tetramer. Cell divisions as shown by CFSE loss were monitored over time.

3.15b In vivo homeostatic proliferation

OT.1 cells (10^6) were injected i.v. into B6129F1 mice followed by an injection of 10^3 ST-OVA or LM-OVA i.v. 7 days later. Spleens were removed at late time points post-infection (i.e. >60 days) and a cell suspension was prepared in PBS (20 x 10^6/ml). Cells were first stained with CFSE (0.125 μM) and re-suspended in R8 medium at 10 x 10^6 cells/ml. CD8$^+$ T cells were purified by STEMCELL negative selection as described in section 3.09c. CD8$^+$ T cells were re-suspended in HBSS and 3 x 10^6 - 4 x 10^6 cells were injected i.v. into RAG$^{-/-}$ mice. Spleens were removed from recipients 7 days later and stained with anti-CD8 antibody and $OVA_{257-264}$-tetramer, and cell divisions were evaluated by loss of CFSE by flow cytometric analysis.

3.15c CD8$^+$ T cell primary cultures

Cell suspensions were obtained from pooled spleens from infected mice (n = 2-3). Splenocytes (10^8) in 10 ml R8 medium were incubated with 10^4 LM-OVA in T-75 tissue culture flasks (Falcon, BD Biosciences) at 37 ^oC and 8 % CO_2. A high dose of gentamicin, (50 μg/ml), was added to the cultures 15 h later, to kill any live LM-OVA. Subsequently at 40 h after *in vitro* antigen exposure, cells were transferred to a T-75 tissue culture flask in fresh media supplemented with IL-7 and IL-15 (1 ng/ml). Cultures were thereafter expanded, and supplemented with fresh media and cytokines every two days.

3.16 Intracellular IL-2 and IFN-γ production by OVA-specific $CD8^+$ T cells

Aliquots of spleen cells (10 x 10^6 /ml) were stained with anti-CD8 antibody and H-$2K^bOVA_{257–264}$ tetramer for 30 min, as described in section 3.10. Cells were then washed, reconstituted in R8 medium plated into 96-well plates (2 x 10^6 /well), and stimulated with $OVA_{257–264}$ peptide (1 μg/ml) in the presence of GolgiStop (BD Biosciences). After 1 h, cells were harvested, washed, permeabilized, and stained for intracellular IL-2 and IFN-γ using an intracellular cytokine staining kit (BD Biosciences) and acquired by flow cytometry.

Technical Acknowledgements

It is acknowledged that the following procedures were carried out by Technical Officers in the laboratory of L. Krishnan and S. Sad at the NRC-IBS; bone marrow cell preparations by Komal Gurnani, intracellular IL-2 staining and maintenance of bacterial stocks by Renu Dudani. I also gratefully acknowledge the assistance provided by Komal Gurnani for carrying out some *in vivo* CTL, ELISPOT and primary $CD8^+$ T cell culture experiments.

4.0 CHAPTER 4: RESULTS

4.1 Modulation of anti-tumour CD8$^+$ T cell responses by LM-OVA and ST-OVA

To investigate efficient and inefficient CD8$^+$ T cell responses against tumour antigens, I employed the use of two well characterized intracellular bacteria, LM-OVA and ST-OVA. LM-OVA infection in mice causes an acute infection with a classical activation of CD8$^+$ T cells within the first week and the long-term maintenance of CD62L^{high} memory CD8$^+$ T cells (T_{CM}). In contrast, ST-OVA infection in B6129F1 mice causes a chronic infection, protracted CD8$^+$ T cell response that does not peak until 2 - 3 weeks and a long-term maintenance of CD62L^{low} memory CD8$^+$ T cell population (T_{EM}). My first aim was to correlate the differential CD8$^+$ T cell activation by these two vector systems, with the anti-tumour response against B16 melanoma. I hypothesized that the generation of a predominantly CD62L^{high} CD8$^+$ T_{CM} cell population can provide superior tumour protection due to the proliferative and/or cell homing potential rather than differential functionality (cytolytic ability and cytokine production).

4.1-01 LM-OVA induced better tumour protection compared with ST-OVA

Protection against murine melanoma expressing ovalbumin (B16-OVA) was monitored in mice after prophylactic exposure to LM-OVA and ST-OVA. Non-vaccinated naïve mice or non-vaccinated mice that received OT.1 splenocytes (OT.1 parked) rapidly developed large tumours following s.c. tumour challenge, succumbing by 3 weeks. When vaccinated mice were challenged with tumours ~90 days post-infection, only 20 % of LM-OVA-vaccinated mice developed tumours, whereas 50 % of ST-OVA-vaccinated mice developed tumours (Figure 3A). Based on 3 independent experiments wherein mice were challenged 51 to 136 days post-infection, non-vaccinated mice had a median survival of 20

days, and ST-OVA–vaccinated mice exhibited a median survival of 41 days. In contrast, the majority of LM-OVA-vaccinated mice survived beyond 100 days (Figure 3B). In some experiments, mice received 10^6 OT.1 splenocytes prior to infection such that the frequency of responding naïve $CD8^+$ T cells was increased and this enabled long-term tracking of antigen-specific $CD8^+$ T cell responses. Of the transferred OT.1 splenocytes, approximately 20 % were $CD8^+$ and >95 % of them were specific for the OVA epitope SIINFEKL ($OVA_{257-264}$). It is possible that the addition of OT.1 splenocytes in combination with vaccination enhanced tumour protection; however, even in the absence of OT.1 cell transfer, LM-OVA vaccination conferred better tumour protection compared to ST-OVA vaccination (Figure 4A & B). Tumour growth in mice injected with non-recombinant LM or ST was similar to uninfected mice (Figure 5A-E), confirming lack of bystander vector effects. Therefore, LM-OVA and ST-OVA clearly afforded diverging long term antigen-specific tumour protection.

4.1-02 LM-OVA and ST-OVA induced distinct infection patterns

To determine the correlates of the differential tumour protection afforded by ST-OVA and LM-OVA, I evaluated the bacterial growth kinetics and the magnitude and quality of the $CD8^+$ T cell response. LM-OVA infection peaked within the first three days and was not detectable after 7 days of infection in the various organs of infected mice, consistent with acute infection. In contrast, ST-OVA infection showed a delayed peak of bacterial burden at ~3 weeks of infection followed by gradual clearance consistent with chronic infection. Nevertheless, after ST-OVA infection bacterial numbers dramatically decreased ~1000-fold in all three organs tested by 60 days and remained undetectable thereafter (Figure 6).

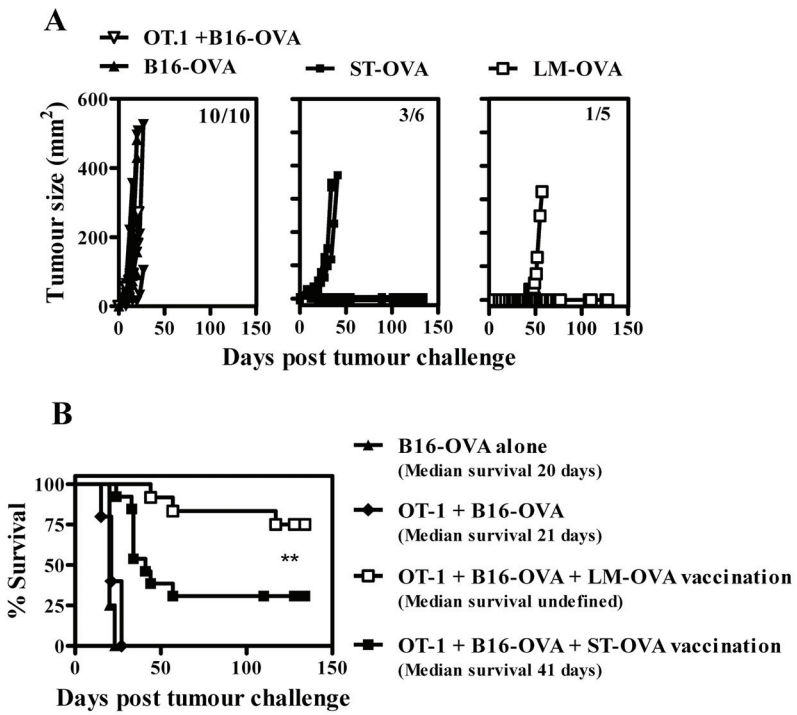

Stark et.al. Cancer Research . May 15;69(10):4327-34. 2009.

FIGURE 3: LM-OVA mediated superior prophylactic protection against B16-OVA tumour development.

B6129F1 mice were injected with 10^6 OT.1 splenocytes and 10^3 LM-OVA or ST-OVA, and challenged with 10^6 B16-OVA tumours (s.c.) on day 90 or 92, respectively. (A) Solid tumour progression in individual mice is indicated. Inset: number of mice developing tumours relative to total number in the group. (B) Percent survival (endpoint marked when tumours reach 300 mm^2). This experiment was performed 5 times with tumour challenge on 51, 56, 62, 90 to 92, and 136 days after infection. As no significant difference was observed between these time points, data was pooled for graphical display (n = 5 – 13 mice per group). Log-rank test shows significance at the 99 % confidence interval for LM-OVA vaccination relative to ST-OVA (p=0.0095).

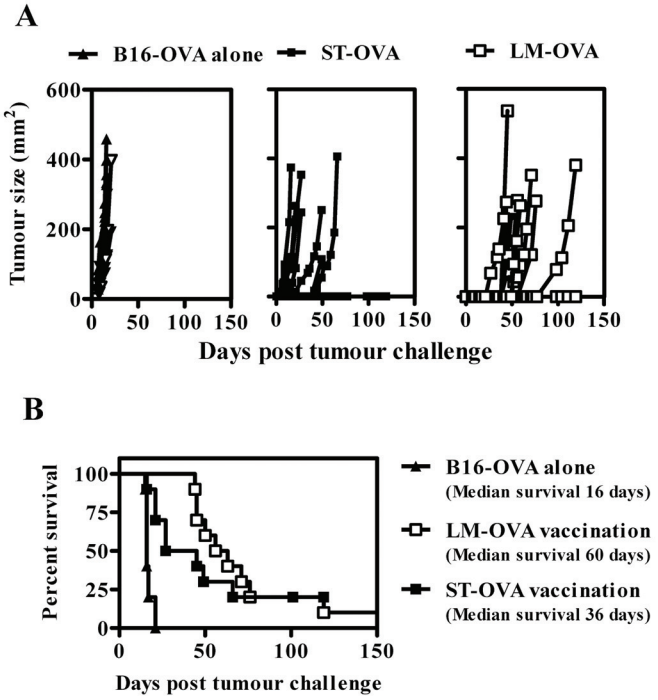

Stark et.al. Cancer Research . May 15;69(10):4327-34. 2009.

FIGURE 4: Endogenous $CD8^+$ T cell responses against LM-OVA mediated superior prophylactic protection against B16-OVA tumour development in the absence of OT.1 cells.

B6129F1 mice were infected (i.v.) with 10^3 LM-OVA or ST-OVA, and challenged s.c. 60 days later with 10^6 B16-OVA tumours. (A) Individual solid tumour growth is displayed. (B) Percent Survival (endpoint marked when tumours reach 300 mm^2). Survival proportions are based on n=10 per group. The median survival of control tumour bearing mice was 16 days. For ST-OVA and LM-OVA vaccinated mice the median survival was 36 and 60 days, respectively.

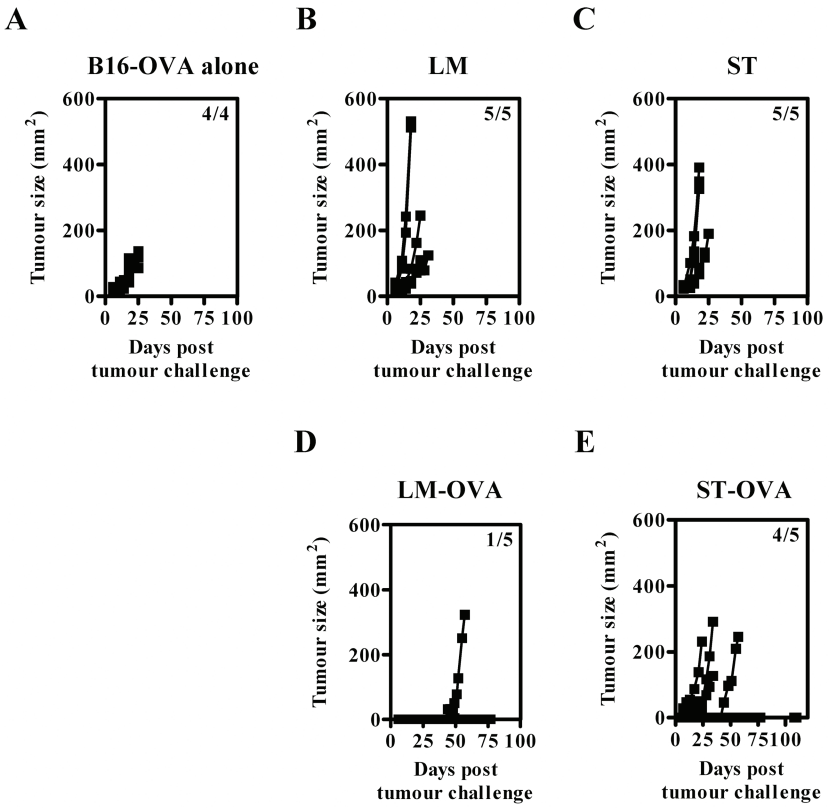

FIGURE 5: LM-OVA and ST-OVA mediated tumour protection is antigen dependent. B6129F1 mice were injected with 10^6 OT.1 splenocytes and infected (i.v.) with 10^3 LM, LM-OVA, ST, or ST-OVA organisms. 91-136 days later they were challenged with 10^6 B16-OVA tumours. (A-E), Solid tumour growth in individual mice is displayed. (n=5) Inset numbers indicate number of mice in each group that succumbed to tumour burden. The median survival of control tumour bearing mice was 25 days. For LM and ST vaccinated mice, the median survival was 25 and 18 days, respectively. ST-OVA vaccinated mice had a median survival of 34 days and LM-OVA survival was undefined.

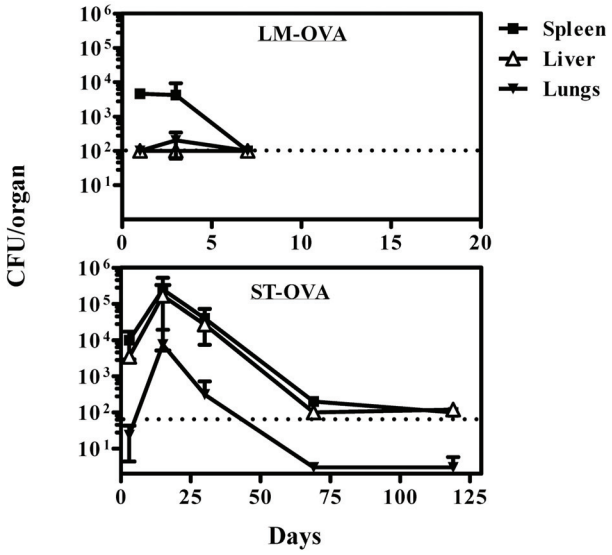

Stark et.al. Cancer Research . May 15;69(10):4327-34. 2009.

FIGURE 6: Contrasting bacterial burden kinetics in LM-OVA and ST-OVA infections.

B6129F1 mice were infected (i.v.) with 10^3 LM-OVA or ST-OVA. Bacterial burden is displayed as mean CFU ± SD (n = 2 – 4 per time point per group). Detection limits were 100 CFU (dotted line) except for the lung tissue where the detection limit was 1 CFU.

Furthermore, LM-OVA were present in the purified DC fraction on day 1 after infection but not detectable at day 15 (Figure 7, top/left). In contrast, ST-OVA were absent from DCs on day 1 after infection, and were detected on day 15 (Figure 7, bottom/left). Accordingly, antigen presentation by LM-OVA infected DCs (based on OT.1 $CD8^+$ T cell proliferation) occurred as early as day 1 after infection. In contrast, the delayed uptake of ST-OVA by DCs corresponded to delayed antigen presentation (Figure 7, right).

4.1-03 LM-OVA and ST-OVA induced distinct $CD8^+$ T cell kinetics

I measured the kinetics of the $OVA_{257-264}$ $CD8^+$ T cell response during LM-OVA and ST-OVA infection using PE-tetramer that recognizes the TCR of $CD8^+$ T cells specific for the $OVA_{257-264}$ peptide. LM-OVA induced blood resident $OVA_{257-264}$ specific $CD8^+$ T cells proliferated and peaked in number by day 7; this was followed by a massive contraction resulting in 10-fold reduction in cell number (Figure 8). Alternatively, ST-OVA infection induced delayed $OVA_{257-264}$ specific $CD8^+$ T cell priming; the response peaked at day 21, followed by a prolonged contraction phase with only a 2-fold reduction in cell number occurring over a 40 day time period (Figure 8). Thus, the $CD8^+$ T cell response kinetics closely followed the infection kinetics, and even for ST-OVA infection there was a clear $CD8^+$ T cell priming phase at ~21 days post infection [141]. Moreover at later time points, $OVA_{257-264}$ specific $CD8^+$ T cell frequencies were similar for LM-OVA and ST-OVA infections.

4.1-03a LM-OVA memory $CD8^+$ T cells expand after B16-OVA tumour challenge

I surmised that expansion of the memory cells would be required for efficacious tumour clearance, and this may be defective in ST-OVA vaccinated mice.

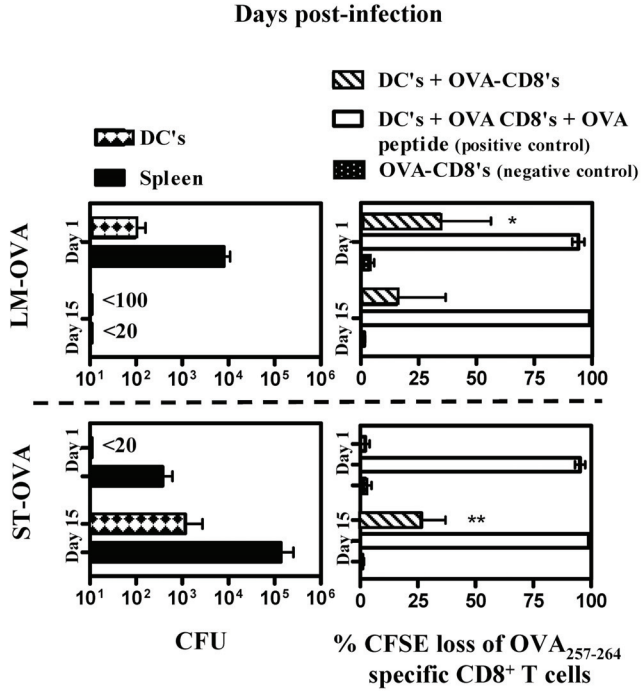

Stark et.al. Cancer Research . May 15;69(10):4327-34. 2009.

FIGURE 7: Contrasting antigen presentation mediated by DCs of ST-OVA and LM-OVA infected mice.

B6129F1 mice were infected with 10^3 LM-OVA or ST-OVA. CFU *(left)* were enumerated in the spleens and purified DCs of individual mice (n = 3 per time point). DCs were purified with the Miltenyi method and cells were co-cultured at a ratio of 1:1 (1 x 10^5 DC/well and 1 x 10^5 OT.1 cells/well). Antigen presentation *(right)* is based on % CFSE dye loss ±SD in OT.1 $CD8^+$ splenocytes cultured for 4 days with purified DCs (obtained from 3 individual mice per time point). Two-tailed *t* test with Welch's correction for unequal variance at each time-point reveals a significant difference between: top/right; Day 1, DC vs. negative control (p=0.0209) and bottom/right; Day 15, DC vs. negative control (p=0.0018).

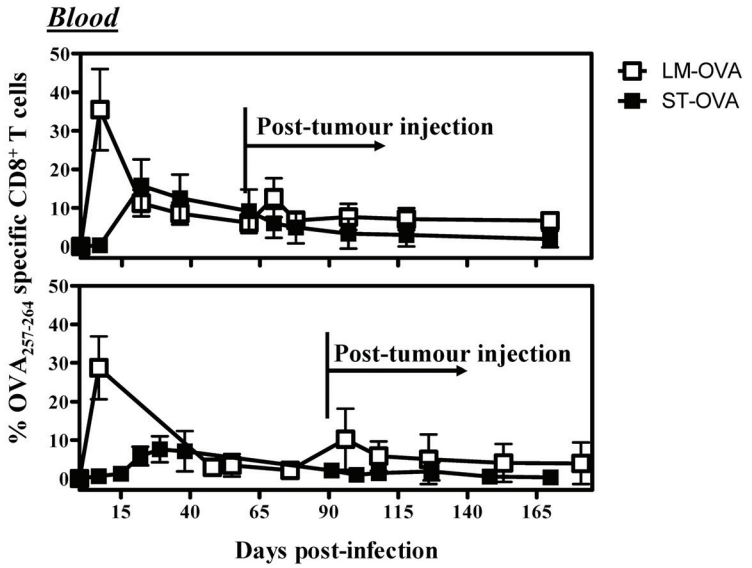

Stark et.al. Cancer Research . May 15;69(10):4327-34. 2009.

FIGURE 8: Kinetics of an $OVA_{257-264}$ specific $CD8^+$ T cell response induced by ST-OVA and LM-OVA.

10^6 OT.1 splenocytes were adoptively transferred into B6129F1 mice. 3-10 days later mice were infected with 10^3 LM-OVA or ST-OVA. The % $OVA_{257-264}$ specific $CD8^+$ T cells ±SD were measured pre- and post-tumour challenge. n = 3 - 5 mice per group per time point. For post-tumour time points in the ST-OVA group, data are representative of surviving mice only. Tumour challenge occurred 62 days (top) or 90 to 92 days (bottom) post-infection. After tumour challenge, the number of antigen-specific $CD8^+$ T cells in the LM-OVA group increased significantly ($P < 0.05$ by unpaired two-tailed *t* test). All data are representative of two to three separate experiments conducted.

At 60 days and beyond of infection, when tumour challenge was carried out, the number of peripheral blood memory cells were low (3-8 %) but similar in LM-OVA and ST-OVA vaccinated mice (Figure 8). In LM-OVA vaccinated mice, tumour challenge at day 62 to 92 caused a rapid expansion of $OVA_{257-264}$ specific $CD8^+$ T cells (to ~10 %) in the blood ($p=0.0314$). In contrast, no such increase was observed in ST-OVA vaccinated mice ($p=0.1017$) (Figure 8). Moreover, the numbers of $OVA_{257-264}$ specific $CD8^+$ T cells remained constant even 100 days post-tumour introduction in ST-OVA infected mice. Thus, the lack of $CD8^+$ T cell expansion following tumour introduction in the ST-OVA group could not be attributed to lower numbers of pre-existing memory $CD8^+$ T cells or to a delayed secondary response.

4.1-03b LM-OVA memory $CD8^+$ T cells differentiated to a predominant $CD62L^{high}$ phenotype

In order to analyze the phenotype of the responding $CD8^+$ T cells to infection, I monitored the kinetics of expression of CD62L, which is expressed at high levels on naïve and T_{CM} $CD8^+$ T cells, and IL-7Rα which is upregulated on naïve and memory T cells [234]. The differentiation pattern of $CD8^+$ T cells during an LM-OVA infection was similar to what is seen in many virus models. An immediate effector phenotype ($CD127^{low}$, $CD62L^{low}$) population was observed early after infection, followed by a progressive increase in T_{CM} cells that correlates with the contraction phase seen after day 7 (Figure 9). In contrast, at 3 weeks of ST-OVA infection a predominant effector phenotype ($CD44^{high}CD62L^{low}$) was seen (Figure 9). The expression of CD62L on ST-OVA induced $CD8^+$ T cells increased from 15 % to 30 % by day 60 in the spleen; however, this was lower than the high levels (~70 %) observed on LM-OVA induced $CD8^+$ T cells (Figure 9A). IL-7Rα expression which is classically upregulated on naïve and memory T cells was initially high in both infection

models decreased as expected at the respective peak of priming. In LM-OVA infection, a majority of $OVA_{257-264}$ specific $CD8^+$ T cells in the blood and spleen appeared to take on the memory phenotype (IL-7Rα^{high}) as early as 21 days and ~80 % of the cells were IL-7Rα^{high} thereon (Figure 9B). In contrast, during ST-OVA infection, the reduction in IL-7Rα expression was delayed until 3 weeks after infection correlating with the delay in priming. Subsequently, IL-7Rα expression gradually increased over time (Figure 9B). Comparing the relative numbers of $OVA_{257-264}$ specific $CD8^+$ T_{CM} cells (CD62L^{high}IL-7Rα^{high}), by day 76, the LM-OVA group exhibited around 86 % whereas the ST-OVA group had only 28 % of such cells. Nevertheless at this time point, ~80 % of $OVA_{257-264}$ specific $CD8^+$ T cells in ST-OVA–infected mice were IL-7Rα high, indicating that a majority of the cells were of the T_{EM} phenotype (Figure 9C). Overall, ST-OVA triggered a delayed effector response and a protracted T_{EM} response, whereas LM-OVA evoked a T_{CM} response.

4.1-04 ST-OVA induced memory $CD8^+$ T cells were fully functional

Next, I determined whether LM-OVA and ST-OVA infection evoked a disparity in $OVA_{257-264}$ specific $CD8^+$ T cell function. The *in vivo* cytotoxicity assay measures the killing ability of $CD8^+$ T cells in an immediate 24 hour time period in a physiological setting. Seven days post-infection, 99.8 % of target cells were eliminated in LM-OVA–infected mice, whereas the peak of cytolytic activity in ST-OVA–infected mice was ~86 % but not observed until 30 to 60 days after infection (Figure 10A). Markedly, the $OVA_{257-264}$ specific $CD8^+$ T cell cytolytic response was low (~20 %) in LM-OVA–infected mice by day 14 (Figure 10A), which corresponded with clearance of the infection and contraction of the response. In contrast, ST-OVA $OVA_{257-264}$ specific $CD8^+$ T cells maintained strong immediate cytolytic functions up to 60 days post infection (Figure 10A).

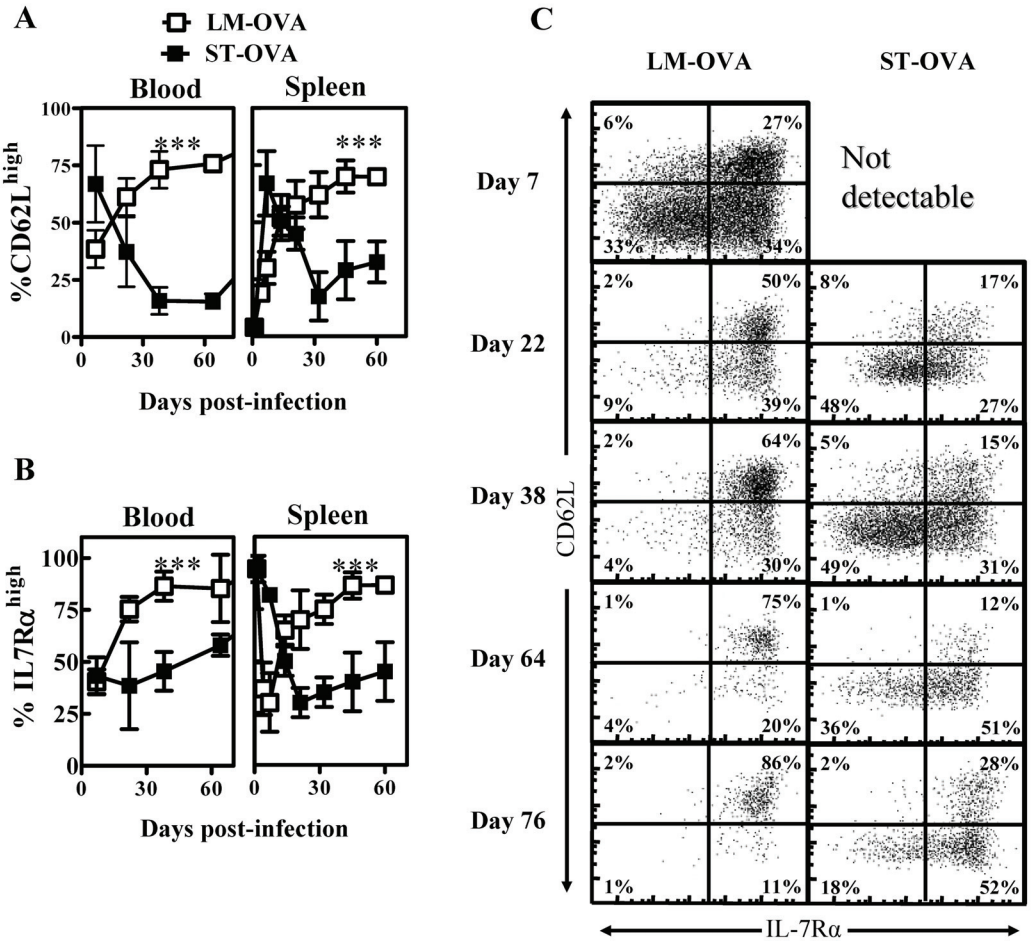

Stark et.al. Cancer Research . May 15;69(10):4327-34. 2009.

FIGURE 9: Differential expression of cell surface memory markers on ST-OVA and LM-OVA induced CD8$^+$ T cells.

The expression of (A) CD62L and (B) IL-7Rα gated on CD44$^+$, OVA$_{257-264}$ specific CD8$^+$ T cells in the blood and spleen over time of mice that received 10^6 OT.1 splenocytes followed by 10^3 LM-OVA or ST-OVA. Data are based on expression levels in n=4-10 mice per group per time point for blood and n=2 per group per time point for spleen (mean ± SD). (C), Representative plot demonstrating co-expression of CD62L and IL-7Rα on gated CD44$^+$, OVA$_{257-264}$ specific CD8$^+$ T cells at various times in the blood. Note that at day 7, ST-OVA numbers cannot be plotted as there is no discernable OVA$_{257-264}$ specific CD8$^+$ T cell population at this time in this group. Numbers indicate % within each quadrant. Data are representative of 2 such individual experiments conducted. ***, A two-way ANOVA was performed and shows a significant difference ($p < 0.001$) between treatment groups over time. Figure A & B were kindly provided by Subash Sad, NRC-IBS.

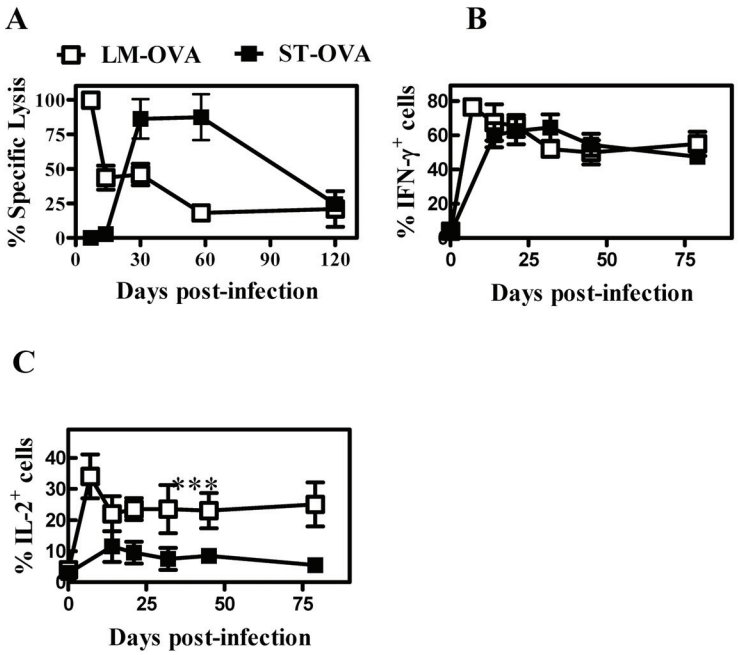

Stark et.al. Cancer Research . May 15;69(10):4327-34. 2009.

FIGURE 10: *In vivo* cytolytic activity, intracellular IFN-γ and IL-2 expression of $OVA_{257-264}$ specific $CD8^+$ T cells.

(A) B6129F1 mice were infected with 10^3 LM-OVA or ST-OVA. At various time points after infection % specific *in vivo* lysis of transferred target cells was calculated. Data were derived from the analysis of individual mice spleens (mean ± SD of n=3) per time point. Experiment was representative of three such experiments. (B & C), B6129F1 mice were first injected with 10^6 OT.1 splenocytes and then infected with 10^3 LM-OVA or ST-OVA. At various time intervals, the numbers of (B) IFN-γ or (C) IL-2 secreting $OVA_{257-264}$-tetramer specific $CD8^+$ T cells were evaluated after 1 h stimulation of cells with $OVA_{257-264}$ peptide. Mean percentage ± SD of (A) IFN-γ and (B) IL-2 secreting antigen-specific $CD8^+$ T cells for various time points is shown. Data was derived from the analysis of 2 individual spleens per time point, and is representative of two such experiments conducted. ***, IL-2 production was significantly ($p < 0.001$) different after LM-OVA and ST-OVA vaccination by a two-way ANOVA. This figure was kindly provided by Subash Sad, NRC-IBS.

$OVA_{257-264}$ specific $CD8^+$ T cells induced against LM-OVA and ST-OVA expressed similar levels of IFN-γ at all time points tested (Figure 10B). However, only LM-OVA induced

$OVA_{257-264}$ specific $CD8^+$ T cells expressed increased intracellular IL-2, and remarkably, their numbers were stably maintained over prolonged periods (Figure 10C). ST-OVA induced $OVA_{257-264}$ specific $CD8^+$ T cells showed lower levels of intracellular IL-2 production at all time points (Figure 10C). Thus, although $CD8^+$ T cells generated against ST-OVA were fully functional in their ability to kill targets and produce IFN-γ, they produced less IL-2 to support their proliferation and expansion.

4.1-05 ST-OVA infected mice had a higher frequency of T_{regs} in the lymph nodes

T_{regs} are known to have a suppressive affect on activated $CD8^+$ T cells and can be hijacked by the pathogen and tumour as a mechanism of immune evasion [235,236]. While T_{regs} play an important role in normal immune homeostasis, they can be recruited to diminish a protective $CD8^+$ T cell response [237]. T_{regs} ($CD4^+CD25^{high}FoxP3^+$) were identified in the spleen of infected mice over time and were found to occur at similar frequencies as a percentage of all lymphocytes (Figure 11). As lymphocyte numbers are greatly increased in the spleen of ST-OVA infected mice compared to LM-OVA infected mice (Figure 12A), I considered it was important to determine the total number of T_{regs} as well. An increased overall number in the spleen could translate to a greater presence in the periphery including tumour sites. In the spleen of ST-OVA infected mice there was an increase in the number of $CD4^+$ T cells (Figure 12B), as well as an increase in the number of T_{regs} (Figure 12C); however, the frequency of T_{regs} of all $CD4^+$ T cells is similar to that of LM-OVA infected mice (Figure 12D).

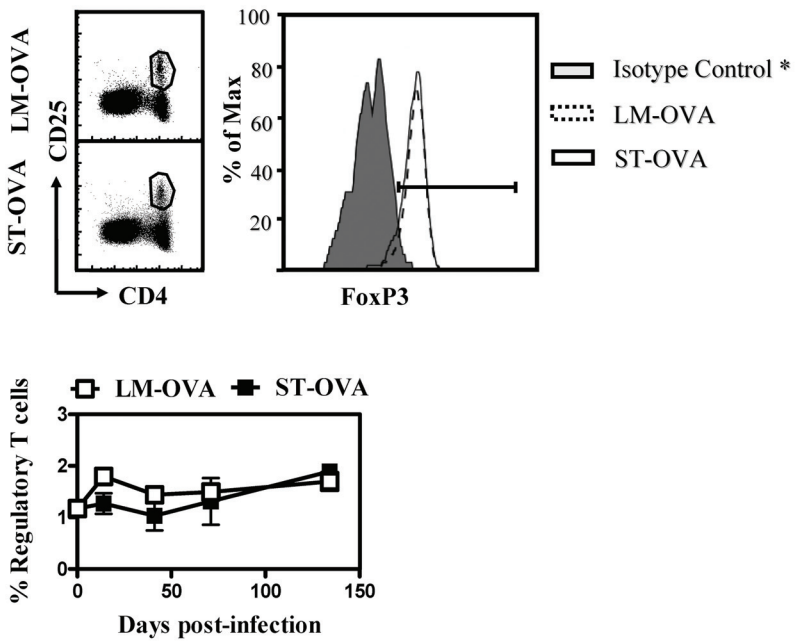

Stark et.al. Cancer Research . May 15;69(10):4327-34. 2009.

FIGURE 11: Percentage of splenic T_{regs} after ST-OVA and LM-OVA infection.
B6129F1 mice were infected with 10^3 LM-OVA or ST-OVA. At various time points after infection, spleens were processed and stained for T_{regs}. % of $CD4^+$ $CD25^{high}$ $FOXP3^+$ splenic cells of all lymphocytes after infection is indicated. Gating strategy and mean ± SD (n = 3/group/time point) is shown. (A) Two-way ANOVA reveals significant difference over time between infections ***.

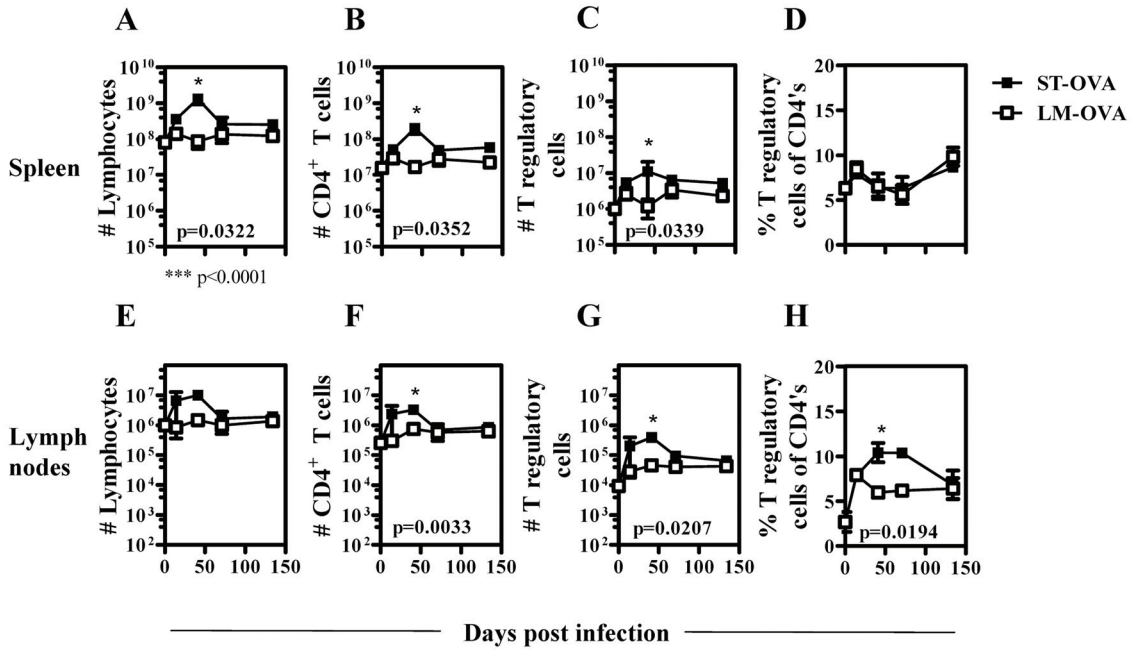

FIGURE 12: Number of lymphocytes, CD4$^+$ T cells, and T_{regs} following ST-OVA and LM-OVA infection.

B6129F1 mice were infected with 10^3 LM-OVA or ST-OVA. At various time points after infection spleen and lymph nodes were processed and stained for T_{regs}. The number of lymphocytes, CD4$^+$ T cells, T_{regs} and the frequency of T_{regs} among CD4$^+$ T cells is shown in (A-D) spleen and (E-H) peripheral inguinal lymph nodes (mean ± SD). (H) Two-tailed *t* test with Welch's correction for unequal variance at each time-point reveals significant differences in T_{reg} cell number and frequency.

A different trend was observed in the peripheral lymph nodes of infected mice; while the number of lymphocytes, $CD4^+$ T cells and T_{regs} were similarly increased in ST-OVA infected animals (Figure 12E, F, G), the frequency of T_{regs} among CD4 T cells was markedly increased (Figure 12H). Thus, there appears to be a dichotomous distribution in the number versus the frequency of T_{regs} evoked following ST-OVA infection. While the number of T_{regs} was greater in the spleen and lymph nodes after 40 days of infection with ST-OVA, the frequency was greater only in the lymph nodes. It is however, unclear how this may impact the anti-tumour $CD8^+$ T cell response.

4.1-06 ST-OVA generated memory $CD8^+$ T cells exhibited defective homeostatic proliferation

Responding $OVA_{257-264}$ specific $CD8^+$ T cells will need to expand and replenish in parallel to counteract an aggressive tumour. Thus, in addition to antigen induced proliferation, homeostatic proliferation of $CD8^+$ T cells may be important for effective tumour control. $OVA_{257-264}$ specific $CD8^+$ T cells generated after LM-OVA infection were able to homeostatically proliferate (based on CFSE reduction) in the presence of growth cytokines for a significantly prolonged period compared with those generated after ST-OVA infection (Figure 13A&B). Negative controls showed that $OVA_{257-264}$ specific $CD8^+$ T cells died rapidly in culture in the absence of cytokine supplementation (Figure 13A). The transfer of 90 day old $OVA_{257-264}$ specific $CD8^+$ T cells into naïve $RAG^{-/-}$ recipients resulted in significantly higher proliferation for LM-OVA memory cells compared with ST-OVA (Figure 13C&D). Because $RAG^{-/-}$ mice lacked endogenous T cells, adoptively transferred memory $CD8^+$ cells inhabited a lymphopenic environment and were able to expand to greater numbers upon homeostatic proliferation. Thus, ST-OVA $OVA_{257-264}$ specific $CD8^+$ T cells were qualitatively defective in this homeostatic expansion ability.

4.1-07 LM-OVA induced CD8$^+$ T cells were better able to traffic to multiple sites

An important determinant of a successful anti-tumour CD8$^+$ T cell response is the ability of CD8$^+$ T cells to traffic to peripheral sites to encounter tumour antigen within lymph nodes and migrate towards tumour sites. Therefore, I compared the mobility of $OVA_{257-264}$ specific CD8$^+$ T cells generated in both infection models. Memory CD8$^+$ T cells were purified from infected mice and adoptively transferred to naïve or tumour bearing B6129F1 mice and then tracked for their ability to traffic efficiently to various organs in response to tumour challenge. The relative proportion of adoptively transferred cells in tumour bearing mice compared to non-tumour bearing mice is shown in Figure 14. In this scenario, greater numbers of LM-OVA (but not ST-OVA) memory CD8$^+$ T cells trafficked to lymphoid compartments (spleen and bone marrow) 3 days after tumour challenge relative to non-tumour-bearing recipients. Thus, ST-OVA induced $OVA_{257-264}$ specific CD8$^+$ T cells were qualitatively defective in homeostatic expansion ability and homing capacity. LM-OVA induced $OVA_{257-264}$ specific CD8$^+$ T cells exhibited superior homing capacity to lymphoid compartments in response to tumour antigen.

4.1-08 Adoptively transferred LM-OVA CD8$^+$ T cells confer superior tumour protection

Since infections cause the activation of APCs and inflammation that may modulate tumour protection in a bystander fashion, I tested the intrinsic anti-tumour ability of CD8$^+$ T cells purified from vaccinated animals when adoptively transferred into naïve hosts. ST-OVA and LM-OVA memory CD8$^+$ T cells were purified 71 days post-infection and similar numbers of $OVA_{257-264}$ specific CD8$^+$ T cells were injected into naïve recipients. Seven days later, recipients were challenged with B16-OVA cells (Figure 15).

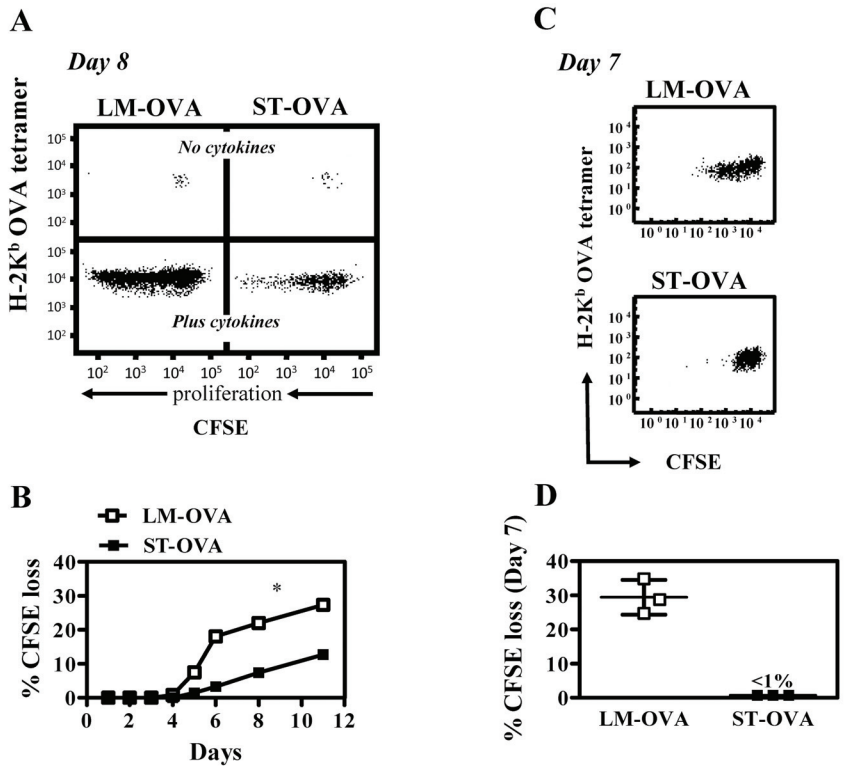

Stark et.al. Cancer Research . May 15;69(10):4327-34. 2009.

FIGURE 13: Homeostatic proliferation of CD8$^+$ T memory cells generated by LM-OVA or ST-OVA infection.

B6129F1 mice were injected with 10^6 OT.1 splenocytes and infected with (i.v.) 10^3 ST-OVA or LM-OVA 7 days later. (A), 125-146 days post-infection spleens were removed and cell suspensions were stained with CFSE. Representative dot plot showing CFSE reduction in CD8$^+$ T cell cultured for 11 days with cytokines. The majority of the cells cultured in the absence of cytokines died within 4 days with < 0.1 % proliferation. Spleens from 10 mice were pooled for each group 125-146 days post-infection and cultured for this representative experiment. (B), Line graph showing kinetics of CFSE reduction in cells cultured with cytokines deduced by periodic flow cytometric analysis of an aliquot of cells. Data are representative of four such separate experiments conducted with both individual and pooled spleen cells obtained from infected mice 66, 84, 125, 125-146 days post-infection. *In vitro* proliferation of LM-OVA CD8$^+$ T cells was significantly different ($P < 0.05$) over time by two-way ANOVA. (C), 91 days post-infection spleens were removed and CD8$^+$ T cells were purified using the Dynabead method and stained with CFSE. 3.2-3.4x10^6 CD8$^+$ T cells were injected i.v. to 3 RAG$^{-/-}$ mice. 7 days later RAG$^{-/-}$ spleens were removed and stained for anti-CD8 and $OVA_{257-264}$-tetramer, and cell divisions were assessed by CFSE loss (mean ± SD). (D), Proliferation is shown for 3 individual mice each receiving either ST-OVA or LM-OVA CD8$^+$ T cells. Based on the analysis of purified CD8$^+$ T cells, 1.52x10^5 antigen-specific cells were transferred per mouse from LM-OVA and 1.33x10^5 antigen-specific cells were transferred from ST-OVA donors.

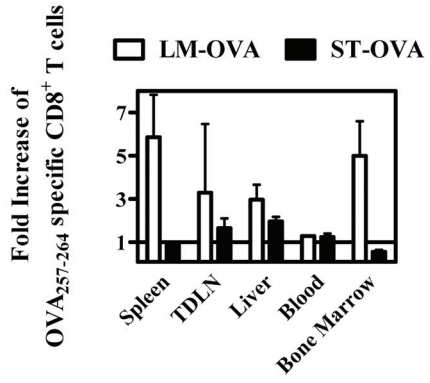

Stark et.al. Cancer Research . May 15;69(10):4327-34. 2009.

FIGURE 14: *In vivo* trafficking of memory CD8$^+$ T cells in B6129F1 mice.
B6129F1 mice were injected with 10^6 OT.1 cells followed by an infection (i.v.) of 10^3 ST-OVA or LM-OVA 7 days later. One hundred sixteen days post-infection, 15 x 10^6 CFSE-labelled CD8$^+$ T cells were purified using the Miltenyi enrichment method and adoptively transferred to naïve B6129F1 mice (mean ± SD, n = 3 per group). Data represent fold-increase in numbers of CFSE-labelled antigen-specific cells in recipients on day 3 of tumour challenge, relative to non-tumour-bearing recipients receiving the same kind of memory cells. TDLN, tumour-draining lymph node.

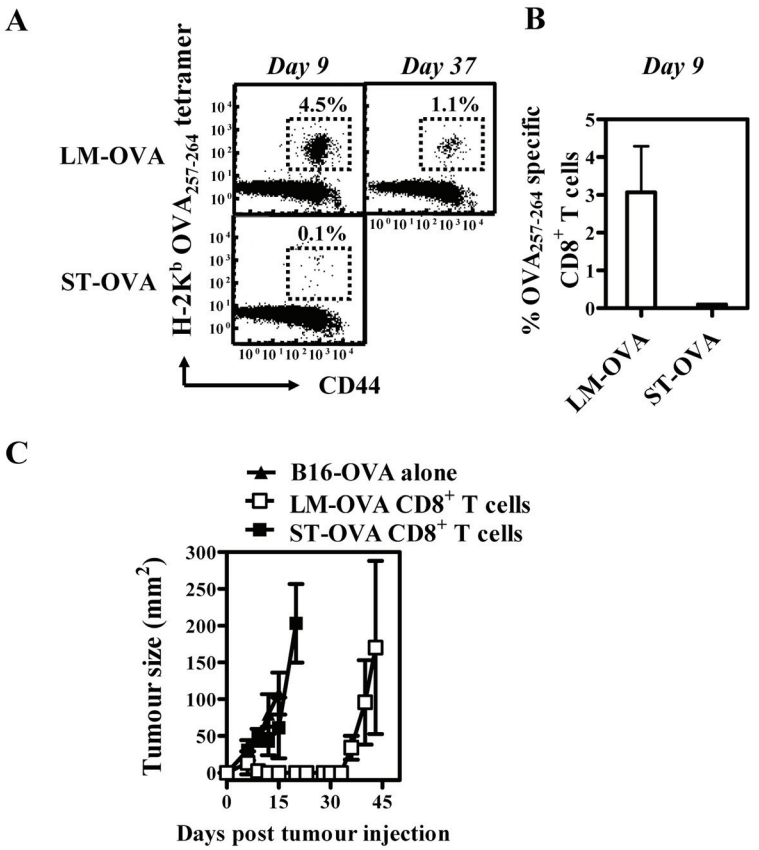

Stark et.al. Cancer Research . May 15;69(10):4327-34. 2009.

FIGURE 15: Therapeutic adoptive transfer of CD8$^+$ T memory cells from LM-OVA and ST-OVA infected mice.

B6129F1 mice were given 10^6 OT.1 splenocytes on day 0 followed by an injection (i.v.) of 10^3 ST-OVA or LM-OVA on day 6. 71 days post-infection spleens were removed and CD8$^+$ T cells were purified with the Miltenyi enrichment method. 3.6 x 10^6 – 4.1 x 10^6 CD8$^+$ T cells were injected i.v. to recipient B6129F1 mice. Based on the analysis of purified CD8$^+$ T cells, this accounted for 1.75 x 10^5 OVA$_{257-264}$ specific CD8$^+$ T cells for LM-OVA and 1.6x10^5 OVA$_{257-264}$ specific CD8$^+$ T cells for ST-OVA. 7 days later, 10^6 B16-OVA tumours were injected (s.c.) into recipient mice. (A), flow cytometric profile of OVA$_{257-264}$ specific CD8$^+$ T cells at day 9 or 37 after adoptive transfer. Note that recipients receiving ST-OVA CD8$^+$ T cells did not survive until 37 days. (B), Bar graph indicating the mean percentage ± SD (n=3 mice per group) of antigen-specific T cells 9 days after adoptive transfer and tumour challenge in recipient mice (C), Solid tumour progression in recipients receiving adoptively transferred CD8$^+$ T cells and tumour challenge. Mean ± SE was indicated for n=3 mice per group.

A significant increase was observed 9 days post-tumour injection only in recipients that received memory $CD8^+$ T cells from LM-OVA–infected mice (Figure 15A and B). Accordingly, mice that received LM-OVA memory cells survived 42 days compared with those given ST-OVA $CD8^+$ T cells that succumbed to tumours by 15 to 18 days. As the adoptively transferred $CD8^+$ T cells harboured no bacteria (confirmed by absence of colonies by plating purified $CD8^+$ T cells), an inherent defect of ST-OVA–generated $CD8^+$ T cells was apparent rather than effects of inflammation or bacterial persistence.

4.1-09 Concluding Remarks:

To conclude, ST-OVA infection in B6129F1 mice generates a protracted $CD8^+$ T cell response with an ultimate T_{EM} phenotype that was inefficient at maintaining an anti-tumour response. This correlated with the lack of homeostatic proliferation, decreased intracellular IL-2 production, and impaired mobility of the ST-OVA $CD8^+$ T cells. Consequently, ST-OVA $CD8^+$ T_{EM} cells were unable to provide long-term tumour protection upon adoptive transfer. In contrast, while the $CD8^+$ T_{CM} cell response generated by LM-OVA infection yielded similar IFN-γ production and cytolytic responses compared to ST-OVA, their increased ability to homeostatically proliferate and expand upon antigen re-exposure combined with superior ability to home to lymphoid compartments correlated with their ability to provide long term protection from tumour. Thus, the phenotypic quality of $CD8^+$ T cells is an important determinant in long-term control of tumour growth.

4.2 Role of functional selectin ligand interactions in the anti-tumour $CD8^+$ T_{CM} response.

CD62L (L-selectin) is an early adhesion molecule present on naïve T cells as well as T_{CM} $CD8^+$ T cells. To further investigate the correlation between $CD62L^{high}$ $CD8^+$ T cells

(T_{CM}) with their enhanced mobility towards lymphoid sites which may bear an implication on their anti-tumour ability as observed in Figure 12, mice deficient for the ligand of CD62L were tested for their ability to generate a T_{CM} memory $CD8^+$ T cell response and respond to tumour. FtDKO mice lack fucosyltransferase IV and VII that are involved in a terminal fucosylation event during post-translational modification events of the sLe^x antigen of many selectin ligands such as PSGL-1, CD34 and MAdCAM-1 [62]. The lack of functional selectin ligands impairs the binding of CD62L (L-selectin) along high endothelial venules and severely compromises T cell trafficking [66,227]. My aim was to determine the kinetics of LM-OVA infection, $CD8^+$ T cell phenotype, functionality and mobility in FtDKO mice and elucidate the importance of selectin ligand interactions to confer long-term tumour protection.

4.2-01 Tumour protection was impaired in LM-OVA vaccinated FtDKO mice

To test the ability of vaccinated FtDKO mice to protect against a tumour challenge, C57BL/6J (wild-type) and FtDKO mice were vaccinated with LM-OVA and challenged with B16-OVA, 21, 93 or 126 days after infection. A significant delay in subcutaneous tumour development was observed in both FtDKO and wild-type vaccinated mice compared to non-vaccinated controls (Figure 16A, B, C). However, all vaccinated FtDKO mice succumbed to subcutaneous tumours significantly quicker relative to vaccinated wild-type group ($p=0.0082$, 0.0015, 0.03 for panels A, B and C respectively). In a metastatic model, mice were challenged i.v. with B16-OVA and were monitored for weight loss. Again, vaccinated wild-type mice were afforded longer survival rates relative to vaccinated FtDKO mice (Figure 16D). In the metastatic challenge model, wild-type mice exhibited an undefined median survival compared to a median survival of 95 days for vaccinated FtDKO mice

(p=0.125). Metastatic tumour burden was confirmed postmortem by confirming presence of black metastatic foci in the lung. In a separate experiment mice were euthanized 15 days after intravenous tumour challenge and lung foci were enumerated. Non-vaccinated Wild-type and FtDKO mice were found to harbour similar number of metastatic foci on day 15 post-tumour challenge (Figure 16E). Furthermore, vaccinated mice (wild-type and FtDKO) did not exhibit visible tumour burden in the lungs at this early time point (Figure 16E) demonstrating a protective effect of vaccination in both mouse strains. Overall, these data indicate that B16-OVA grew subcutaneously and metastatically at a similar pace in non-vaccinated FtDKO and wild-type mice. However, vaccination with LM-OVA afforded longer tumour protection in wild-type mice, whereas FtDKO showed significantly shorter median survival. Furthermore, the deficiency in tumour protection in FtDKO mice was evident when tumour challenge was carried out either early (day 21) or late (day 126) post-vaccination.

4.2-02 LM-OVA induced a $CD8^+$ T cell response in FtDKO mice

The frequency of $OVA_{257-264}$ specific $CD8^+$ T cells responding to LM-OVA vaccination were monitored in the blood over time and found to proliferate and contract at a similar pace in both wild-type and FtDKO mice. Blood was tracked in 3 independent experiments wherein animals were vaccinated with LM-OVA and later challenged with B16-OVA on day 21 (Figure 17A), day 93 (Figure 17B), or day 126 (Figure 17C). The frequency of $OVA_{257-264}$ specific $CD8^+$ T cells in FtDKO mice was significantly greater on day 7 post LM-OVA infection in 2 out of the 3 experiments. Further analysis of seven independent experiments, confirmed a higher frequency of $OVA_{257-264}$ specific $CD8^+$ T cells in FtDKO mice on day 7 post-infection.

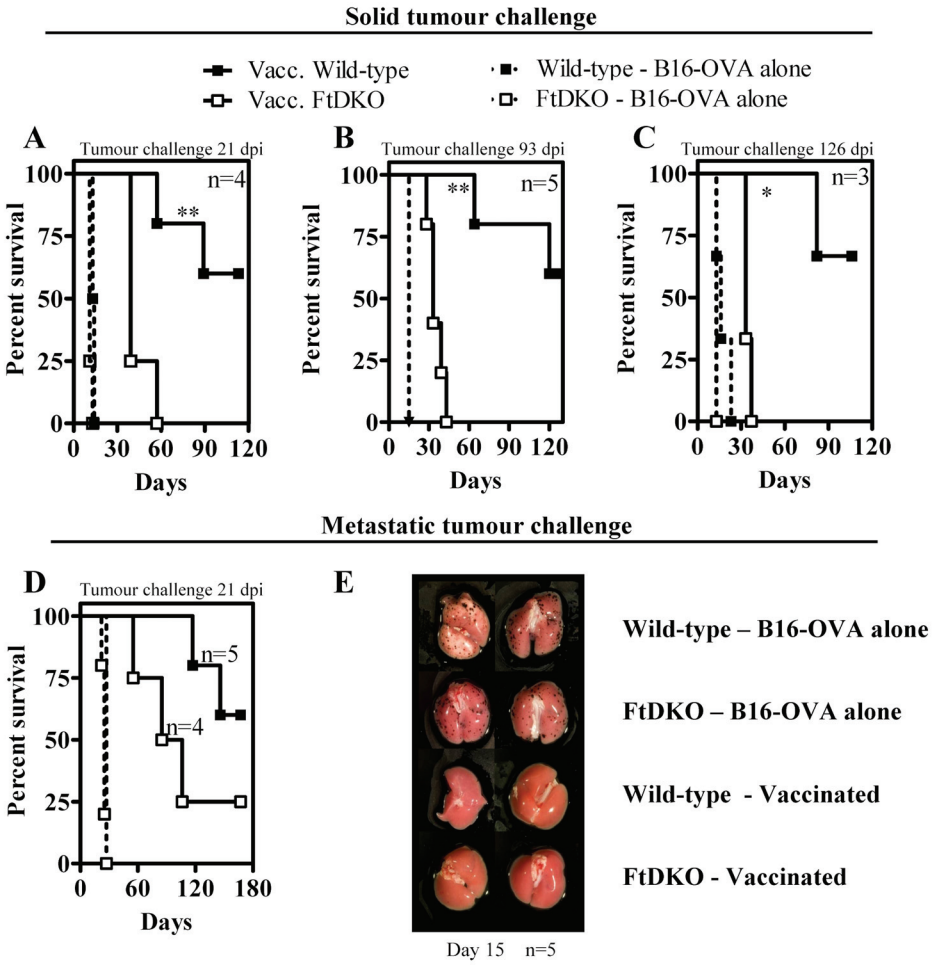

FIGURE 16: Prophylactic vaccination against B16-OVA in FtDKO mice.
C57BL/6J (Wild-type) and FtDKO mice were infected i.v. with 10^4 LM-OVA. Mice were later challenged with 10^6 B16-OVA (s.c.), (A) 21 days, (B) 93 days or (C) 126 days post-infection (dpi). For the survival graphs, mice were euthanized upon reaching a maximum tumour size of 300 mm^2. (D), For the metastatic model, mice were challenged with 5 x 10^5 B16-OVA (i.v.) 21 days post-infection. (E), A separate experiment was carried out whereupon lungs were removed 15 days after tumour challenge and tumour foci visualized. A log rank Mantel Cox survival test was carried out with GraphPad Prism 5.01 software; significant differences were observed in panel A (p=0.0082), panel B (p=0.0015) and panel c (p=0.0347). (Vacc.: Vaccinated with 10^4 LM-OVA prior to tumour)

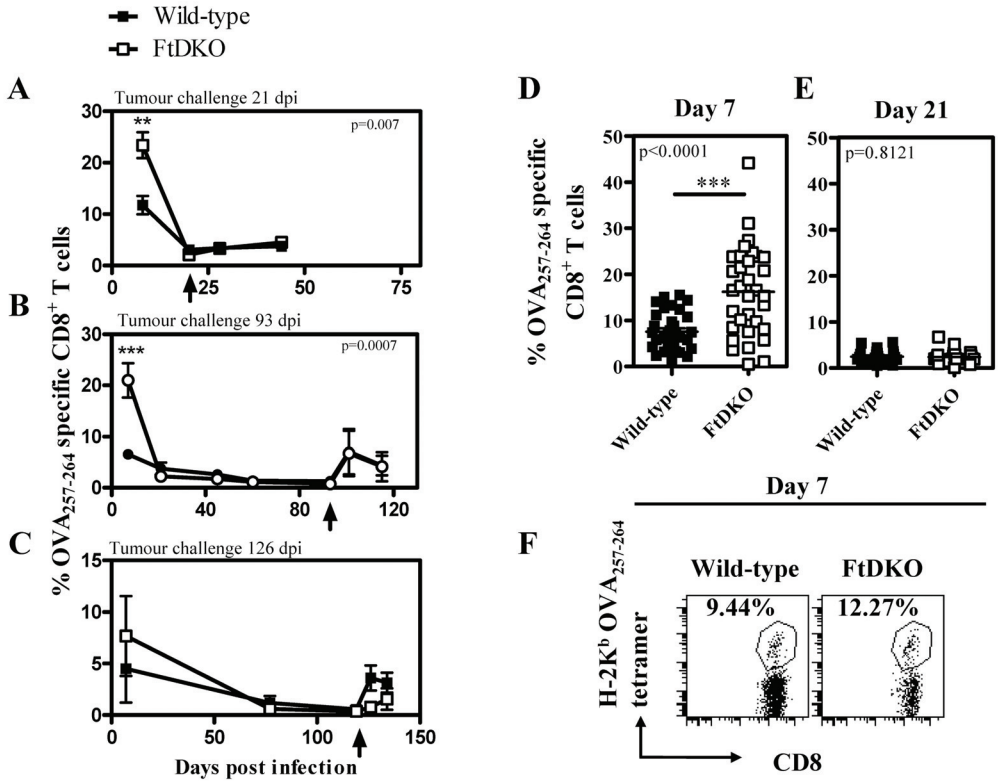

FIGURE 17: Frequency of responding $OVA_{257-264}$ specific $CD8^+$ T cells in the blood of FtDKO mice.

As in Figure 1, Wild-type and FtDKO mice were infected i.v. with 10^4 LM-OVA and challenged s.c. with 10^6 B16-OVA (A) 21 days, (B) 93 or (C) 126 dpi. Blood samples were taken at different time points throughout infection and after tumour, stained for $OVA_{257-264}$ specific $CD8^+$ T cells and plotted as frequency of all $CD8^+$ T cells (mean ± SD). Tumour injection time point is indicated by an arrow. (D&E) The frequency of responding $OVA_{257-264}$ specific $CD8^+$ T cells at day 7 and 21 was pooled from seven independent experiments and, (F) representative flow cytometric dot plots are presented. A two tailed *t*-test was performed with Welch's correction for unequal variance with GraphPad Prism 5.01 software. Fold increase of responding $OVA_{257-264}$ specific $CD8^+$ T cells 7 to 8 days after tumour challenge from 3 pooled experiments with tumour given at 21, 93 or 126 days after infection. There was no correlation between an increased number of responding cells and increased tumour protection.

Notably, the timing of $CD8^+$ T cell contraction was found to be similar as the frequency declined from day 7 to 21 in both wild-type and FtDKO mice (Figure 17E). Additionally, a low steady frequency of $OVA_{257-264}$ specific $CD8^+$ T cells was detectable in the blood (~1 %) up to 119 days post-infection in both wild-type and FtDKO mice (Figure 17B & C). Upon tumour challenge a small but notable expansion of $OVA_{257-264}$ specific $CD8^+$ T cells in the blood 7 or 8 days later was similarly observed for both mice strains. Therefore, upon LM-OVA vaccination, FtDKO mice exhibited a $CD8^+$ T cell response similar in magnitude, kinetics and maintenance to wild-type mice.

4.2-03 LM-OVA induced a similar phenotype of $CD8^+$ T cells in Wild-type and FtDKO mice

Naïve $CD8^+$ T cells have a high level of surface receptor IL-7Rα and CD62L expression. Once activated, $CD8^+$ T cells down-regulate the expression of both IL-7Rα and CD62L. Later on in the memory phase, IL-7Rα is again up-regulated and CD62L expression is variable depending on the type of infection or vaccine [238,239]. Seven days after LM-OVA infection, $CD8^+$ T cells had a similar low level of IL-7Rα and CD62L in both wild-type and FtDKO mice (Figure 18A) indicative of an effector response. In the memory phase, 93 days after infection, the up-regulation of IL-7Rα and CD62L on $OVA_{257-264}$ specific $CD8^+$ T cells occurred similarly in both strains of mice, with an increased expression of both cell surface receptors over time (Figure 18A). Eight days after the introduction of a subcutaneous B16-OVA melanoma, the expression of IL-7Rα and CD62L was down regulated on $OVA_{257-264}$ specific $CD8^+$ T cells indicating a return to a predominant effector phenotype. Furthermore, the proportion of $CD62L^{high}IL\text{-}7R\alpha^{high}$ T_{CM} (Figure 18B), $CD62L^{low}IL\text{-}7R\alpha^{high}$ T_{EM} (Figure 18C) and $CD62L^{low}IL\text{-}7R\alpha^{low}$ effector (Figure 18D) $CD8^+$ T cells was comparable between wild-type and FtDKO at each time point.

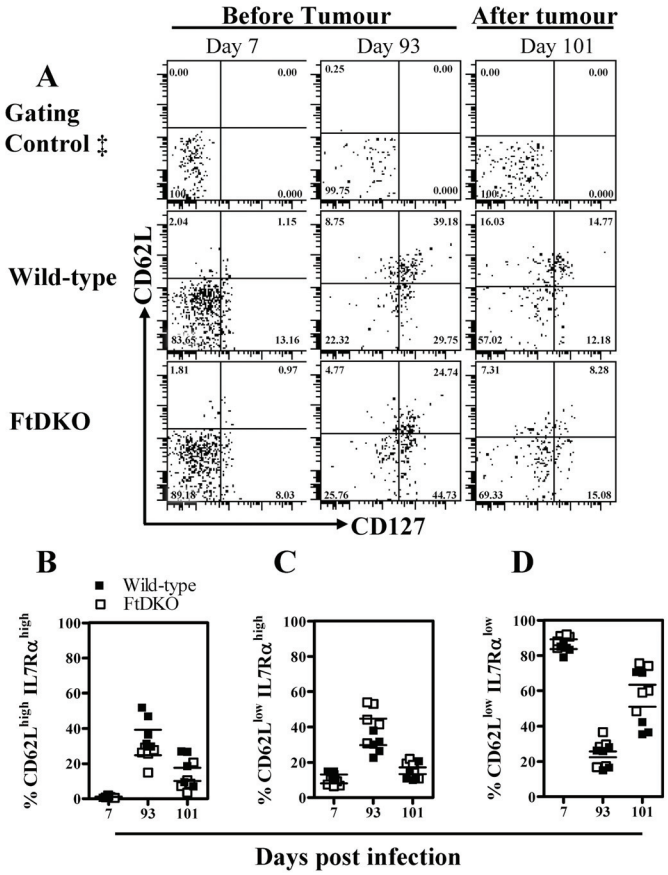

FIGURE 18: Phenotype of responding $OVA_{257-264}$ specific $CD8^+$ T cells in LM-OVA infected FtDKO mice.

The expression of CD62L and IL-7Rα on $OVA_{257-264}$ specific $CD8^+$ T cells is graphed for (A) day 7 and 93 after infection and again 8 days after tumour was introduced (day 101). Inset numbers represent the mean percent of cells in each quadrant ± standard deviation (n=5). Dot plots are representative of n=5 mice per group. ‡Fluorescence minus one (FMO) controls were used to set the gates for IL-7Rα and CD62L. 'Gating control' dotplots do not contain IL-7Rα or CD62L antibody but do contain anti-CD8 and $OVA_{257-264}$ tetramer to best illustrate the gating strategy. Data from individual mice was analyzed and graphed to illustrate the frequency of (B) T_{CM}, (C) T_{EM} and (D) T_E as a percent of all $OVA_{257-264}$ specific $CD8^+$ T cells.

These results indicate that FtDKO mice induce $CD8^+$ T cell responses of similar kinetics and phenotypic proportions as that of wild-type mice during both the effector and memory phases of the immune response.

4.2-04 $CD8^+$ T cells from FtDKO mice are fully functional

FtDKO mice have non functional selectin ligands. Since the expression of selection ligands is induced upon activation of $CD8^+$ T cells [28], I next sought to investigate whether there was any difference in the functionality of $OVA_{257-264}$ specific $CD8^+$ T cells after vaccination. Within 7 days of infection both wild-type and FtDKO mice showed similar cytotoxicity against specific targets *in vivo*, with nearly 100 % of target cells eliminated. Over time, the killing ability of $CD8^+$ T cells waned equally in both strains of mice (Figure 19A). Similarly, the frequency of IFN-γ secreting $CD8^+$ T cells was similar in both strains of mice (Figs. 19B, C & D). Furthermore, the $CD8^+$ T cell frequencies by ELISPOT were similar for both mice strains not only in lymphoid tissue but also liver. Notably, over later time points, lymph node $CD8^+$ T cell frequencies in FtDKO mice could not be ascertained due to lymph node atrophy. Taken together these data indicate that $OVA_{257-264}$ specific $CD8^+$ T cells generated in an FtDKO mouse were equally capable of secreting IFN-γ in response to antigen, and they were functionally capable of killing a substantial amount of adoptively transferred circulating target cells. Therefore, the lack of long-term tumour protection in FtDKO mice cannot be attributed to non-functional $CD8^+$ T cell response.

4.2-05 $CD8^+$ T cells from FtDKO respond to systemic bacterial re-challenge

I next ascertained if LM-OVA infection itself was differentially controlled in FtDKO mice. Bacterial burden was enumerated in the spleen and liver following infection with 10^4 LM-OVA (Figure 20A & B). A diminished splenic bacterial burden was noted in FtDKO

mice relative to wild-type on day 1 post-infection whereas no differences in liver bacterial burden were observed at any time point (Figure 20B). Overall, both strains of mice cleared LM-OVA infection within 5 days. In a separate experiment WT mice were challenged with a lower dose of LM-OVA (10^3 instead of 10^4 CFU) resulting in a lower bacterial burden similar to FtDKO mice 1 day after infection. Twenty-one days after infection they were challenged with B16-OVA; again WT mice were afforded longer lasting protection from tumour compared to FtDKO mice vaccinated with a higher dose (Figure 20C & D).

In order to test the recall ability of $OVA_{257-264}$ specific $CD8^+$ T cells following initial priming with 10^4 LM-OVA, a re-challenge infection of 10^5 LM-OVA was administered 21 days after initial vaccination. As observed above, non-vaccinated FtDKO mice had a significantly decreased splenic bacterial burden compared to WT (Figure 20E) with an infective dose of 10^4 or 10^5 LM-OVA. However, in vaccinated mice, both FtDKO and WT had undetectable splenic LM-OVA burden upon re-challenge indicating a rapid secondary response. Concurrently, the LM-OVA re-challenge caused the rapid expansion of blood resident $OVA_{257-264}$ specific $CD8^+$ T cells in both mouse strains indicative of a strong memory recall response (Figure 20F). Thus, while FtDKO mice exhibited diminished protection against tumour challenge, their $CD8^+$ T cell response was effective against infection re-challenge.

4.2-06 DC Antigen presentation is similar in LM-OVA infected Wild-type and FtDKO mice

Next, to investigate any potential defect in antigen presentation, I measured the ability of splenic DCs to present OVA antigen to OT.1 derived $CD8^+$ T cells *ex vivo*. Successful DC presentation of OVA peptide (SIINFEKL) to $CD8^+$ T cells was measured by robust $CD8^+$ T cell proliferation and a significant down-regulation of CD62L.

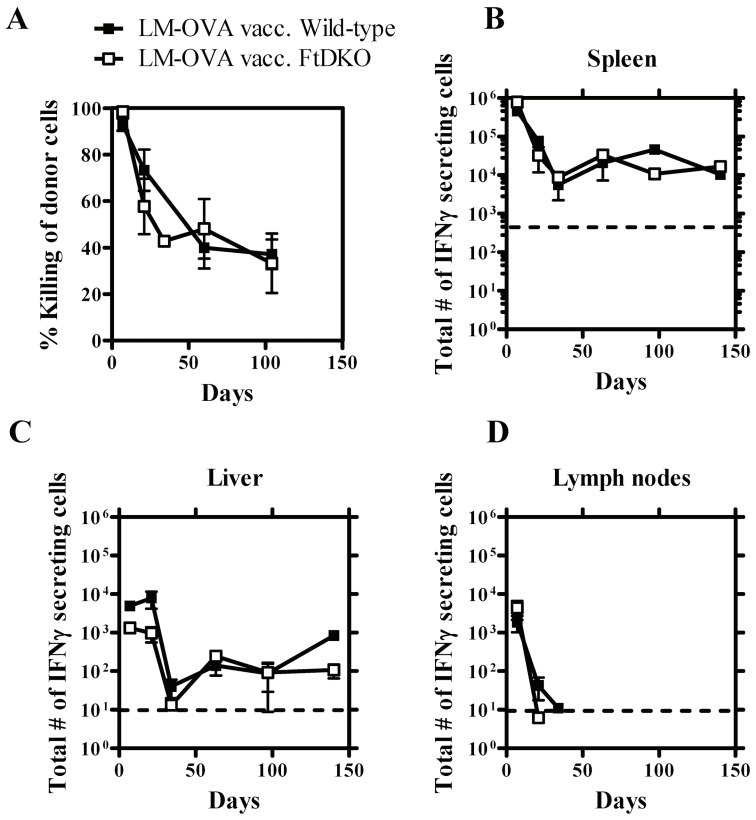

FIGURE 19: FtDKO $OVA_{257-264}$ specific $CD8^+$ T cells are cytolytic.
Wild-type and FtDKO mice were infected i.v. with 10^4 LM-OVA and at different time points after infection the *in vivo* cytolytic potential of responding $OVA_{257-264}$ specific $CD8^+$ T cells was determined (mean ± SE) (A). 2 mice were used for each group at each time point. No significant differences were observed between each group over time. An IFN-γ ELISPOT assay was performed on samples of (B) Spleen, (C) Liver and (D) Lymph nodes at different time points after infection. Two mice were used for each group at each time point and this experiment was repeated twice with similar results.

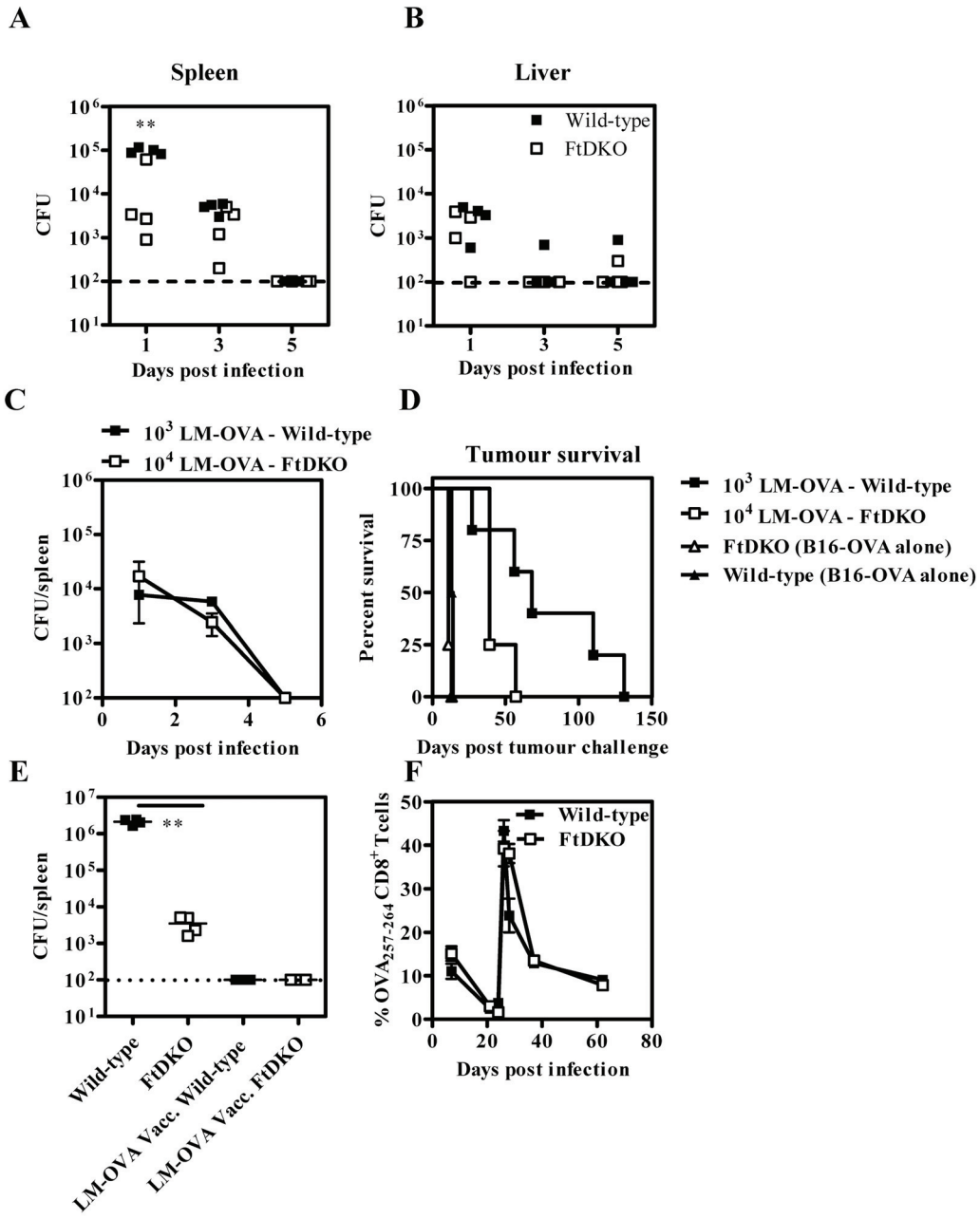

FIGURE 20: LM-OVA clearance and CD8$^+$ T cell response to re-challenge.
Bacterial burden in the (A) spleen, and (B) liver of individual mice on different days post-infection (n=4/time point/group) following 10^4 LM-OVA infection (i.v.). **, P=0.0029 by two-tailed *t* test with Welch's correction for unequal variance. C57BL/6J and FtDKO mice were immunized (i.v.) with 10^3 or 10^4 LM-OVA respectively. (C), Spleens were removed on day 1, 3, or 5 after infection and diluted to determine bacterial burden, (mean ± SE, n=3-4 mice). (D), In a separate study mice were challenged with 10^6 B16-OVA and survival was

monitored. Data is compiled from two such separate studies involving Wild-type or FtDKO mice. Median survival of vaccinated Wild-type mice was 68 days, and for FtDKO mice, 39 days, n=4-5 mice per group. (E & F), In another experiment, mice vaccinated with 10^4 LM-OVA were re-challenged 21 days later with 10^5 LM-OVA. Splenic bacterial burden on day 3 following 10^5 LM-OVA infection (E), n=4/group. **, P=0.0013 relative to Wild-type by two tailed *t*-test with Welch's correction for unequal variance. The frequency of blood $OVA_{257-264}$ specific $CD8^+$ T cells was determined (F) following primary exposure to 10^4 LM-OVA and re-challenge on day 21 with 10^5 LM-OVA (mean ± SE, n=3/group).

FtDKO spleens were notably enlarged compared to wild-type mice (Figure 21), likely due to the increase in circulating monocytes previously reported [66,227]. To determine any defects in antigen presentation of FtDKO mice following LM-OVA infection, splenic DCs were purified from LM-OVA infected mice 1 day after infection. DCs were co-cultured with CFSE stained $OVA_{257-264}$ specific $CD8^+$ T cells and T cell proliferation was measured by CFSE loss using flow cytometry. DCs from LM infected mice served as negative controls and OVA peptide (SIINFEKL) pulsed DCs served as positive controls. Both DCs from FtDKO and wild-type mice were capable of inducing $CD8^+$ T cell proliferation similar to positive control (Figure 22) indicating a comparable level of $OVA_{257-264}$ antigen presented by FtDKO to wild-type control. These results suggest that there was no intrinsic defect in the antigen-presentation capacity of DCs from FtDKO mice.

4.2-07 FtDKO and Wild-type $CD8^+$ T cells had a similar proliferative potential

The superior ability of T_{CM} cells to contain tumour growth is attributed to their proliferative ability. Hence I sought to determine whether $CD8^+$ T memory cells from FtDKO mice have a reduced ability to rapidly proliferate in response to antigen. Splenic cultures from vaccinated mice stimulated *in vitro* with LM-OVA and cytokines, and analyzed 4, 6 and 12 days later exhibited a steady expansion of antigen-specific $CD8^+$ T cells over time (Figure 23). Moreover, in two out of three experiments, a greater number of antigen-specific $CD8^+$ T cells were noted for FtDKO cells relative to wild-type cultures. Overall, the number of $OVA_{257-264}$ specific $CD8^+$ T cells increased in both groups. Thus, the lack of selectin ligands on $CD8^+$ T cells did not impair their antigen-dependant proliferation.

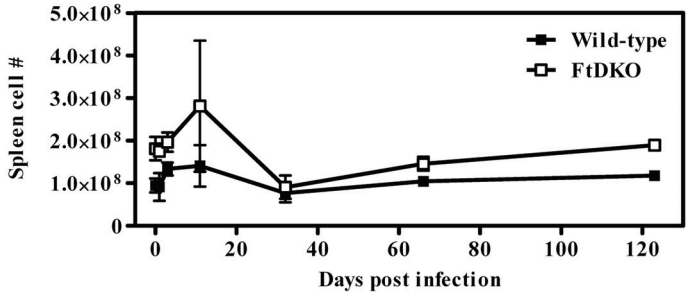

FIGURE 21: Splenomegaly of FtDKO mice.
Wild-type and FtDKO mice were infected with 10^4 LM-OVA. Spleens were isolated at varying time points after immunization and the number of lymphocytes enumerated by microscopy with trypan exclusion. Mean ± SD, n=2-4/group/time-point.

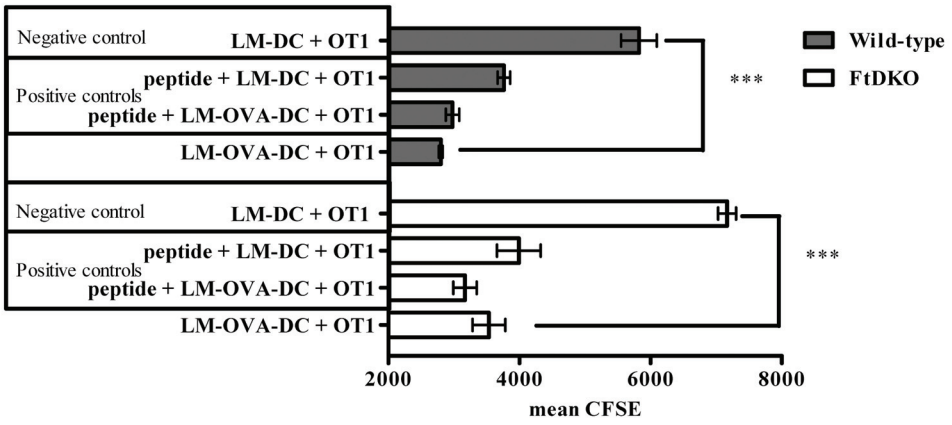

FIGURE 22: Antigen presentation by FtDKO DCs.
Mean ± SD of triplicate cultures of CFSE reduction correlates to proliferation of OT.1 $CD8^+$ T cells in response to DCs from LM or LM-OVA infected mice. DCs were purified using the STEMCELL method and co-cultured at a ratio of 3:1 (3×10^5 DCs and 1×10^5 OT.1 cells/well). Positive controls were pulsed with $OVA_{257-264}$ peptide *in vitro*. Data were significantly different, *** ($p<0.0001$), relative to negative control (LM infected DCs) by two tailed *t* test with Welch's correction for unequal variance. Data are representative of 2 independent DC isolation experiments.

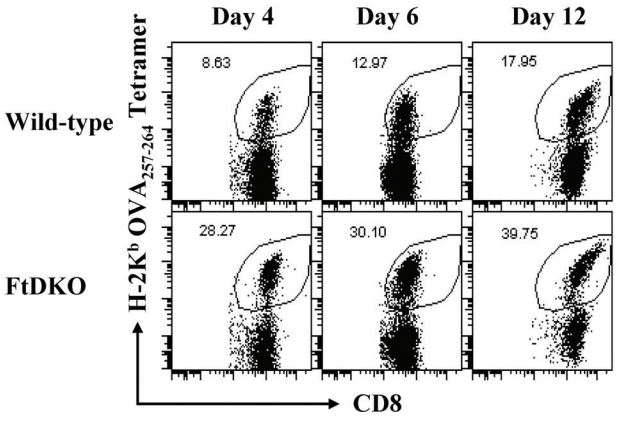

FIGURE 23: *In vitro* proliferation of FtDKO CD8$^+$ T cells.
Wild-type and FtDKO mice were primed and boosted (34 to 76) with 10^4 and 10^5 LM-OVA, respectively. 7 days after boosting, spleens were harvested and processed for cell culture. Initial FACS analysis reveals $OVA_{257-264}$ specific $CD8^+$ T cell frequency at 2-3 %. Representative flow cytometric profile indicating *in vitro* antigen-dependent proliferation of $OVA_{257-264}$ specific $CD8^+$ T cells on different days of *in vitro* culture is shown. Inset numbers represent percentage of gated cells. Data are representative of three independent experiments conducted.

4.2-08 $CD8^+$ T cell infiltration into FtDKO draining lymph nodes and tumours was impaired

Since FtDKO mice displayed normal antigen-presentation, $CD8^+$ T cell expansion, contraction and function, I next analyzed their tumour infiltrative properties upon adoptive transfer. $CD8^+$ T cells were expanded *in vitro* from vaccinated mice, and adoptively transferred into non-tumour and tumour bearing recipients (Figure 24A). Firstly, significantly greater numbers of $OVA_{257-264}$ specific $CD8^+$ T cells infiltrated the lymph nodes of wild-type compared to FtDKO recipients (Figure 24B & C). This trend was noted for both non-tumour (Figure 24B) and tumour bearing (Figure 24C) recipients and for wild-type or FtDKO donor cells. In contrast FtDKO recipients harboured more donor cells (wild-type or FtDKO) in the spleen (Figure 24D). In wild-type recipients, FtDKO and wild-type donor cells migrated to the lymph node and spleen at similar levels (Figure 24B, C & D). Therefore, the FtDKO host environment appeared to skew the trafficking of donor cells away from the peripheral lymphoid compartment. Furthermore, significantly lower numbers of FtDKO donor cells were recovered from the tumour tissue of both wild-type and FtDKO recipients (Figure 24E). However, high numbers of donor wild-type cells were found in tumours of both wild-type and FtDKO hosts. Taken together, these results indicate a defect in homing of antigen specific $CD8^+$ T cells (wild-type or FtDKO) to the lymph nodes of FtDKO recipient mice and compromised migration of FtDKO deficient $CD8^+$ T cells into the subcutaneous tumour.

4.2-09 Transferred FtDKO effector $CD8^+$ T cells mediated long term tumour protection

Effector $CD8^+$ T cells were generated *in vivo* and stimulated *in vitro* as described above and delivered to naïve FtDKO and wild-type hosts at the same time as tumour introduction.

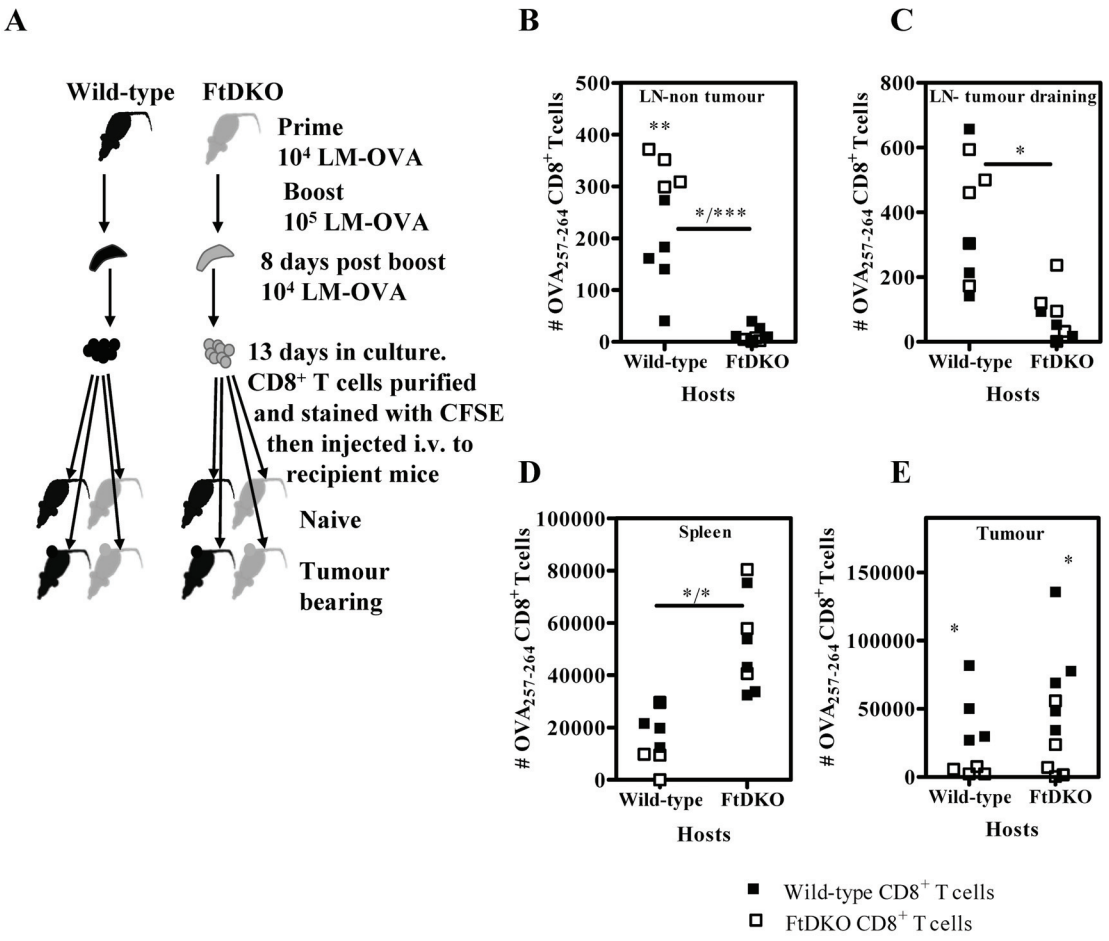

FIGURE 24: Adoptive transfer and tracking of Effector CD8$^+$ T cells.
An adoptive transfer experiment was carried as indicated in the schematic diagram (A). 2.5-5 X 10^6 $OVA_{257-264}$ specific CD8$^+$ T cells were transferred i.v. into naïve or tumour bearing (9 days post tumour injection) recipient mice. Donor cells in the various organs of recipients were enumerated 4-5 days later. Mean ± SD (n=4/group) of $OVA_{257-264}$-specific CD8$^+$ T cells recovered from (B) non-tumour bearing mouse lymph nodes, (C) tumour bearing mouse lymph nodes, (D) tumour bearing mouse spleen and (E) tumour of recipient Wild-type or FtDKO mice. (B), **, Wild-type cells in FtDKO compared to Wild-type hosts, p=0.0022; ***, FtDKO cells in FtDKO compared to Wild-type hosts, p<0.0001. (C), *, Wild-type cells in different hosts, p=0.048; **, FtDKO cells in different hosts, p=0.007. (D), *, Wild-type cells in different hosts, p=0.027; * FtDKO cells in different hosts, p=0.011. (E), **, Wild-type cells vs. FtDKO cells in Wild-type hosts, p=0.004; *, FtDKO versus Wild-type cells in FtDKO hosts, p=0.018. Data were analyzed by unpaired *t* test.

Surprisingly, effector FtDKO $CD8^+$ T cells were able to provide similar or longer lasting tumour protection in both wild-type and FtDKO mice respectively (Figure 25A-E). Importantly, this observation correlates with the finding that the cytolytic capacity of FtDKO $CD8^+$ T cells was not impaired. In contrast, direct vaccination of FtDKO mice resulted in weakened long-term tumour protection (Figure 16A-D). Thus, it appears that while endogenous memory $OVA_{257-264}$ specific $CD8^+$ T cells were not as adept at long term tumour protection, a large number (1×10^6 $OVA_{257-264}$ specific $CD8^+$ T cells) of activated effector $CD8^+$ T cells can circumvent the need to home via lymph nodes and mediate direct tumour protection.

4.2-10 Concluding Remarks

The absence of selectin ligands abrogates long term tumour protection afforded by LM-OVA vaccination. Upon further investigation it was determined that antigen presentation and $CD8^+$ T cell activation was not impaired in response to the intravenous LM-OVA infection in FtDKO mice. Additionally the proliferation of FtDKO $CD8^+$ T cells in response to antigen was similar or greater than wild-type control. Strikingly, the migration of anti-tumour FtDKO $CD8^+$ T cells into peripheral lymph nodes was reduced. Additionally, the absence of selectin ligands on $CD8^+$ T cells impaired migration towards subcutaneous tumour sites. In contrast, the migration of $OVA_{257-264}$ specific $CD8^+$ T cells into the spleen of FtDKO hosts was enhanced compared to wild-type. This may be due to the observation of increased numbers of circulating monocytes and lymphocytes observed in FtDKO mice, which may be attributable to hypotrophic lymph nodes. Finally, the absence of selectin ligands in lymphoid compartments appeared to impair $CD8^+$ T cell entry and/or retention to the tumour site.

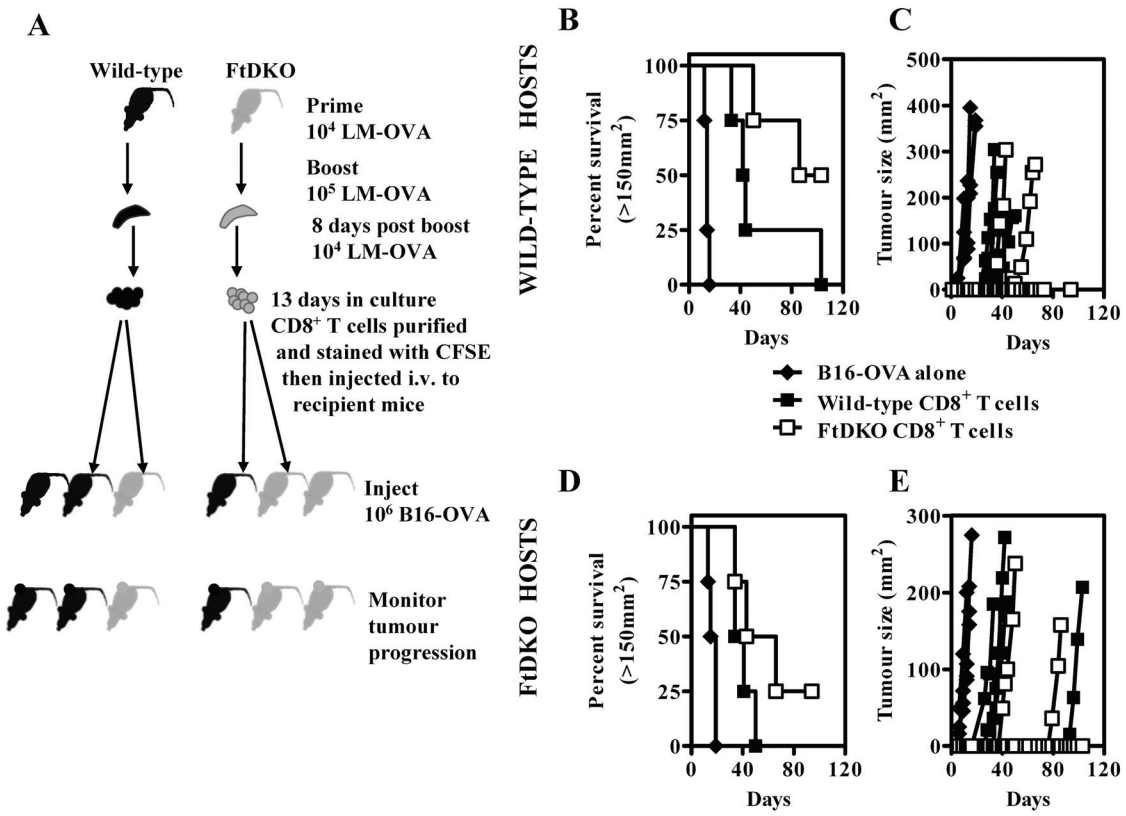

FIGURE 25: Adoptive transfer and of Effector $CD8^+$ T cells and tumour progression. $CD8^+$ T cells were generated, cultured and purified as described in Figure 24. FACS analysis revealed that 1 X 10^6 $OVA_{257-264}$ specific $CD8^+$ T cells were transferred into recipient mice. 10^6 B16-OVA tumour cells were injected s.c. the same day as $CD8^+$ T cells were injected i.v. (A), A schematic diagram is provided to describe the derivation of $CD8^+$ T cells and their transfer into naïve hosts. (B), % survival was monitored in Wild-type hosts as was (C) tumour progression in individual mice. (D), % survival was monitored in FtDKO hosts as was (E) tumour progression in individual mice.

Overall, the presence of selectin ligands on the host endothelium and $CD8^+$ T cells appeared to be important for long-term tumour protection in the murine melanoma model.

4.3 Archaeosomes as a model for understanding the properties of anti-tumour $CD8^+$ T cells

While live vectors such as LM-OVA and ST-OVA can deliver tumour antigen to the MHC-class I processing machinery for the induction of anti-tumour $CD8^+$ T cell responses, there are limitations for the use of live vectors in humans. One such limitation is the activation of host response against the vector which limits further boosting with the same vector which is normally required to break host tolerance to self tumour antigens. Use of heterogenous live vectors for priming and boosting may overcome the problem; however, there remains a risk of reversion to virulence for live pathogens making it less desirable for human use. Archaeosomes are liposomes made up of TPL derived from Archaea which can serve as vehicles for the delivery of antigens to MHC-class I processing machinery leading to activation of $CD8^+$ T cells [203]. The uniqueness of this liposome lies within the lipid structure that provides greater stability and elicits no known anti-lipid immune response. Thus, archaeosomes are a convenient model vaccine-delivery-vehicle to determine the quantitative threshold of $CD8^+$ T cell immunity required for prophylactic and therapeutic tumour protection.

4.3-01 Vaccination with OVA-Archaeosomes provided long lasting tumour protection

In a preliminary experiment, confirming previous observations on the adjuvant ability of archaeosomes, I compared the efficacy of OVA antigen delivery by 3 types of archaeosomes derived from TPL of *Methanobrevibacter smithii* (MS), *Halobacterium salinarum* (HS) *or Halococcus morrheae* (HM). The efficacy of these liposomes to generate

an $OVA_{257-264}$ specific $CD8^+$ T cell response was evaluated and followed by a subcutaneous B16-OVA tumour challenge given 42 days post vaccination (Figure 26A, B). Mice vaccinated with MS-OVA showed an expansion of the $OVA_{257-264}$ specific $CD8^+$ T cells upon tumour challenge unlike mice vaccinated with HS-OVA or HM-OVA (Fig 26A). Nevertheless, all vaccinated groups exhibited detectable levels of $OVA_{257-264}$ specific $CD8^+$ T cells. Despite the disparate boost of responding $OVA_{257-264}$ specific $CD8^+$ T cells, all vaccinated groups were protected from a subcutaneous tumour challenge relative to non-vaccinated controls (Figure 26B). This suggests that the threshold of the memory $CD8^+$ T cell response maintained after vaccination with all three OVA-archaeosomes was sufficient to afford prophylactic tumour protection.

4.3-02 MS-OVA therapy induced OVA-$CD8^+$ T cells and modest tumour protection

The infiltration of a large number of $OVA_{257-264}$ specific $CD8^+$ T cells into tumour sites has been correlated with an improved outcome in colorectal, epithelial, ovarian and metastatic tumours [10,240,215]. As MS-OVA vaccination afforded detectable expansion of the $CD8^+$ T cell response, it was deemed the most promising archaeosome candidate and was utilized to evaluate therapeutic tumour protection. MS-OVA, comprising a low dose of antigen (20 μg), was used to vaccinate (s.c.) mice on days 4, 8 and 18 after tumour challenge. Non-vaccinated control mice succumbed to tumour burden within 10 days, whereas therapeutic MS-OVA vaccination extended survival to 31 days (Figure 27A). Vaccination initiated a strong $CD8^+$ T cell response and tumour growth was suppressed to an undetectable size. However, tumour growth resumed at later time-points despite the maintenance of a large number of $OVA_{257-264}$ specific $CD8^+$ T cells (Figure 27B).

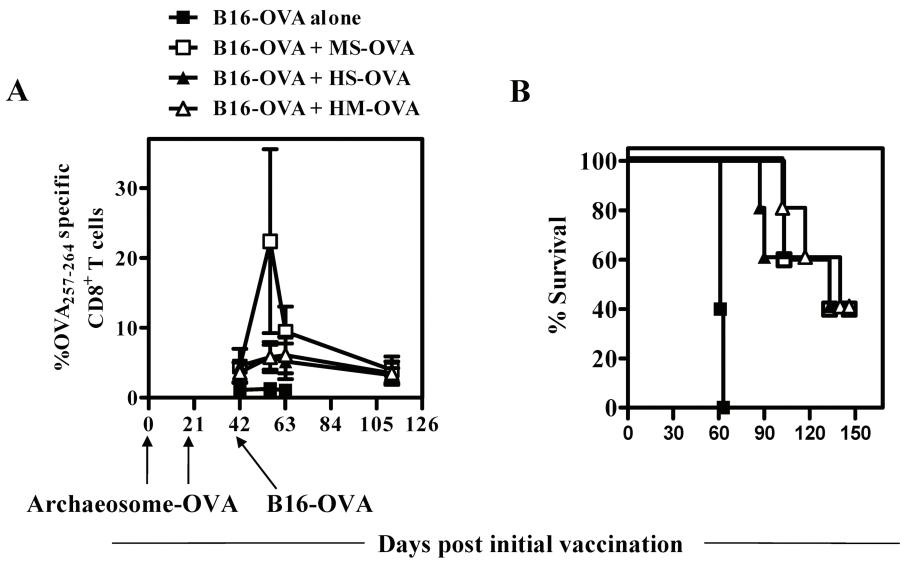

FIGURE 26: Prophylactic protection against B16-OVA by OVA-archaeosomes.
C57BL/6J mice were vaccinated on day 0 and 21 with MS-OVA, HS-OVA or HM-OVA. Subsequently, all mice were challenged (s.c.) with 10^6 B16-OVA. (A), The frequency of $OVA_{257-264}$ specific $CD8^+$ T cells was measured in the blood over time and (B) survival was measured over time (n=5/group). While all vaccinated mice significantly delayed the onset of tumour compared to control (Log Rank Mantel Cox test: p=0.005) no statistically significant differences between vaccinated groups were observed (p=0.9577).

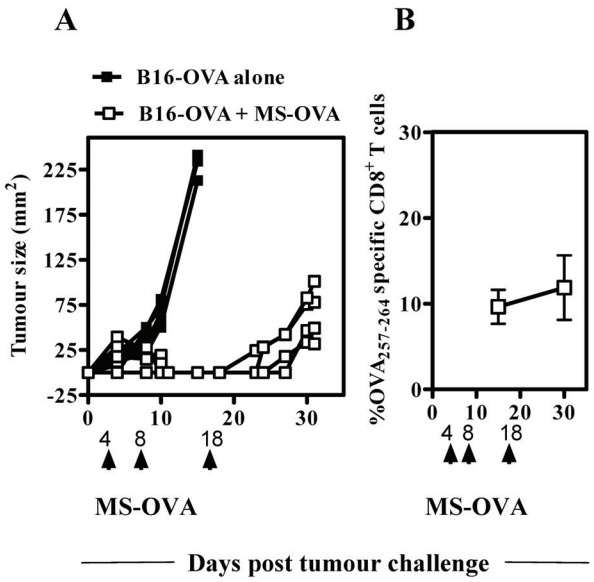

FIGURE 27: Therapeutic treatment of subcutaneous B16-OVA with MS-OVA.
C57BL/6J mice were challenged (s.c.) with 10^6 B16-OVA. 4, 8 and 18 days after tumour challenge, MS-OVA was injected (s.c.) 1-2 cm away from tumour site. (A), Tumour growth in individual mice is shown for vaccinated mice and non-vaccinated mice. (B), The mean frequency ± SD of $OVA_{257-264}$ specific $CD8^+$ T cells is shown at two time points for vaccinated mice (n=4/group).

B16-OVA tumours grow aggressively; a dose of 10^6 tumour cells is sufficient to ensure all mice succumb to tumour burden with a median survival of 10-12 days. In order to lengthen the window of opportunity for therapeutic treatment, the growth rates of lower doses of B16-OVA (10^5 and 10^4) in non-vaccinated mice was evaluated (Figure 28). The injection of 10^4 B16-OVA tumours provided a long window to therapeutically treat mice; however, the dose was not substantial enough to ensure tumour growth in all control mice. A dose of 10^5 B16-OVA cells provided a median survival of 20 days; thus lengthening the window of opportunity for therapeutic treatments by ~8 days. In a subsequent experiment with 10^5 B16-OVA tumour cells injected, mice were treated with MS-OVA 3 days later; 3 of the 5 mice were given extra doses of MS-OVA at day 10 and 29. While MS-OVA treatment afforded a longer window of tumour protection compared to control, a second and third injection did not provide significant additional protection (Figure 29A) even though the frequency of $OVA_{257-264}$ specific $CD8^+$ T cells increased in the blood (Figure 29B). Many current vaccination strategies, aimed at inducing $CD8^+$ T cell responses to intracellular infections or cancer, have the primary goal of generating a large amount of tumour reactive $CD8^+$ T cells. On the contrary, my data suggested that increasing numbers of circulating $OVA_{257-264}$ specific $CD8^+$ T cells alone was insufficient for long lasting tumour protection.

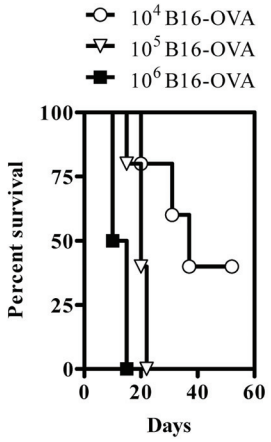

FIGURE 28: Optimization of B16-OVA cell number for tumour challenge studies. C57BL/6J mice were challenged (s.c.) in the dorsal flank with 10^6, 10^5, or 10^4 B16-OVA. Tumour burden was monitored over time.

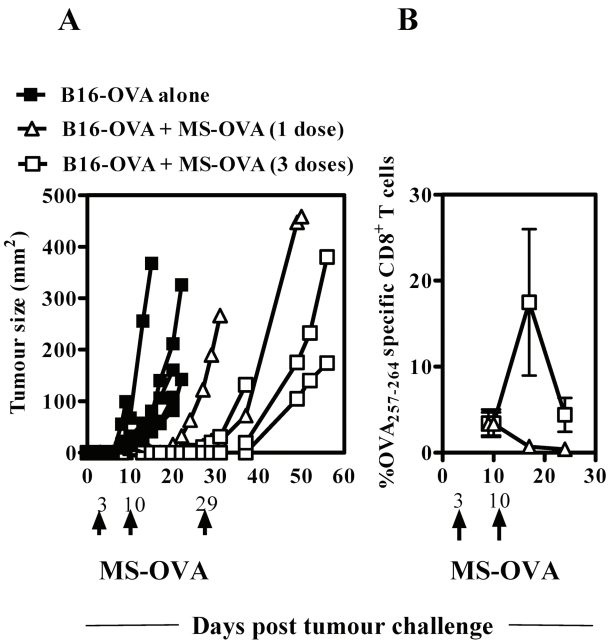

FIGURE 29: Optimizing MS-OVA boosting regimen in tumour immunotherapy. C57BL/6J mice were challenged (s.c.) with 10^5 B16-OVA. 3, 10 and 29 days after tumour injection, MS-OVA treatment was administered s.c. (A), Tumour growth in individual mice is shown for non-vaccinated, singly vaccinated (day 3 only) and thrice vaccinated mice. (B), The frequency of $OVA_{257-264}$ specific $CD8^+$ T cells is shown at 3 time points after tumour (mean ± SD, n=2-3/group). No significant difference in survival was observed between mice vaccinated once or three times with MS-OVA (Log-rank Mantel-Cox Test p=0.2072).

4.3-03 MS-OVA treatment affords therapeutic protection against B16-OVA tumour following adoptive transfer of OT.1 cells

After MS-OVA vaccination, the endogenous levels of $OVA_{257-264}$ specific $CD8^+$ T cells are low; this makes it difficult to track the phenotype of subpopulations over time. Therefore, I increased the pool of $OVA_{257-264}$ specific $CD8^+$ T cells by adoptively transferring splenocytes from an OT.1 mouse in which >95 % of the $CD8^+$ T cells are specific for the OVA epitope SIINFEKL. B16-OVA is considered an immunogenic tumour and many melanoma $CD8^+$ T cell epitopes have been identified resulting in endogenous activation of $CD8^+$ T cells [241]. Therefore, it was possible that OVA tumour antigen of B16-OVA could activate transferred OT.1 $OVA_{257-264}$ specific $CD8^+$ T cells even in non-vaccinated mice. Hence, I first measured the rate of OT.1 $CD8^+$ T cell activation in the absence of vaccination. Mice were injected with a large number of B16-OVA cells (10^6) and 3 days after tumour challenge, 10^4, 10^5 or 10^6 OT.1 splenocytes were transferred (i.v.) and the frequency of $OVA_{257-264}$ specific $CD8^+$ T cells was monitored over time (Figure 30A). The overall frequency of $OVA_{257-264}$ specific $CD8^+$ T cells was low (0.1 % - 0.6 %) in all tested doses, and no significant increase occurred over time. Importantly there were no differences in B16-OVA tumour growth patterns in mice adoptively transferred with OT.1 cells (Figure 30B). Since OT.1 $CD8^+$ T cells were not activated by the presence of tumour, in subsequent experiments OT.1 cells were transferred prior to tumour challenge for convenience and a non-vaccinated OT.1 parked control was included in each experiment. In the next experiment, OT.1 parked tumour bearing mice were therapeutically treated with MS-OVA, 3 and 8 days after tumour challenge. Similar to previous results, MS-OVA conferred protection from tumour growth with a median survival of 37 days compared to non-vaccinated controls that had a median survival of 13 days (Figure 31A).

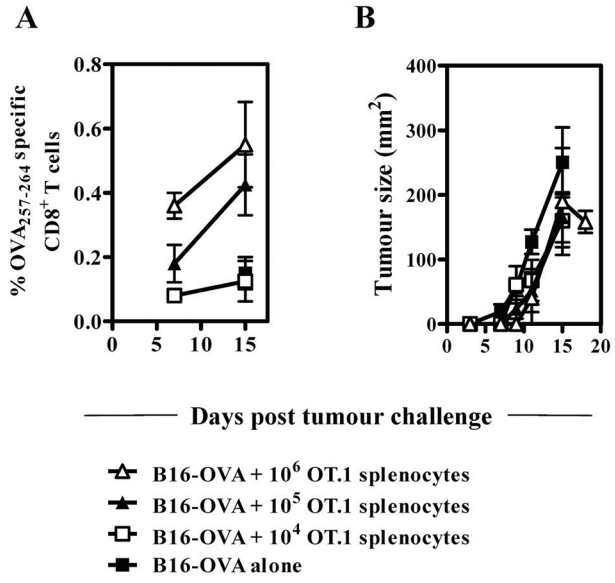

FIGURE 30: OT.1 cell transfer and tumour challenge.
C57BL/6J mice were challenged s.c. with 10^6 B16-OVA. 3 days later 10^4, 10^5 or 10^6 OT.1 splenocytes are injected i.v. (A) Blood samples are taken to monitor $OVA_{257-264}$ specific $CD8^+$ T cells. (B) Tumour size was monitored over time. (Mean ± SE, n=5/group).

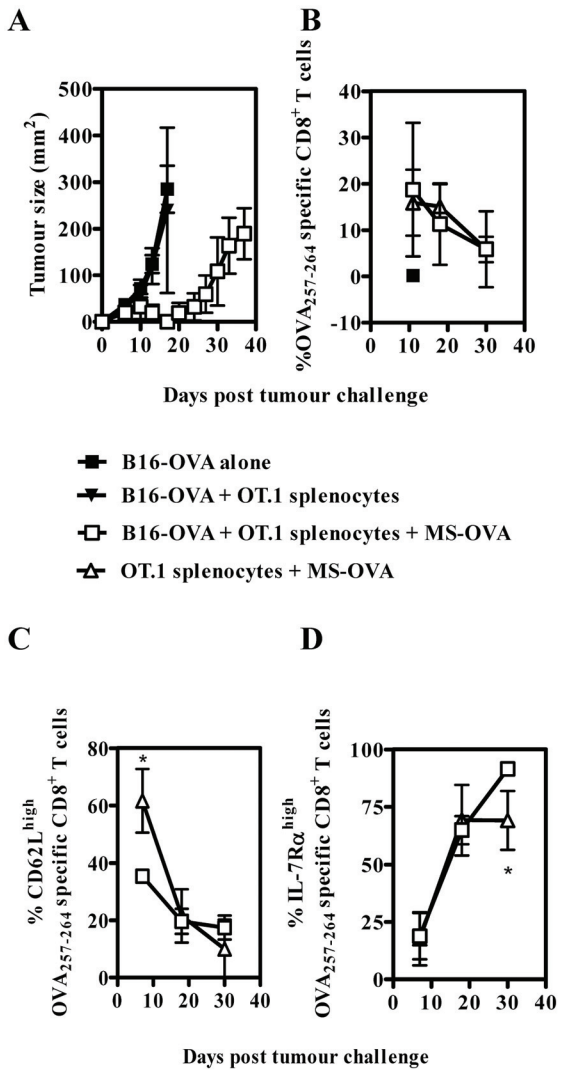

FIGURE 31: Phenotype of responding $OVA_{257-264}$ specific $CD8^+$ T cells following tumour challenge.

C57BL/6J mice were first injected i.v. with 10^6 OT.1 splenocytes. 7 days later, 10^6 B16-OVA tumour cells were injected s.c. in the dorsal flank. 3 and 8 days after tumour injection, MS-OVA was injected s.c. on the dorsal flank (away from tumour site). (A) Tumour progression was monitored. (B), The frequency of $OVA_{257-264}$ specific $CD8^+$ T cells was measured in the blood and the % expression of (C) CD62L and (D) IL-7Rα was determined. Mean ± SD, n=5/group. Two-tailed *t*-test with Welch's correction for unequal variance. (C) *, p=0.02, (D) *, p=0.04.

The presence of tumour did not alter the frequency of responding $OVA_{257-264}$ specific $CD8^+$ T cells compared to a non-tumour bearing vaccinated mouse (Figure 31B). However, CD62L expression on $CD8^+$ T cells in tumour bearing mice was lower compared to non-tumour bearing mice; yet at later time-points, a similar level of expression of this marker was observed in both tumour and non-tumour bearing mice (Figure 31C). IL-7Rα expression on $OVA_{257-264}$ specific $CD8^+$ T cells was slightly higher in tumour bearing mice by day 30, but may be a result of IL-7Rα^{low} $CD8^+$ T cells trafficking to the tumour site to exert effector functions.

4.3-04 LM-OVA treatment activates a profound $CD8^+$ T cell response and provides long-lasting protection against B16-OVA tumours

In order to fully assess the tumour protective $CD8^+$ T cell response of the particulate vaccine, MS-OVA, I next chose to compare it to the well-characterized live vaccine LM-OVA. Therapeutic LM-OVA treatment afforded much longer survival times compared to MS-OVA treatment. Notably, LM-OVA treated mice survive past 60 days with an undefined median survival significantly longer than MS-OVA treated mice (Figure 32E). The frequency of responding $OVA_{257-264}$ specific $CD8^+$ T cells was initially similar between non-tumour and tumour challenged mice; however later on, when tumour was returned, the frequency increased significantly compared to non-tumour challenged mice (Figure 32B). With MS-OVA treatment, the contraction of $OVA_{257-264}$ specific $CD8^+$ T cells was notably protracted compared to the quick contraction observed with LM-OVA vaccination. The early contraction of $OVA_{257-264}$ specific $CD8^+$ T cells observed in LM-OVA vaccinated mice was met with a steeper rise in CD62L expression (Figure 32C) but similar IL-7Rα expression (Figure 32D) indicative of T_{CM} formation.

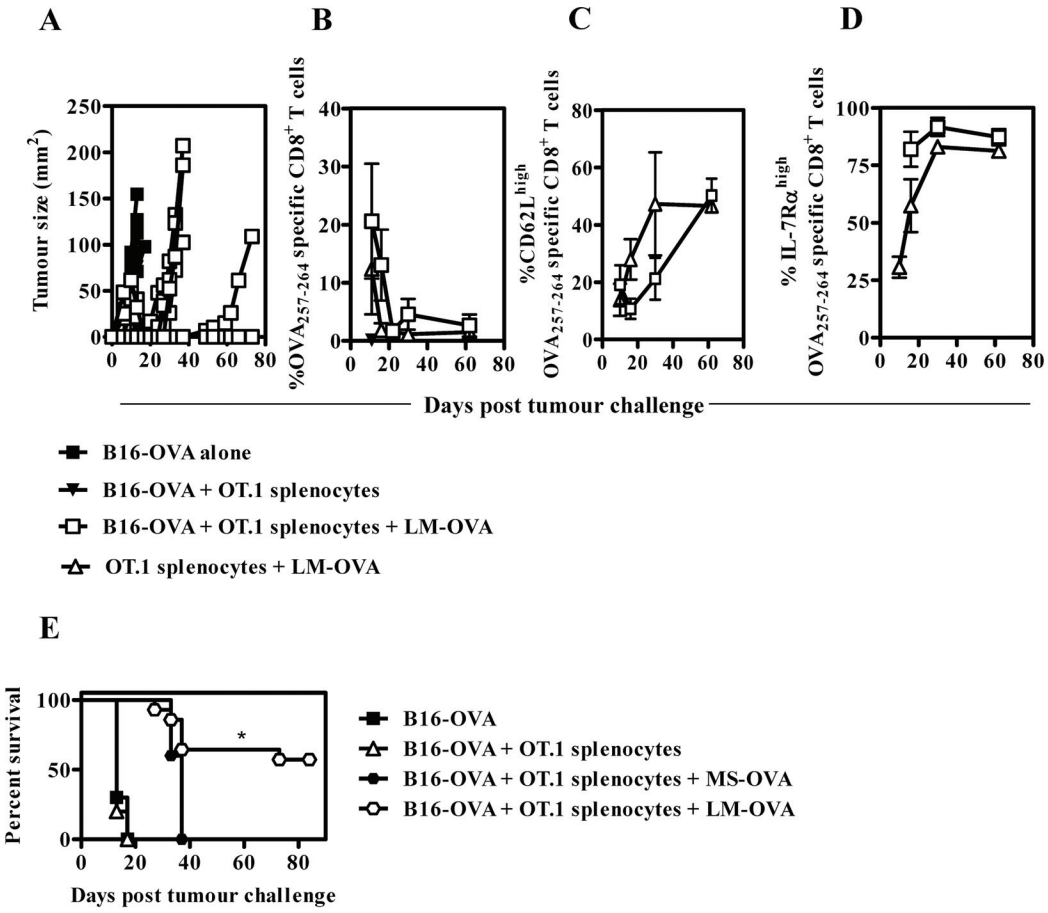

FIGURE 32: Phenotype of responding $OVA_{257-264}$ specific $CD8^+$ T cells following therapeutic treatment of B16-OVA tumours.

C57BL/6J mice were injected i.v. with 10^6 OT.1 splenocytes and 7 days later challenged with 10^6 B16-OVA tumour cells (s.c.). 3 days after tumour injection, 10^4 LM-OVA was injected (s.c.) on the dorsal flank (away from tumour site). (A), Tumour progression was monitored as was the frequency of (B), $OVA_{257-264}$ specific $CD8^+$ T cells in the blood and the % expression of (C) CD62L and (D), IL-7Rα. Mean ± SD, n=5-14. (E), A significant difference in survival is afforded to LM-OVA treated mice compared to MS-OVA treated group as determined by Log rank (Mantel-Cox) test. (E) *p=0.0196.

4.3-05 Tumour infiltrating CD8$^+$ T cells express PD-1 following therapeutic MS-OVA treatment

PD-1 is upregulated on activated CD8$^+$ T cells [242] and its maintained expression mediates the down-regulation of CD8$^+$ T cell cytotoxicity and is thought to play a role in the immune evasion of tumours [115]. After tumour development mice were sacrificed; blood, spleen, tumour and lymph nodes were taken to analyze tissue resident $OVA_{257-264}$ specific CD8$^+$ T cells and their phenotype. In MS-OVA and LM-OVA vaccinated mice, there was an increased frequency of $OVA_{257-264}$ specific CD8$^+$ T cells in the tumour compared to other compartments (Figure 33A & B). Surface expression of IL-7Rα and CD62L was significantly higher on $OVA_{257-264}$ specific CD8$^+$ T cells in the spleen and lymph nodes compared to the tumour (Figure 34 & 35). Interestingly, in MS-OVA vaccinated mice an increased expression of PD-1 was observed on infiltrating CD8$^+$ T cells compared to other sites (Figure 36A). This trend was not observed in LM-OVA treated mice (Figure 36B). Additionally, PD-1 expression was significantly lower on blood resident CD8$^+$ T cells in both MS-OVA and LM-OVA vaccinated mice (Figure 36A & B). Since PD-1 upregulation has been correlated with diminished T cell function [237] this could represent a loss of tumour control and may account for the large disparity of tumour protection between MS-OVA and LM-OVA in the therapeutic setting (Figure 32E).

4.3-06 B16-OVA tumour burden decreased the cytotoxicity of OVA-CD8$^+$ T cells

The upregulation of cell surface markers such as PD-1 or other tumour evasion mechanisms may negatively affect CD8$^+$ T cell function. Therefore, I next tested the killing capacity of *in vivo* $OVA_{257-264}$ specific CD8$^+$ T cells in tumour and non-tumour bearing mice.

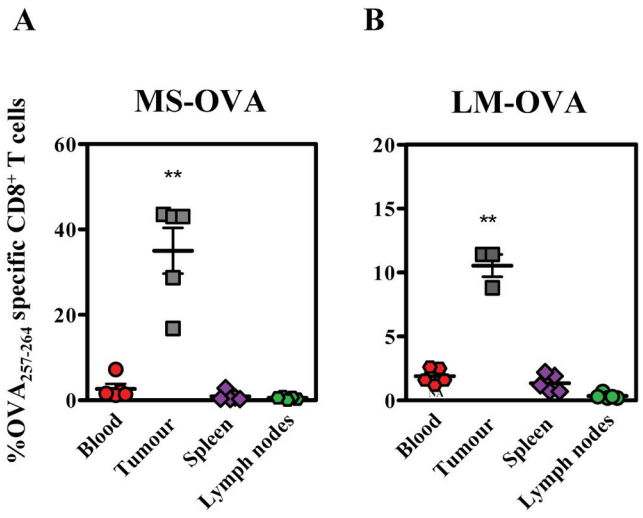

FIGURE 33: Frequency of responding $OVA_{257-264}$ specific $CD8^+$ T cells.
C57BL/6J mice were injected i.v. with 10^6 OT.1 splenocytes. 7 days later 10^6 B16-OVA tumour cells were injected (s.c.) in the dorsal flank. 3 and 8 days after tumour injection, (A) MS-OVA or (B) 10^4 LM-OVA was injected s.c. on the dorsal flank (away from tumour site). At varying time points after infection organs were excised and processed to cell suspensions for FACS analysis. The frequency of $OVA_{257-264}$ specific $CD8^+$ T cells was measured (mean ± SE, n=2-3). Unpaired two-tailed *t* test with Welch's correction for unequal variance: (A) Tumour **p<0.005 (B) Tumour **p<0.01.

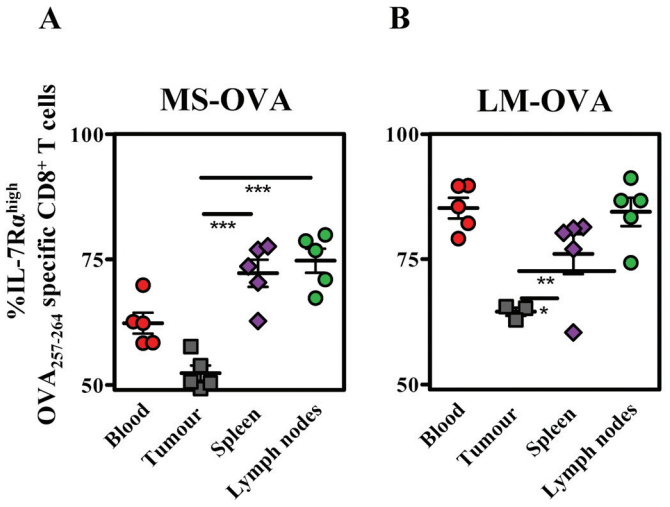

FIGURE 34: IL-7Rα expression of $OVA_{257-264}$ specific $CD8^+$ T cells.
C57BL/6J mice were injected i.v. with 10^6 OT.1 splenocytes. 7 days later 10^6 B16-OVA tumour cells were injected s.c. in the dorsal flank. 3 and 8 days after tumour injection, (A) MS-OVA or (B) 10^4 LM-OVA was injected s.c. on the dorsal flank (away from tumour site). At varying time points after infection organs were excised and processed to cell suspensions for FACS analysis. % IL-7Rα^{high} was plotted of all $OVA_{257-264}$ specific $CD8^+$ T cells were measured (mean ± SE, n=2-3). Unpaired two-tailed *t* test with Welch's correction for unequal variance: (A) Spleen vs. Tumour ***p=0.0007; lymph node vs. Tumour ***, p=0.0002. (B) *, p=0.0475; **, p=0.0025.

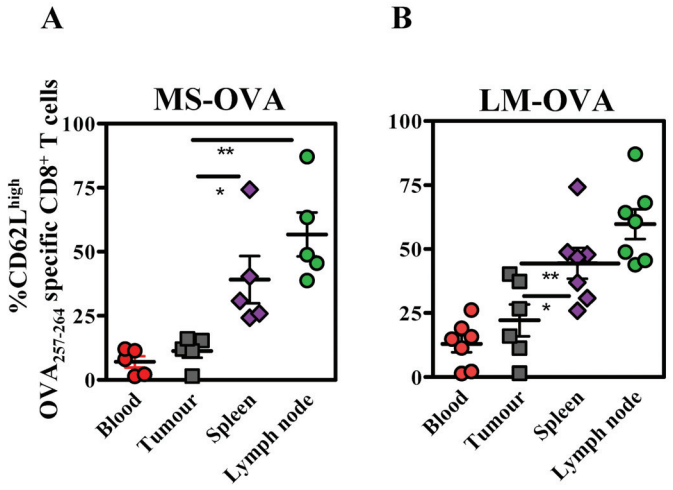

FIGURE 35: CD62L expression of $OVA_{257-264}$ specific $CD8^+$ T cells.
C57BL/6J mice were injected i.v. with 10^6 OT.1 splenocytes. 7 days later 10^6 B16-OVA tumour cells were injected s.c. in the dorsal flank. 3 and 8 days after tumour injection, (A) MS-OVA or (B) 10^4 LM-OVA was injected s.c. on the dorsal flank (away from tumour site). At varying time points after infection organs were excised and processed to cell suspensions for FACS analysis. % $CD62L^{high}$ was plotted of all $OVA_{257-264}$ specific $CD8^+$ T cells were measured (mean ± SE, n=2-3). Unpaired two-tailed *t* test with Welch's correction for unequal variance: (A) *p=0.0436; *, p=0.0072. (B) *, p=0.273; **, p=0.0013.

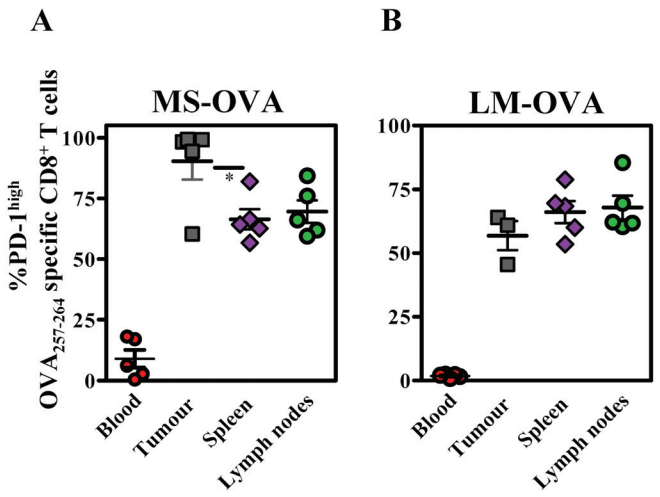

FIGURE 36: PD-1 expression of $OVA_{257-264}$ specific $CD8^+$ T cells.
C57BL/6J mice were injected i.v. with 10^6 OT.1 splenocytes. 7 days later 10^6 B16-OVA tumour cells were injected s.c. in the dorsal flank. 3 and 8 days after tumour injection, (A) MS-OVA or (B) 10^4 LM-OVA was injected s.c. on the dorsal flank (away from tumour site). At varying time points after infection organs were excised and processed to cell suspensions for FACS analysis. % $PD\text{-}1^{high}$ was plotted of all $OVA_{257-264}$ specific $CD8^+$ T cells were measured (mean ± SE, n=2-3).

Briefly, a mixture of peptide-pulsed and non-peptide-pulsed CFSE labeled target cells were injected at a 1:1 ratio into MS-OVA treated tumour bearing or non-tumour bearing mice. 24 h later, spleens were removed from recipient mice and analyzed by flow cytometry for loss of target cells relative to non-target control cells. When C57BL/6J mice were therapeutically treated with MS-OVA on day 3 and 8; dramatic killing of donor cells was observed on day 15 irrespective of their tumour-bearing status. As expected tumour bearing naïve mice did not exhibit any killing of target cells indicating that the endogenous $CD8^+$ T cell response to the tumour immunogen was negligible (Figure 37A). Over time, both non-tumour bearing and tumour bearing animals that were administered MS-OVA showed a steady loss of cytolytic ability. Previous studies have shown that a boost of MS-OVA 21 days later generates $OVA_{257-264}$ specific $CD8^+$ T cells that maintain >80 % cytotoxicity for extended period of times (~100 days post vaccination) [203]. Therefore, I surmised that the boosting schedule I chose for my studies (4 days after priming) may not have been efficient at sustaining the cytolytic activity. Hence in a separate experiment, tumour bearing mice were treated therapeutically with MS-OVA on day 3 and 24 (boosting after 21 days of priming). When this schedule was followed, non-tumour bearing vaccinated mice maintained $CD8^+$ T cell cytotoxicity as observed previously [203] while a marked decrease was observed in tumour bearing mice (Figure 37B). These data suggest that tumour suppressive properties additionally contribute to the loss of sustained $CD8^+$ T cell cytotoxicity.

4.3-07 T regulatory cell depletion prior to MS-OVA therapy delays tumour growth

Recent studies have attributed T_{regs} with dampening anti-tumour $CD8^+$ T cell function [236,237]; therefore T_{regs} were depleted with αCD25 antibody in a therapeutic MS-OVA tumour model.

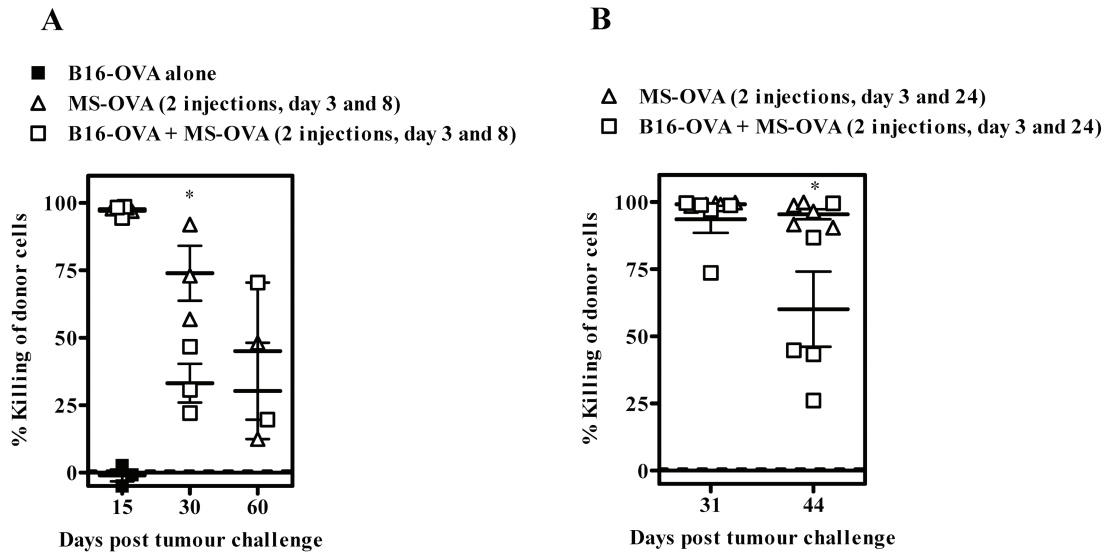

FIGURE 37: *In vivo* CTL during immunotherapy with MS-OVA
10^6 B16-OVA tumour cells were injected s.c. in the dorsal flank of C57BL/6J mice. (A) 3 and 8 days after tumour injection, MS-OVA was injected s.c. on the dorsal flank (away from tumour site). At varying time points after infection, CFSE stained target splenocytes were injected i.v.; 24 h later recipient spleens were removed and processed to measure *in vivo* cytolytic killing. (Mean ± SE, n=2-5/time point/group) *p=0.0308 (B) priming and boosting was carried out with MS-OVA on days 3 and 24 days after tumour injection, and *in vivo* cytolytic activity was measured. *p=0.0370. Unpaired two-tailed *t* tests were performed with GraphPad prism software.

CD25, also known as IL-2Rα is present on T_{regs} as well as activated $CD4^+$ and $CD8^+$ T cells as a part of the IL-2 receptor. Because CD25 is upregulated on activated T cells, it is important that depletion occur prior to vaccination. One day after the intra-peritoneal injection of αCD25, all mice were challenged (s.c.) with B16-OVA and later treated (s.c.) with MS-OVA, 3 and 24 days after tumour. The rate of tumour growth was similar for tumour control (Figure 38A) and αCD25 tumour control (Figure 38B) mice indicating that the loss of T_{regs} prior does not alter tumour growth. Mice given MS-OVA (Figure 38C) or αCD25 and MS-OVA (Figure 38D) had a significant delay in tumour occurrence with substantially greater median survivals compared to non-vaccinated controls (Figure 38E). Furthermore, αCD25 depletion prior to MS-OVA treatment afforded a slightly longer median survival of 40 days compared to 31 days in non-depleted mice. However, a comparison of the survival curves with a Log Rank test show no significant survival difference ($p=0.3228$). However, while αCD25 antibody treatment prior to vaccination can be expected to eliminate constitutive T_{regs}, it may not counter the generation of inducible T_{regs} that could also play a role in dampening anti-tumour $CD8^+$ T cell responses. The delay in tumour onset achieved with T_{reg} removal raises the question of whether increasing the quantity of $CD8^+$ T cells with repeated vaccination can overcome tumour suppression.

4.3-08 Multiple boosting with MS-OVA induced high numbers of circulating $CD8^+$ T cells

Many live vaccines can attribute their success to their immune bolstering components like LPS. By piggy backing target epitopes such as viral nucleoproteins or tumour self proteins within highly immunogenic intracellular vectors (LM) it is possible to induce large numbers of antigen specific $CD8^+$ T cells.

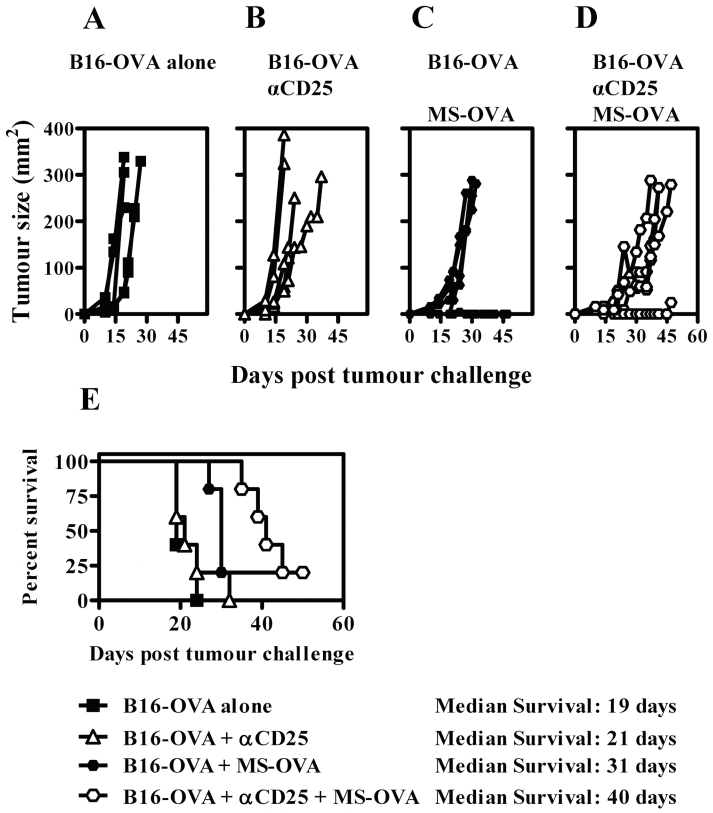

FIGURE 38: T_{reg} depletion prior to tumour immunotherapy with MS-OVA.
C57BL/6J mice were injected intra-peritoneally with αCD25 antibody. One day later, 10^6 B16-OVA tumour cells were injected s.c. on the dorsal flank. 3 and 24 days after tumour MS-OVA was injected s.c. on the dorsal flank away from tumour site. (A, B, C, D) Tumour progression was monitored for individual mice over time. (E) % survival is shown with median survival of each group. No significant survival differences were observed between A & B or between C & D. A significant difference in survival was observed between A & C p=0.0023, as well as between B & D, p=0.0017. n=5/group.

A major drawback to these vectors is their limited use in boosting the $CD8^+$ T cell response due to significant anti-vector antibody responses that sequester and restrict the re-exposure of target epitopes. Significant advances have been made in designing better priming vectors to augment secondary responses [52,243]. The unique adjuvant properties of MS-OVA make it a promising vector in multiple boosting regimens as sufficient co-stimulation is evoked while there is little or no anti-lipid antibody response [203]. In order to determine the maximum quantitative threshold of a $CD8^+$ T cell response that can be achieved, MS-OVA or LM-OVA were administered (s.c.) to C57BL/6J mice at specific time intervals either once, twice or 5 times. The frequency of $OVA_{257-264}$ specific $CD8^+$ T cells were monitored in the blood at regular intervals before vaccination and 7 days after vaccination up to 300 days post initial exposure. One exposure to MS-OVA or LM-OVA (Figure 39A & D) elicited a modest response with ~2 % $OVA_{257-264}$ specific $CD8^+$ T cells by day 7. Long term tracking revealed ~0.3 % $OVA_{257-264}$ specific $CD8^+$ T cells up to 300 days post vaccination (Figure 39A & D). With the administration of a second dose of MS-OVA or LM-OVA at day 21 a noticeable increase in $OVA_{257-264}$ specific $CD8^+$ T cells was detectable by day 28 (Figure 39B & E). With the addition of subsequent vaccinations at day 42, 72 and 110, further boosting of the immune response was observed in the MS-OVA setting only (Figure 39C & F). Notably, 21 days after the second exposure to antigen (day 42), the frequency of $OVA_{257-264}$ specific $CD8^+$ T cells was significantly lower in MS-OVA compared to LM-OVA vaccinated mice ($p=0.04$). Thus, a clear disparity in the timing of contraction is observable between vaccination regimens. Additionally, after the 3rd exposure to LM-OVA, very little T cell expansion occurred (Figure 39F). In contrast, after the second dose of MS-OVA, the $OVA_{257-264}$ specific $CD8^+$ T cells underwent quick contraction, and after the third exposure to MS-OVA a rapid proliferation ensued to more than 30 % $OVA_{257-264}$ specific $CD8^+$ T cells

(Figure 39C). The fourth and fifth exposure of antigen induced very little T cell proliferation in the LM-OVA setting but marked proliferation in the MS-OVA setting. However, no greater than the 30 % of $OVA_{257-264}$ specific $CD8^+$ T cells were observed in the blood after the third dose. 300 days post initial vaccination, ~5 % of $OVA_{257-264}$ specific $CD8^+$ T cells were detectable after multiple MS-OVA vaccinations compared to ~1 % $OVA_{257-264}$ specific $CD8^+$ T cells after multiple LM-OVA vaccinations.

4.3-09 CD62L expression on $CD8^+$ T cells reduces with multiple boosting

To further characterize the $OVA_{257-264}$ specific $CD8^+$ T cell response elicited by MS-OVA or LM-OVA after single or multiple boosting, blood samples were further stained for CD62L. After one exposure to MS-OVA or LM-OVA a significant amount (~75 %) of the few responding $OVA_{257-264}$ specific $CD8^+$ T cells were $CD62L^{high}$ by day 70 (Figure 40A & D). When mice were boosted with MS-OVA, a severe reduction in the number of $CD62L^{high}$ $CD8^+$ T cells was observed indicating a shift in the overall phenotype of memory $CD8^+$ T cells (Figure 40B). The same cannot be said of LM-OVA. After boosting with LM-OVA, a large proportion of the cells remain $CD62L^{high}$, albeit at lower levels compared to priming alone at later time-points (Figure 40E). Subsequent boosting with either MS-OVA or LM-OVA reduces the % $CD62L^{high}$ $CD8^+$ T cells to 25 % and 50 %, respectively, at late time-points (>200 days) (Figure 40C & F). Overall, while boosting with MS-OVA increases the frequency of $OVA_{257-264}$ specific $CD8^+$ T cells to great numbers, a marked decrease in $CD62L^{high}$ T_{CM} cells was observed at later time-points. In the case of LM-OVA, multiple boosting does not augment the frequency of $OVA_{257-264}$ specific $CD8^+$ T cells past the 2^{nd} dose. Additionally, the frequency of $CD62L^{high}$ cells decreases with more exposures to LM-OVA, however it was greater than the frequency observed in MS-OVA vaccinated mice.

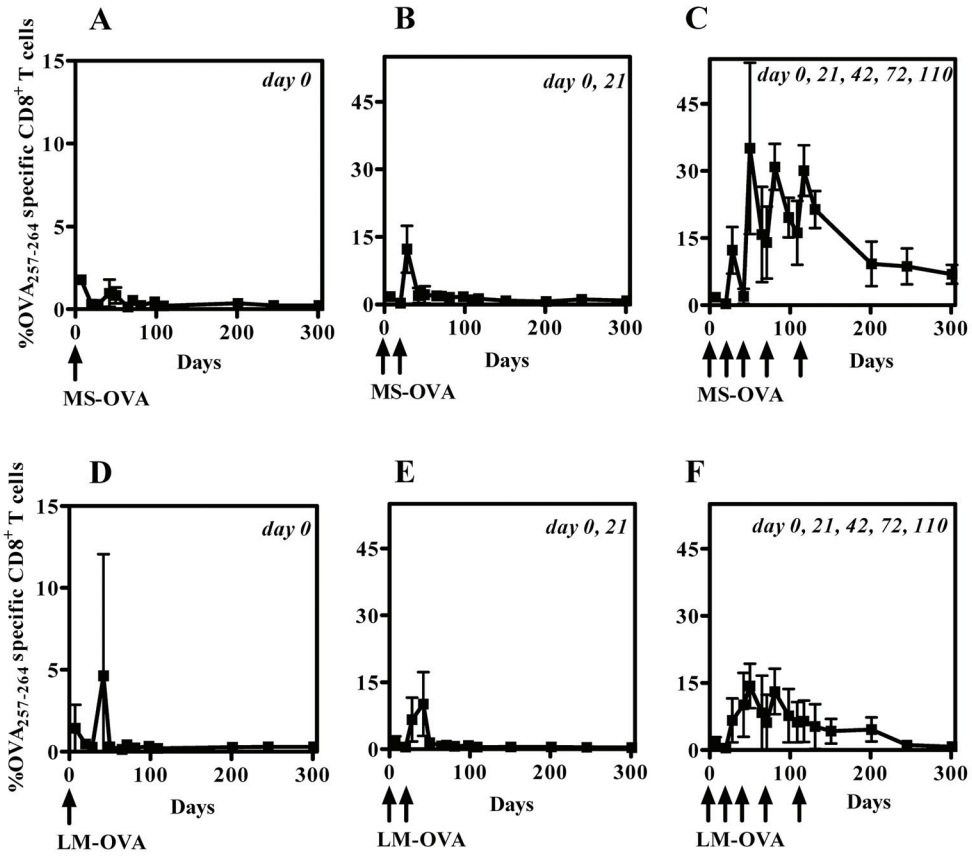

FIGURE 39: Frequency of $OVA_{257-264}$ specific $CD8^+$ T cells following prime-boost vaccinations.

C57BL/6J mice were vaccinated s.c. with (A, B, C) MS-OVA or (D, E, F) 10^4 LM-OVA in the middle of the dorsal flank at day 0, 21, 42, 72, 110 as indicated at the top of each panel. Blood was taken before vaccination, 7 days after and 21 days after each vaccination as well as at later time-points. Blood was stained with anti-CD8 antibody as well as $OVA_{257-264}$ tetramer and analyzed by flow cytometer. n=3/group.

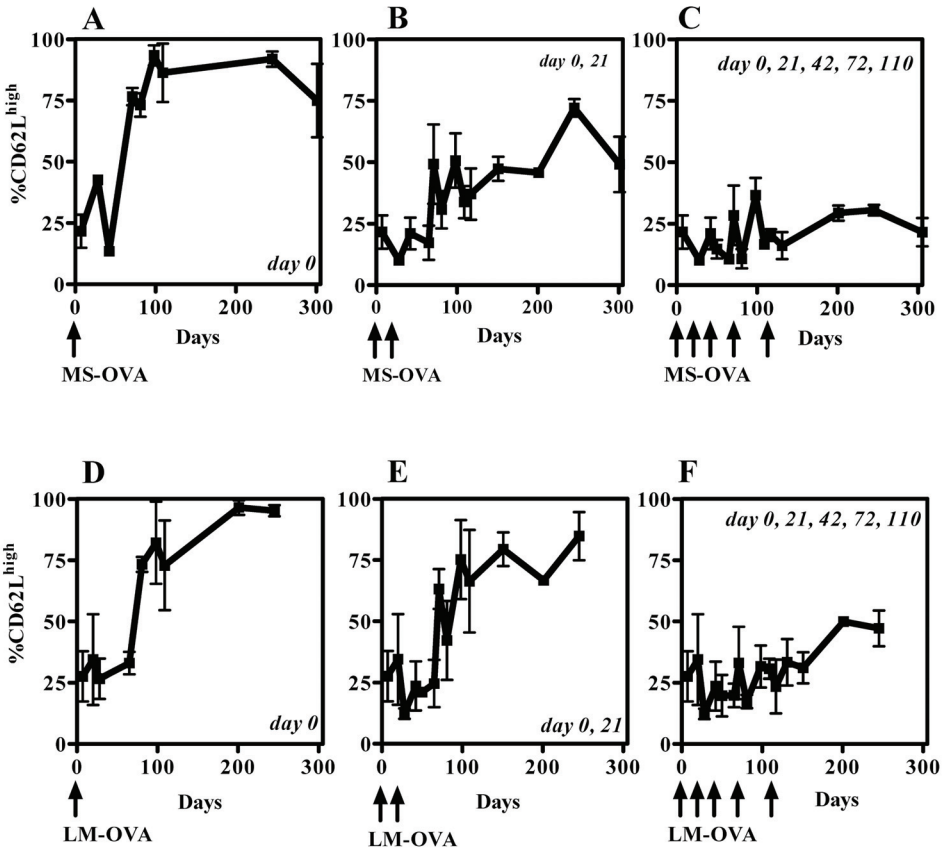

FIGURE 40: CD62L^{high} expression on responding CD8^{+} T cells following prime-boost vaccinations.

C57BL/6J mice were vaccinated s.c. with (A, B, C) MS-OVA or (D, E, F) 10^4 LM-OVA in the middle of the dorsal flank at day 0, 21, 42, 72, 110 as indicated at the top of each panel. Blood samples were taken before vaccination, 7 days after and 21 days after each vaccination as well as at later time-points. Blood was stained with anti-CD8, $OVA_{257-264}$-tetramer and anti-CD62L and analyzed with a BD FACSCanto flow Cytometer. % CD62L was obtained from a gated population of $OVA_{257-264}$ specific CD8^{+} T cells. (Mean ± SD, n=3).

Overall continued boosting with either pathogen decreased the frequency of circulating $CD62L^{high}$ $CD8^+$ T_{CM} cells.

4.3-10 Similar tumour protection after multiple vaccinations with MS-OVA or LM-OVA

323 days after initial vaccination, all mice were challenged with a subcutaneous dose of 10^6 B16-OVA. All MS-OVA vaccinated mice were afforded greater protection from tumour with a median survival of 32 to 42 days compared to control with a median survival of ~16 days (Figure 41A). While all LM-OVA vaccinated mice were afforded similar survival rates, those vaccinated twice or 5 times with LM-OVA survived significantly longer when compared to control mice (Figure 41B). With the exception of 1 LM-OVA vaccinated mouse, all mice succumbed to tumour before 60 days with an average median survival of 37 to 42 days compared to control mice that succumbed to tumour ~16 days post injection.

4.3-11 Staggered boosting increased frequency of OVA-$CD8^+$ T cells and tumour protection

The re-exposure of $CD8^+$ T cells to antigen at short intervals can lessen their proliferation potential and lead to activation induced cell death due to overstimulation [11]. Therefore, in an effort to improve the $OVA_{257-264}$ specific $CD8^+$ T cell response, the 2nd and 3rd vaccinations were delayed to day 29 and 89. While it is currently not known how much of a delay is suitable to maximize the $CD8^+$ T cell response, booster vaccinations were given at increased intervals.

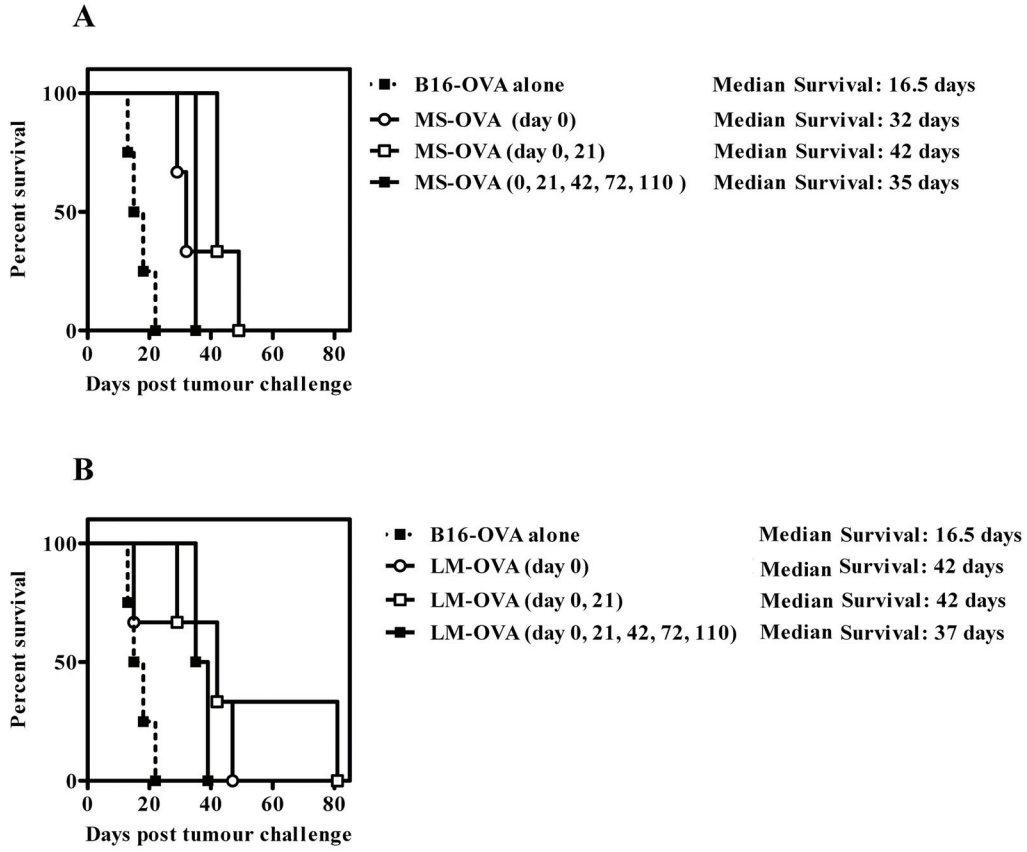

FIGURE 41: Tumour challenge following prime-boost vaccinations with MS-OVA or LM-OVA.

C57BL/6J mice were infected s.c. with (A) MS-OVA or (B) 10^4 of LM-OVA in the middle of the dorsal flank at day 0, 21, 42, 72 and 110 as indicated at the top of each panel. 323 days after initial vaccination, 10^6 B16-OVA cells were injected s.c. in the lower dorsal flank. Survival was measured over time. Log rank (Mantel-Cox) test reveals all MS-OVA vaccinated mice were significantly protected from tumour longer than control (*, $p<0.05$). Mice doubly vaccinated survived longer than mice vaccinated 5 times (**, $p<0.01$). Mice vaccinated twice or 5 times with LM-OVA survived significantly longer compared to control mice (*, $p<0.05$). All LM-OVA vaccinated mice were afforded similar survival rates. (n=2-4/group)

The frequency of $OVA_{257-264}$ specific $CD8^+$ T cells were monitored in the spleen of mice vaccinated with MS-OVA twice (Figure 42A), or three times (Figure 42B). Blood was also taken throughout the experiment from mice vaccinated with MS-OVA once (Figure 42C), twice (Figure 42D) or three times (Figure 42E). Remarkably, up to 50 % of $CD8^+$ cells in the blood were found to be specific for OVA, 10 days after the 3rd vaccination (Figure 42E). In the previous experiment (Figure 41), mice were challenged with tumour almost a year after initial vaccination; in this experimental setup mice were challenged earlier with B16-OVA tumour 216 days post initial vaccination. Mice vaccinated 3 times were afforded a median survival of 91 days which was substantially greater than the median survival (46 days) of mice vaccinated once or twice (Figure 43). Blood samples were taken after tumour and the frequency of $OVA_{257-264}$ specific $CD8^+$ T cells was plotted for mice receiving 3 (Figure 44A) or 2 (Figure 44B) vaccinations. Mice were segregated into two groups to show those that survived tumour challenge past 70 days or those that succumbed to tumour. % $CD62L^{high}$ $OVA_{257-264}$ specific $CD8^+$ T cells were also shown for mice receiving 3 (Figure 44C) or 2 (Figure 44D) vaccinations. Day 0, blood samples were taken immediately before tumour challenge and show a prevalent $CD62L^{high}$ phenotype for the majority of $OVA_{257-264}$ specific $CD8^+$ T cells, most prominently in mice doubly vaccinated compared to mice vaccinated three times (***, $p<0.001$). This indicates that mice given a third vaccination had a more heterogenous $CD62L^{low}$ and $CD62L^{high}$ $OVA_{257-264}$ specific $CD8^+$ T cell population. 8 days after tumour injection the blood profile indicated that the majority of cells obtained had a $CD62L^{low}$ effector T cell (T_E) phenotype (Figure 44C&D) and a substantial expansion of $OVA_{257-264}$ specific $CD8^+$ T cells was evident (Figure 44A&B).

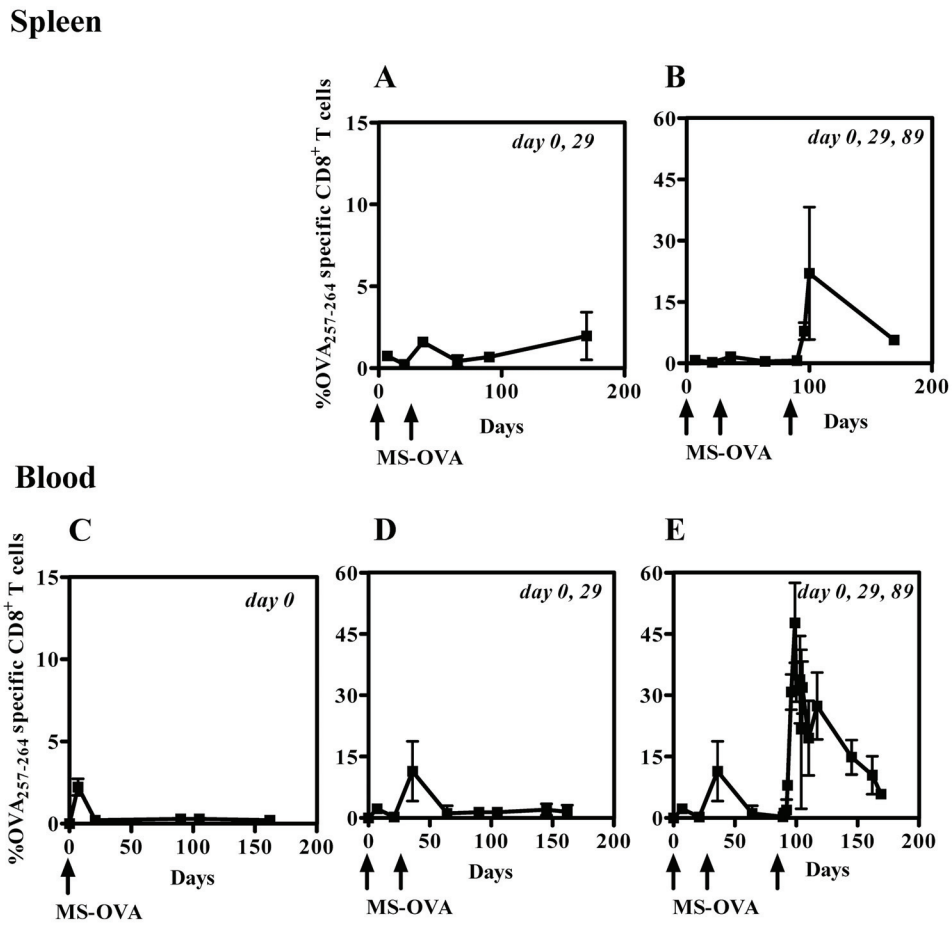

FIGURE 42: CD8$^+$ T cell frequency following staggered prime-boost vaccinations with MS-OVA or LM-OVA.

C57BL/6J mice were vaccinated s.c. with MS-OVA in the middle of the dorsal flank at day 0, 29 and 89 as indicated at the top of each panel. (A, B) Spleen and (C, D, E) blood samples were taken before vaccination, 7 days after and 21 days after each vaccination as well as at later time-points. The blood was stained with anti-CD8 antibody as well as $OVA_{257-264}$ tetramer and analyzed by flow cytometry. (n=3-9/group)

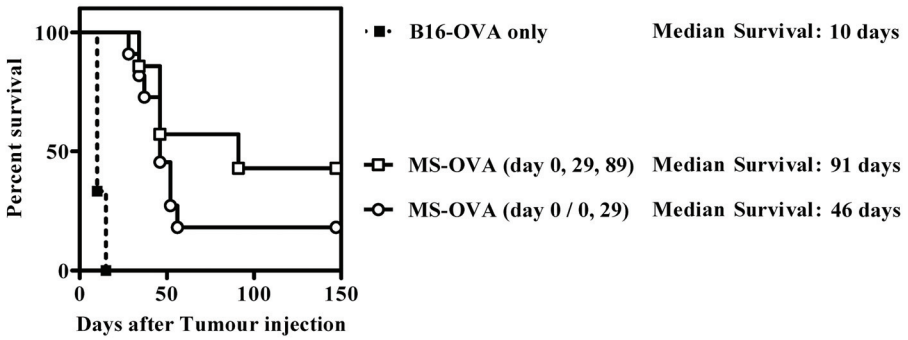

FIGURE 43: Tumour challenge following staggered prime-boost vaccinations with MS-OVA or LM-OVA.

C57BL/6J mice were infected s.c. with MS-OVA in the middle of the dorsal flank at day 0, 29 and 89 as indicated at the top of each panel. 216 days after initial vaccination 10^6 B16-OVA cells were injected s.c. in the lower dorsal flank. Survival was measured over time. Log Rank (mantel-cox) test shows significance of **, $p<0.01$ for control versus all vaccinated groups individually. (n=3-11/group).

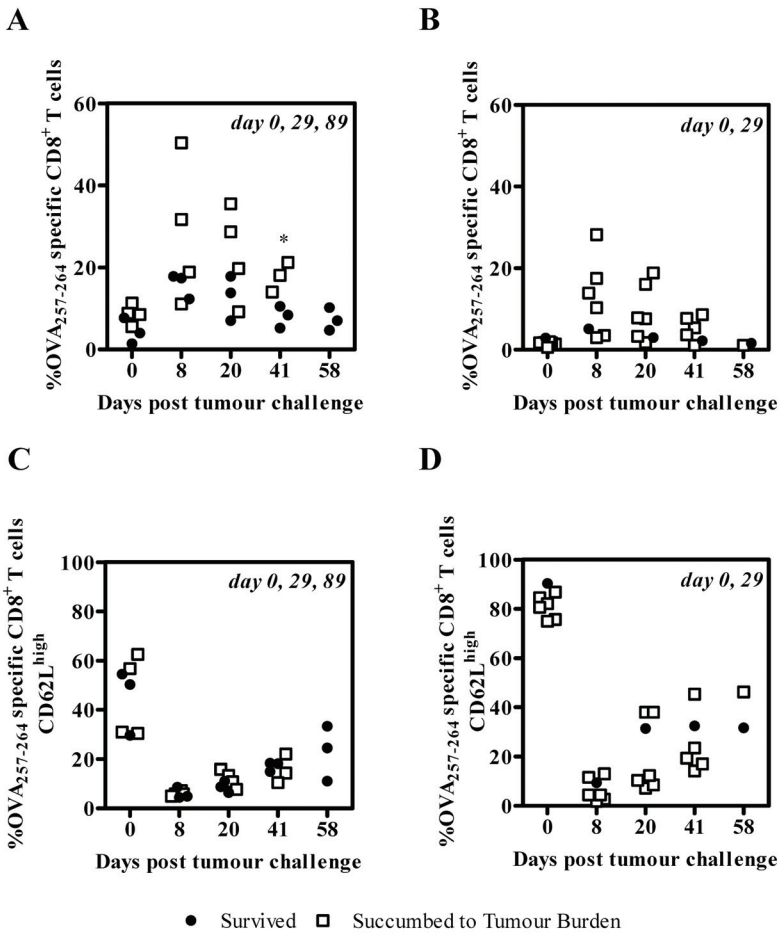

FIGURE 44: CD8$^+$ T cell frequency following tumour challenge after vaccination. C57BL/6J mice were infected s.c. with MS-OVA in the middle of the dorsal flank at day (A, B) 0, 29 and 89 or (C, D) 0, 29 as indicated at the top of each panel. 216 days after initial vaccination 10^6 B16-OVA cells were injected s.c. in the lower dorsal flank. Blood samples were taken after tumour and assayed for the frequency of (A, C) $OVA_{257-264}$ specific CD8$^+$ T cells and their % expression of (B, D) CD62L. Surviving mice and those that succumbed to tumour mice were segregated for analysis. (A) Two-tailed t-test with Welch's correction for unequal variance *, p=0.02. Data are graphed for individual mice.

Notably, the expansion of $OVA_{257-264}$ specific $CD8^+$ T cells was more prominent in those mice that eventually succumbed to tumour burden, likely as a result of larger sources of tumour antigen due to increased tumour burden. Taken together, I observed that >100 days after vaccination, right before tumour challenge, doubly vaccinated mice have significantly less blood resident $OVA_{257-264}$ specific $CD8^+$ T cells (**, $p<0.01$) but they express significantly more CD62L (***, $p<0.001$) compared to mice vaccinated 3 times, yet tumour protection was shorter in duration (Figure 44). This indicates that while a T_{CM} phenotype is desired of an anti-tumour vaccine, the presence of a larger number of $CD8^+$ T cells with effector function (T_{EM}) may compensate, leading to an increased duration of tumour protection.

4.3-12 Concluding Remarks:

4.3-12a Immunotherapy against murine melanoma

MS-OVA liposomes were capable of generating a tumour protective response in both a therapeutic and prophylactic tumour setting. An early boost, just 3 days after priming did not allow long-term maintenance of $CD8^+$ T cell cytotoxicity in either tumour and/or non-tumour bearing mice. In non tumour bearing mice, delaying the boost to 21 days (3 weeks after priming) allowed for the steady maintenance of $CD8^+$ T cell cytotoxicity following MS-OVA vaccination as reported earlier. In the therapeutic setting, the loss of $CD8^+$ T cell cytotoxicity was not merely related to the timing of the boost, as both early boosting (3 days after priming) or delayed boosting (21 days after priming) did not allow for prolonged maintenance of $CD8^+$ T cell cytotoxicity in the progressive tumour growth environment.

In all therapeutic experiments with MS-OVA, tumour growth was initially suppressed but eventually returned. My data suggests that this may correlate to the waning of the anti-

tumour cytotoxic response. The factors associated with tumour recurrence identified in this study include the upregulation of PD-1 on tumour infiltrating $OVA_{257-264}$ specific $CD8^+$ T cells and interference by T_{reg} cells. LM-OVA treated mice fared better with longer overall survival compared to MS-OVA treated mice. The factors associated with prolonged tumour protection in LM-OVA vaccinated mice included a rapid contraction of $OVA_{257-264}$ specific $CD8^+$ T cell frequency and maintenance of T_{CM} phenotype cells.

Overall my data reveals the complexity of achieving sustained tumour regression in a therapeutic setting in the wake of tumour evasion.

4.3-12b Maximizing $CD8^+$ T cell quantity following vaccination

In order to elucidate the maximum possible quantity of $CD8^+$ T cell responses, a multiple boosting regimen was evaluated utilizing MS-OVA. In the prophylactic setting, multiple boosting with MS-OVA effectively increased circulating $CD8^+$ T cells while decreasing the frequency of $CD62L^{high}$ cells. Delaying the MS-OVA booster doses did not further increase the frequency of $OVA_{257-264}$ specific $CD8^+$ T cells; however, the proportion of T_{CM} cells was enhanced with 2 rather than 3 vaccinations. In all vaccinated mice, a tumour challenge similarly increased the number of responding $CD8^+$ T cells. Therefore, increased circulating $CD8^+$ T cells alone did not positively correlate with improved tumour protection. When the interval between priming and boosting was increased, a 3-injection schedule afforded greater tumour protection compared to singly and double vaccinated mice when tumour challenge occurred ~200 days post the first injection. Nevertheless, while it was initially thought that multiple boosts would continually increase $OVA_{257-264}$ specific $CD8^+$ T cell frequencies and confer maximal vaccine efficacy, a regiment of 5 injections of

MS-OVA demonstrated no additional benefit over 3 injections. Thus, the data suggests that the benefits of boosting multiple times may be limited in an immunotherapeutic setting.

5.0 CHAPTER 5: DISCUSSION

5.1 Differential tumour protection by LM-OVA and ST-OVA

Vaccine delivery approaches aimed at inducing $CD8^+$ T cell responses have largely focused on maximizing the quantity of the response to improve efficacy. My findings demonstrate the importance of selecting vaccine delivery approaches that can differentially modulate the phenotype of memory $CD8^+$ T cells for improved tumour immunotherapy. It was previously shown that the T_{CM} memory phenotype confers a better host protection against tumour development compared to T_{EM} [11,44,49,153,244–246]. However, the manner in which beneficial T_{CM} cell types are induced post-vaccination was unclear. In this study I provide evidence that T_{CM} or T_{EM} phenotype $CD8^+$ T cells may be differentially generated *in vivo* by bacterial vectors such as ST-OVA and LM-OVA that have contrasting replicating potential and intracellular niches. I characterized $CD8^+$ T memory cells for their phenotypic expression of CD62L and IL-7Rα, and for their functional ability to produce cytokines and kill specific targets *in vivo*. The acute pathogen LM-OVA, that generated a predominant T_{CM} memory phenotype, was better able to prevent or clear an established B16-OVA melanoma tumour than the T_{EM} memory phenotype generated by the chronic pathogen ST-OVA (Figure 3, 4 & 5). This selective ability of LM-OVA induced $CD8^+$ T memory cells to control tumour burden correlated to their profound capacity for homeostatic proliferation (Figure 13). A similar observation was made with the use of recombinant Adenovirus versus Semliki Forest Virus (SFV) for tumour immunotherapy where a predominant T_{CM} phenotype generated by SFV conferred longer tumour protection [153]. Thus, adjuvants and delivery

systems need to be selected for their capacity to influence the appropriate phenotypic and proliferative quality of memory $CD8^+$ T cells rather than solely for their immediate functional ability, cytotoxicity and cytokine production.

5.1-01 Antigen localization and duration of infection on $CD8^+$ T cell response

It has previously been reported that many factors such as the timing and extent of antigen-presentation and inflammation induced, influences $CD8^+$ T cell differentiation [55,141,176]. While LM-OVA induces a typical T cell memory response [247] first observed in viral infection models [248], ST-OVA induces a delayed and reduced peak of $CD8^+$ T cell response followed by a protracted contraction phase perhaps due to its residence within the phagosomes of infected cells (Figure 8) [141,168]. Differences in bacterial burden were ruled out as a contributing factor because on day 3 after infection, the time when naïve $CD8^+$ T cells are typically primed, both LM-OVA and ST-OVA infections caused a similar bacterial burden (Figure 6) [141]. Furthermore, both LM-OVA and ST-OVA expressed similar levels of OVA [141]. Thus, my results demonstrate that the magnitude and kinetics of the response against the same antigen may be differentially influenced by delivery strategy.

Despite the phagosomal nature of ST-OVA and the delay in antigen-presentation, $CD8^+$ T cell activation does occur, albeit at initial lower levels compared to LM-OVA. However, 60 days after infection with either pathogen, a stable population (3-8 %) of $OVA_{257-264}$ specific $CD8^+$ T cells was detected in the blood (Figure 8). Similar numbers ($\sim 2x10^5$) of $OVA_{257-264}$ specific $CD8^+$ T cells were discernable in the spleen [249]. Therefore, even with a chronic vector such as ST, a priming phase followed by transition to maintenance (memory) occurred correlating with the substantial reduction in antigen burden. Thus, tumour protection was intentionally tested at time periods well beyond 60 days post-infection, when similar

numbers of $OVA_{257-264}$ specific $CD8^+$ T cells were present in LM-OVA and ST-OVA infected mice, and antigen burden was absent or minimal.

5.1-02 Chronic infections and induction of $CD8^+T_{EM}$ cells

The pathway of differentiation of primed $CD8^+$ T cells into T_{EM} or T_{CM} phenotypes remains unclear. Recently, the cytokine conditions necessary for the generation of a predominant T_{CM} memory response have begun to be uncovered [250–252]. It was previously shown that weak antigen presentation as afforded by recombinant *Mycobacterium bovis* BCG-OVA promotes differentiation mainly into T_{CM} phenotype [55]. Furthermore, competition of $CD8^+$ T cells for access to APCs also influences the phenotype distribution [55,251]. BCG-OVA and ST-OVA are both phagosomal resident pathogens that evoke delayed antigen presentation. However, BCG vectors cause T_{CM} generation and afford strong tumour protection [157], suggesting that chronicity itself may not be a detriment for cancer vaccine delivery. Overall, several aspects of ST-OVA infection such as prolonged inflammation, rapid rate of replication [141], delayed uptake by DCs, and delayed clearance likely contribute to continued low-level antigen presentation disallowing differentiation to T_{CM} phenotype.

5.1-03 ST-OVA generated T_{EM} cells and exhaustion and/or anergy

Chronic antigen exposure has been associated with an eventual ineffective immune response against viral infections [253–255]. Chronically stimulated T cells can also become senescent in a tumour bearing host [241]. However, $CD8^+$ T cells induced against ST-OVA were not anergic, or non-functional since they were cytotoxic and expressed IFN-γ rapidly (Figure 10). The drop in the *in vivo* cytolytic activity in LM-OVA infected mice from day 7 to day 30 is commensurate with the contraction of the $OVA_{257-264}$ specific $CD8^+$ T cell response that

occurs following priming (Figure 8). Similarly, the delayed and prolonged T_E and T_{EM} phase during ST-OVA infection correlates with the kinetics of *in vivo* cytotoxicity data (Figure 9). However, at day 60 after infection, while similar numbers of $OVA_{257-264}$ specific $CD8^+$ T cells were present in LM-OVA and ST-OVA infected mice, the latter group showed greater *in vivo* cytolytic activity in comparison to the former. T_{EM} cells have been shown to exhibit stronger immediate effector function [42], although this remains controversial [256]. Nevertheless, despite the induction of a potent immediate cytolytic $CD8^+$ T-cell response, long-term anti-tumour killing was compromised. Furthermore, no differences were detected of IFN-γ expression in $OVA_{257-264}$ specific $CD8^+$ T cells in the spleens of LM-OVA versus ST-OVA infected mice. A majority of the cells in ST-OVA infected mice had differentiated into memory phenotype by day 64 since they had up-regulated IL-7Rα expression that correlates to memory transition [156]. Thus, the precipitous reduction in the bacterial burden that occurs prior to day 45 of ST-OVA infection (Figure 4) [141] probably reduced the antigen levels enormously, thereby preventing T cell anergy, and facilitating the development of memory cells. Regardless of whether ST-OVA induced $CD8^+$ T cells may be considered as memory cells, my study reiterates how varied vectors that appear to evoke cytolytic $CD8^+$ T cells may differentially modulate cancer vaccine efficacy due to the quality of the memory $CD8^+$ T cell response.

5.1-04 Tissue homing properties of T_{CM} cells

The ability of ST-OVA and LM-OVA generated $CD8^+$ T cells to protect against tumours correlated to their differential proliferation and capacity to traffic to the tumour site. Memory $CD8^+$ T cells are characterized by their ability to persist with homeostatic cytokines IL-7 and IL-15 independently of antigen [238,257,258]; however, the rate of proliferation can differ between infections. Only LM-OVA induced memory $OVA_{257-264}$ specific $CD8^+$ T cells were

able to proliferate substantially in the absence of antigen (*in vivo* and *in vitro*) (Figure 13). Additionally, LM-OVA induced $OVA_{257-264}$ specific $CD8^+$ T cells were better able to produce IL-2 compared to ST-OVA (Figure 10c). Similarly, in response to tumour challenge, the expansion of memory $OVA_{257-264}$ specific $CD8^+$ T cells occurred only in LM-OVA–vaccinated mice (Figure 15a). While this expansion was small it was significant because tumours lack the danger signals that activate APC co-stimulation and cytokine production. Additionally, $OVA_{257-264}$ specific $CD8^+$ T_{CM} cells evoked by LM-OVA were better able to home to lymphoid organs including TDLN, 3 days after tumour challenge (Figure 14). Therefore, the advantage for LM-OVA induced $OVA_{257-264}$ specific T_{CM} cells may be their overall capacity for expansion (antigen-dependant and independent) and extravasation to lymphoid tissues allowing them to efficiently combat an aggressively growing tumour. The enhanced ability of T_{CM} cells to extravasate into lymphoid tissues appears to be related to the high expression of CD62L. Its expression on memory $CD8^+$ T cells might be of pivotal importance to concentrate tumour reactive $CD8^+$ T cells in lymphoid areas where they can encounter mature APCs presenting tumour antigen.

5.1-05 ST-OVA infection and T_{reg} cell induction

It has previously been shown that because ST-OVA becomes sequestered in the phagosomes of phagocytic cells by preventing lysosome formation, bacterial antigens are prevented from accessing MHC-class I presenting machinery and evoking a prompt $CD8^+$ T cell response [141,142]. Recently, it has been suggested that an influx of T_{regs} cells during early ST-OVA infection might play a role in maintaining ST chronicity. It was shown that the suppressive potency of T_{regs} during ST infection was heightened early during infection (3-4 weeks) and removal of T_{regs} accelerated bacterial eradication [259]. It is possible that T_{regs} are

recruited during ST infection as a way to suppress anti-microbial $CD8^+$ T cell responses, providing a niche for the microbe to maintain a persistent infection [235,260–262]. Similarly, I found that the frequency of T_{regs} in the spleen remained stable during ST-OVA infection [259] (Figure. 10D). However, an increase in the overall number of T_{regs} occurred by day 41 of ST-OVA infection. This may be attributable to the generalized inflammation-induced splenic enlargement seen following murine ST-OVA infection. Indeed, I also observed an increase in the total number of lymphocytes and $CD4^+$ T cells. However, since the number of IFN-γ secreting $OVA_{257-264}$ specific $CD8^+$ T cells in the spleen after 30 days of infection is similar in both infection models [142], the increased ratio of T_{regs} to $OVA_{257-264}$ specific $CD8^+$ T cells during ST-OVA infection may enhance immunosuppression. Supporting this premise, there was an increased frequency of T_{regs} in the lymph nodes on day 41 after ST-OVA infection (Figure 12H). Since T cell activation typically occurs in lymphoid sites, it remains possible that the increased frequency of T_{regs} in ST-OVA infection, albeit in the lymph nodes alone, may play a role to suppress adaptive immunity; a possible mechanism to maintain ST chronicity (Figure 12).

5.1-06 Concluding Remarks

Virulent and attenuated strains of ST have been investigated as live vectors for use in cancer therapy [156,226]. While such studies reveal an induction of $CD8^+$ T cells, their long-term protective ability has not been characterized in detail. Furthermore, ST can elicit profound inflammation and may lead to bystander tumour protection and has been used for its direct oncolytic properties [263,264]. LM is also considered an efficient vector for cancer vaccines [177,265,266]. While both vectors used in this study are highly virulent and may not be desirable for human vaccines, they were intentionally chosen as they consistently drive extreme phenotypes

of the $CD8^+$ T cell response, T_{CM} and T_{EM}. Thus, they constitute convenient model systems for critically defining the role of T cell quality evoked by the vector/adjuvant in influencing vaccine efficacy. Overall, I think that attenuated LM or muted vectors such as *Mycobacterium bovis* BCG [157], or adjuvants augmenting TLR-independent responses [165] may beneficially direct differentiation of T_{CM} cells desirable for cancer immunotherapy by limiting persistent and/or overt activation.

One consideration is that a 10-fold reduction in pathogen burden by memory T cells may be sufficient to provide complete protection against infection when complemented with the ability of the innate immune system to eliminate the remaining pathogens. However, a meager 10-fold reduction in tumour burden by memory T cells is insufficient in cancer immunotherapy, as the remaining low number of cancer cells may potentially expand and lead to recurrence and/or metastasis. Furthermore, as tumour cells are not associated with danger signals, consequently the innate immune system is unable to complement adaptive immunity for tumour clearance. Thus, while T_{EM} cells alone may be sufficient to facilitate protection against pathogens, they may be impaired when it comes to tumour control.

5.2 Lack of functional selectin ligands compromises long term tumour protection.

Adhesion events that occur between antigen-specific $CD8^+$ T cells and their environment may facilitate tumour surveillance from the initial activation, maintenance as a memory cells, reactivation and extravasation to a tumour site. Induced expression of adhesion molecules such as chemokine receptors, integrins or selectins on T cells has been reported to enhance migration to the periphery [267–269]. Furthermore, reducing the expression of the late adhesion molecule, VLA-4 on $CD8^+$ T cells, reduces their recruitment into tumours [270]. In many cancer models the infiltration of $CD8^+$ T cells into a tumour site

correlates with an improved prognosis [10,240,215]. Therefore, understanding the events that draw tumour reactive $CD8^+$ T cells into a tumour environment is vital for the development of efficacious anti-tumour vaccines. Among the many adhesion molecules involved in cell adherence, selectin/selectin ligand interactions occur early on and mediate rolling and tethering of lymphocytes along the endothelium. The complete loss of selectin ligand binding activity in the FtDKO mice [227,271,272] offered a convenient model to study the role of these interactions among anti-tumour $CD8^+$ T cells.

5.2-01 Response to tumours in FtDKO mice

I utilized LM-OVA vaccination as a model system to evoke anti-tumour T cell immunity as this leads to the induction of $CD62L^{high}$ T_{CM} cells and consequent long-term protection against B16-OVA melanoma as described above and previously [249]. The presence of the selectin, CD62L, on antigen experienced T_{CM}, has been correlated with superior tumour protective ability [11,49,273]. CD62L is capable of binding a number of cell associated selectin ligands including GlyCAM-1, CD34, PSGL-1, MAdCAM-1 and sulfated glycoprotein – 200kDa (Sgp200) [274,275]. A final reaction in the synthesis of these glycan ligands is a fucosylation reaction mediated by α(1,3) fucosyltransferase [276]. Mice singly deficient in α(1,3)fucosyltransferase-VII ($FucTVII^{-/-}$) have reduced cell numbers in lymph nodes [66] as well as reduced $CD4^+$ and $CD8^+$ T cell homing into the skin as shown by a contact hypersensitivity assay [272,274]. However, $FucTVII^{-/-}$ mice exhibit an incomplete inhibition of E-selectin ligand formation. Complete inhibition of selectin ligand binding including E-selectin interactions occurs in FtDKO mice doubly deficient for α(1,3)fucosyltransferase-IV and VII. Using this model, selectin/ligand interactions have been credited to mediate effector $CD8^+$ T cell recruitment to the myocardium [271] as well as

naïve and memory $CD8^+$ T cell entry into lymph nodes [67]. I observed that despite the normal ability of FtDKO mice to mount a classic acute immune response to LM-OVA vaccination, including induction of $CD62L^{high}$ T_{CM} cells, (Figure 17 & 18) their ability to maintain a long-term anti-tumour $CD8^+$ T cell response was compromised (Figure 16). Thus, the interaction of CD62L on $CD8^+$ T cells with its fucosylated ligands appears to be important for their ability to infiltrate peripheral tumours.

Vaccinated FtDKO mice succumbed to tumour at a faster pace than wild type mice. However, they exhibited a delay in tumour development relative to non-vaccinated controls. This suggests that a deficiency in fucosylation events may not fully negate short-term effector function of antigen-specific $CD8^+$ T cells. Similarly, the adoptive transfer of 10^6 FtDKO effector $CD8^+$ T cells into naïve recipients conferred protection from tumour challenge (Figure 25) indicating the functional efficacy of a large number of recently activated cells. It may thus be envisaged that the defect *in vivo* relates to the required movement and expansion of memory $CD8^+$ T cells in an FtDKO host from lymph node to the tumour site. Nevertheless, the expression of selectin ligands is induced on some activated $CD8^+$ T cells and has been suggested to play a role in their extravasation into sites of injury by binding to P-selectin and E-selectin [28].

5.2-02 Metastatic tumour protection in vaccinated FtDKO mice

In a previous study, vesicular stomatitis virus (VSV) vaccinated singly deficient $FucTVII^{-/-}$ mice challenged i.v. 14 days later with EL-4N1 tumours (thymoma cell line expressing VSV-nucleoprotein) exhibited similar protection as wild-type controls [274]. However, in that study, tumour protection was reported only up to 50 days post-tumour challenge. Similarly, I observed that following intravenous challenge with B16-OVA,

FtDKO mice were protected similar to wild-type controls when observed a few weeks after tumour challenge. However, FtDKO mice succumbed to tumours at later time-points at a faster rate relative to wild type controls. Nevertheless, the protection against metastatic tumour challenge appeared to be less severely compromised in FtDKO mice (Figure 16). This may be attributed to previous observations that T cell homing to non-lymphoid organs such as lung and liver remains efficient in the absence of selectin ligand interactions.

5.2-03 Response to LM-OVA infection in FtDKO mice

Previously it was shown that FtDKO mice exhibit similar kinetics of clearance of *Mycobacterium tuberculosis* and lymphocytic choriomeningitis virus infections in visceral organs [67,277], despite a disparate frequency of $CD8^+$ T cells in the lymph node but similar frequencies in other organs [68,274,277]. My results show that FtDKO mice had significantly decreased splenic burden of LM-OVA as early as 1 day after infection (Figure 20). However, this did not result in reduced priming of $CD8^+$ T cells, as evident by the efficient antigen-presentation by splenic DCs of FtDKO mice (Figure 22). Furthermore, FtDKO mice had more double the splenocytes compared to wild type (Figure 21). Similar observations were made previously as this strain of mice has significant increases in circulating leukocytes and monocytes [66,67]. Moreover, 7 days after LM-OVA infection, FtDKO mice had significantly higher frequencies of blood resident $OVA_{257-264}$ specific $CD8^+$ T cells (Figure 17). Overall, the enhanced innate immune response combined with an uncompromised $CD8^+$ T cell response seen in the spleens and livers of FtDKO mice may have contributed to accelerated clearance of LM-OVA that shows natural tropism for spleen and liver.

5.2-04 Homeostasis of CD8$^+$ T cells in FtDKO mice

The ability of T_{CM} cells to afford superior long-term tumour protection has been attributed to their improved homeostatic proliferation. I therefore postulated that the lack of selectin/ligand interactions may impede memory CD8$^+$ T cell homeostasis. However, I often observed an increased proliferation of FtDKO $OVA_{257-264}$ specific CD8$^+$ T cells compared to wild type when cultured *in vitro* with cytokines IL-7 and IL-15 (Figure 23). Furthermore, the frequency of $OVA_{257-264}$ specific CD8$^+$ T cells remained similar between vaccinated FtDKO and wild type mice up to day 126. Increased homeostasis of memory CD8$^+$ T cells in FtDKO mice *in vivo* may be triggered by the lymphopenic environment of the low density lymph nodes [67]. However, it is unclear how selectin-ligand deficiency may modulate homeostatic proliferation *in vitro*. As CD8$^+$ T cells can express both selectin ligands and selectins, further study is needed to determine if T cell - T cell interactions differentially modulate proliferative ability.

5.2-05 Infiltration of FtDKO CD8$^+$ T cells into tumour

Adoptive transfer experiments were designed to determine any defects of cellular extravasation into various tissues. Following adoptive cell transfer, antigen-specific FtDKO CD8$^+$ T cells were recovered in substantially lower numbers in the tumours of wild type recipients (Figure 24). This suggests that selectin ligand deficient CD8$^+$ T cells may have an intrinsic extravasation defect. This observation agrees with an earlier study showing fewer FucTVII$^{-/-}$ $OVA_{257-264}$ specific OT.1 CD8$^+$ T cells entering an inflamed footpad compared to wild type [271]. It is however possible that the low numbers of FtDKO cells at the tumour site correlated to a reduced retention and/or replenishment of these cells over time. Indeed,

lymphoid proliferation of T cells and peripheral migration may be required for sustained tumour killing.

Schuster et al., [278] showed that naïve antigen-specific CD62L$^{-/-}$ T cells adoptively transferred to a RAG$^{-/-}$ host bearing a MC57-SIY-IND fibrosarcoma were defective in responding to tumour antigen and affording protection relative to CD62L$^{+/+}$ T cells. Selectin-ligand interactions have been shown to influence naïve T cell trafficking to LNs [43,272]. Recently it was postulated that antigen-experienced CD8^{+} T cells are able to traffic to lymphoid compartments via other non-high endothelial venules such as afferent lymph [67]. Harp et al., also reported reduced T cell egress from the lymph nodes of FtDKO resulting in enrichment of CD44^{high} CD8^{+} T memory cells [67] which may be attributed to differential recirculation of lymphocytes in a reduced cell density environment [279]. Similarly, it may be envisaged that circulating CD8^{+} T cells may migrate to highly vascularized B16-OVA tumours directly via the blood vasculature, utilizing selectin-ligand independent interactions, thus providing some level of short-term protection. Thus, the absence of selectin ligands on the FtDKO CD8^{+} T cells may have a secondary consequence of reducing their retention at the tumour site and/or abrogating sustained egress of these cells from the lymph node into the peripheral tumour, compromising long-term protection (Figure 24E). Overall, it appears that the presence of selectin ligands on both the host high endothelial venules as well as CD8^{+} T cells may be important for efficient and continued extravasation and/or retention within peripheral tumours.

5.2-06 Concluding Remarks

In the last decade, adoptive T cell transfer-based cancer immunotherapy has gained prominence in clinical trials including the use of genetically engineered T lymphocytes that

express high affinity TCRs of known cancer antigen specificity [280,281]. Furthermore, focus is shifting towards refining the qualities in a candidate anti-tumour T cell, such as increased homeostatic proliferation and increased expression of co-stimulatory molecule CD27 along with reduced expression of regulatory molecules such as KLRG-1, CD57 and Eomes such that tumour evasive properties are effectively counteracted while optimizing the functionality of anti-tumour T cells [11]. The optimization of selectin ligand interactions on $CD8^+$ T cells in adoptive transfer T cell preparations may be yet another important criterion for maintenance of a long-term anti-tumour $CD8^+$ T cell response.

5.3 Archaeosomes as models for understanding the properties of anti-tumour $CD8^+$ T cells

In the previous sections, I discussed the role of $CD8^+$ T_{CM} cells, selectin ligand interactions and the manner in which vaccine vectors may influence these parameters, thus impacting immunotherapy. However, a central concern in many cancer immunotherapy clinical trials has been inability to explain the reason for recurrence of tumours following an initial period of remission. Archaeosomes are potent inducers of $CD8^+$ T cell immunity and can also break tolerance to cancer self antigen [104]. Archaeosomes also rival live vectors such as LM-OVA in the potency of the $CD8^+$ T cell response but can also be advantageously utilized in multiple vaccination regimens without the development of anti-vector antibody responses. Therefore, archaeosomes constituted a convenient antigen delivery system to address the mechanisms of $CD8^+$ T cell activation and dysfunction in a tumour environment. A fundamental immunological question in the context of cancer immunotherapy is: what is the maximal threshold of antigen-specific $CD8^+$ T cells that can be evoked by vaccination? Archaeosomes are optimal for the inquiry of such basic vaccinology questions as they are a

non-replicating particulate vaccine delivery system whose efficacy may not be compromised with repeated boosting due to circulating neutralizing antibodies.

5.3-01 Archaeosomes and induction of $CD8^+$ T cell responses

In previous studies, various archaeosomes differing in total polar lipid sources were compared for their potency in augmenting $OVA_{257-264}$ specific $CD8^+$ T cell responses. MS archaeosomes were identified to have the appropriate mixture of core archaeol and caldarchaeol content [282,283] leading to long-term $CD8^+$ T cell memory. My studies initially confirmed these findings that upon B16-OVA tumour challenge, MS-OVA vaccinated mice induced a rapid proliferation of $OVA_{257-264}$ specific $CD8^+$ T cells (Figure 26). Interestingly, many caldarchaeol archaeosomes evoke potent T cell memory, suggesting their role in providing an antigen depot effect [284]. An additional feature of MS lipids is that they are high in archaetidylserine headgroups [200], allowing receptor mediated endocytosis via the Phosphatidylserine (PS) receptor on APCs [167]. Following PS-receptor mediated endocytosis, acidification of the phagosome facilitates fusion of the archaeosome membrane with phagosomes leading to expulsion of antigen into the cytosol, and subsequently TAP-mediated processing and MHC-class I presentation of antigen occurs [167]. However, as antigen entrapped in *M. smithii* also evokes antibody responses and T helper cells, it appears that some degradation of the archaeosomes occurs in the endosome as well, allowing release of antigenic material for loading onto MHC-class II molecules. Directing antigenic presentation towards MHC-class I evokes a strong $CD8^+$ T cell response by archaeosomes and favours strong anti-tumour responses [201]. While, my studies describe the potency of MS archaeosomes in a prophylactic setting, other archaeosomes types lacking caldarchaeol lipids also evoked strong anti-tumour responses (Figure 26). Therefore, it appears that the minimal

threshold of $CD8^+$ T cell numbers required for prophylactic protection against B16 tumours may have been reached even with other archaeosome types, thus masking any additional benefit of potent T cell activation by MS archaeosomes. Prophylactic tumour protection, not unlike protection against infection, may require substantially low quantitative levels of $CD8^+$ T cells; however, the therapeutic protection against a rapidly growing tumour may require high levels of $CD8^+$ T cells.

5.3-02 Maintenance of effective anti-tumour $CD8^+$ T cell response in a tumour environment

It has been shown in numerous studies that the presence of anti-tumour $CD8^+$ T cells within a tumour is a positive prognostic factor [10,240,215]. In line with this, I observed that therapeutic treatment with MS-OVA, 3 to 4 days after tumour inoculation caused tumour burden to decrease to an undetectable size within 11 days (Figure 27). Furthermore, a tumour-free period was maintained for 10-15 days followed by a gradual re-growth of tumour. While the delay in tumour recurrence was substantial, it highlights the less than optimal benefit for long term host survival. I therefore first examined if the induction of large frequencies of anti-tumour $CD8^+$ T cells could be achieved by repeated booster vaccinations. Prime-boost regimes often utilize different adjuvants to induce maximal cell-mediated immunity [285,286]. However, previous studies have demonstrated that archaeosomes work effectively for both priming and boosting and there is no benefit of an alternate adjuvant [104,203]. My data reveals that while priming and boosting resulted in increased frequencies of $CD8^+$ T cells, overall tumour protection in the therapeutic setting did not significantly improve compared to a single dose vaccine.

The therapeutic treatment of tumour bearing mice treated with 1, 2 or 3 MS-OVA injections resulted in a similar rate of tumour occurrence, regardless of boosting interval or

$OVA_{257-264}$ specific $CD8^+$ T cell frequency (Figure 27A). To amplify any differences in tumour protection between treatment regimes, I reduced the initial tumour challenge. While the onset of tumour was expectedly delayed following challenge with 10^5 versus 10^6 B16-OVA cells, no difference in vaccine efficacy could be achieved (Figure 29A). In all vaccination scenarios, providing an MS-OVA booster vaccination increased the frequency of circulating $OVA_{257-264}$ specific $CD8^+$ T cells, however tumours still returned (Figure 27B and 29B). While generating a high frequency of tumour specific $CD8^+$ T cells is a good initial step towards combating a growing tumour, it appears that treatment regimes must be further refined or supplemented to enhance $CD8^+$ T cell function by minimizing evasive mechanisms at play.

5.3-03 Role of PD-1 in cancer immunotherapy

Immune suppressive mechanisms can be evoked to reduce the effectiveness of anti-tumour $CD8^+$ T cells. One such mechanism includes the upregulation of PD-1 on $CD8^+$ T cells. PD-1 is known to be expressed on a subpopulation of $CD4^-$ $CD8^-$ T cells in the thymus, is transiently expressed on some early activated T cells [53,287] as well as upregulated on chronically activated exhausted $CD8^+$ T cells in LCMV [288], Hepatitis C [289] and HIV models [290–292]. It has also been shown that PD-1 is upregulated on exhausted persistently stimulated $CD8^+$ T cells [293,294], including tumour infiltrating $CD8^+$ T cells [113,295]. Using a blocking antibody against PD-1 can rescue $CD8^+$ T cell lytic abilities [114]. Mice treated therapeutically with MS-OVA successfully suppressed tumour for a short window, however when tumour returned, $CD8^+$ T cells located within the tumour tissue, spleen and lymph nodes notably exhibited high levels of PD-1 expression (60-75 %) (Figure 36). The percentage of PD-1 on $OVA_{257-264}$ specific $CD8^+$ T cells was increased in the tumours of

MS-OVA versus LM-OVA vaccinated mice. These increases of PD-1 expression on $CD8^+$ T cells highlight a possible cause for relapse of tumour growth in this vaccination scenario. Many strategies to reduce the effects of PD-1 signaling in tumour reactive $CD8^+$ T cells are being investigated and some are currently in Phase I and Phase II clinical trials [131,140]. Targeting PD-1 expression on $CD8^+$ T cells has been shown to reverse exhaustion thereby enhancing lytic capabilities [294,296,297]. Conversely, targeting PD-L1 and PD-L2 on APCs and tumour cells has also been shown to increase T cell activation [298] and cytolytic activity [297]. PD-1 blocking antibodies have been shown to rescue $CD8^+$ T cell function in both mice and human assays [115,294,299]. A feature of antibody mediated immune manipulations is that it's a non-self-replicating tool with a short half life, administration of which can be easily regulated in a clinical setting. A drawback for the use of pan-PD-1 antibodies is that PD-1 will become impaired on all $CD8^+$ T cells including those that are inherently inhibited to provide peripheral tolerance and avoid autoimmunity. When blocking antibodies were delivered in clinical trials against an inhibitory T cell co-stimulatory molecule, CTLA-4 [300], patients developed immune-related adverse events such as colitis/diarrhea, dermatitis, hepatitis, nephritis, and inflammatory myopathy [301]. While treatment strategies such as use of corticosteroids are in place to counteract autoimmune events, an alternate method is the use of PD-1 siRNA introduced directly into tumour reactive $CD8^+$ T cells by stable transduction with a retrovirus [296]. This technique limits the PD-1 blockade to tumour reactive $CD8^+$ T cells and represents a promising technique to supplement current therapeutic adoptive T cell therapies.

5.3-04 Role of T_{regs} cells in cancer immunotherapy

Another mechanism of tumour evasion is the activation and recruitment of T_{regs} cells that impair cytolytic $CD8^+$ T cells. From a perspective of peripheral tolerance T_{regs} have an important role in limiting cytotoxic T cell responses to keep inflammation in check and prevent harmful autoimmunity [302]. Thus, the collateral damage caused by T_{regs} inadvertently can compromise the function of self-specific anti-tumour $CD8^+$ T cell responses [303]. Additionally, T_{regs} can become activated and recruited during chronic infections, a fail-safe regulatory mechanism to limit the damaging effects of inflammation induced with an ever-present pathogen and constant antigen exposure [259,262]. Interfering with T_{reg} action has been shown to restore cytolytic $CD8^+$ T cell function and their anti-tumour abilities [100–102,117,304,305]. I also observed that T_{regs} were recruited to the lymph nodes of chronically ST-OVA infected B6129F1 mice with a 2-fold increase in the frequency of T_{regs} of all CD4s. Acute infection with LM-OVA also caused an early increase in the frequency of T_{regs} but contraction occurred quickly (Figure 12). This suggests that the use of live vectors for cancer therapy might activate inducible T_{regs} thus dampening vector efficacy.

T_{regs} are defined by a number of cell surface markers including CD25, which is the alpha subunit of the IL-2 receptor and is upregulated during T cell activation. Antibody depletion of CD25 to delete T_{regs} is currently being investigated in combination with immunotherapy to augment sustained T cell proliferation and tumour cytotoxicity [102,305]. I also observed that depletion of T_{regs} with anti-CD25 antibody prior to therapeutic treatment of tumours with MS-OVA lengthened the tumour-free period (from 31 to 40 days) compared to non-anti-CD25 depleted mice (Figure 38).

Recently, it was shown that whole body radiation prior to ACT augments the anti-tumour responsiveness of transferred cells. While a reduction of T cells by lymphoablation

provides room for an increased proliferation of transferred T cells, irradiation also removes T_{regs} that would otherwise impair the cytotoxicity of transferred T cells [11,216]. In pre-clinical studies with mice and humans, the anti-CD25 antibody Daclizumab® depletes $CD25^+$ $Foxp3^+$ $CD4^+$ T cells from the blood for at least 3 weeks [303]. Unfortunately, a recent clinical trial with Daclizumab® showed effective depletion of $CD25^{high}$ immune cells but no overall improvement in T cell activation and cytotoxicity after DC vaccination [306]. As the antibody is detectable up to 3 weeks after treatment, DC therapy (provided 4 or 8 days later) was likely impaired as residual anti-CD25 would prevent the formation of IL-2 receptor complex, and impair $CD8^+$ T cell proliferation [307]. Thus, it is important to balance the advantages of T_{reg} removal with the disadvantageous removal of activated T cells when designing optimal anti-CD25 treatment regimens. The use of short-lived anti-CD25 antibodies might prove more successful in tumour immunotherapy treatments.

5.3-05 Therapeutic tumour protection by MS-OVA versus LM-OVA

A longer period of tumour protection was conferred by LM-OVA versus MS-OVA treatment. The peak of $CD8^+$ T cell frequency for both treatments was similar at around 20 % (Figure 31 & 32). Therefore, the difference in protection could not be attributed to a higher initial $OVA_{257-264}$ specific $CD8^+$ T cell frequency. Since MS-OVA was administered twice after tumour, the frequency of $OVA_{257-264}$ specific $CD8^+$ T cells persisted at a higher number by day 20 compared to LM-OVA treated mice. LM-OVA induced $OVA_{257-264}$ specific $CD8^+$ T cells underwent a relative fast contraction in the blood and generated a predominant IL-7Rα^{high} $CD62L^{high}$ T_{CM} memory response. In contrast, MS-OVA induced $OVA_{257-264}$ specific $CD8^+$ T cells maintained a low surface expression of CD62L in the blood, but high IL-7Rα, indicative of the generation of a T_{EM} response. Previously, Krishnan

et al., have shown that MS-OVA vaccination alone, evokes a balanced T_{EM} versus T_{CM} phenotype of memory $CD8^+$ T cells, in contrast to LM-OVA that predominantly evokes T_{CM} cells [165]. Quick contraction of $OVA_{257-264}$ specific $CD8^+$ T cells after therapeutic LM-OVA infection could occur as a result of an anti-vector response that limits the exposure of OVA antigen, driving T_{CM} formation (Figure 32). On the other hand, archaeosomes are quite stable, lasting upwards of 90 days when injected s.c. [308]; a low constant delivery of OVA antigen could be responsible for maintaining a higher frequency of effector $OVA_{257-264}$ specific $CD8^+$ T cells (Figure 31). Additionally, since tumour burden was noticeably greater on MS-OVA treated animals at earlier time-points, tumour derived OVA antigen could also drive $OVA_{257-264}$ specific $CD8^+$ T cells to adopt a $CD62L^{low}$ phenotype, similar to what was observed during chronic ST-OVA infection (Figure 9). Overall, my results suggest that even in a therapeutic setting, where the presence of a large number of antigen-specific $CD8^+$ T cell effectors has been considered beneficial for rapid tumour control, T_{CM} cells appear to provide superior protection.

Interestingly, the frequency of $OVA_{257-264}$ specific $CD8^+$ T cells was higher in the tumour of MS-OVA versus LM-OVA treated mice (Figure 33). Since LM-OVA treated mice survived longer, the mere presence of more $OVA_{257-264}$ specific $CD8^+$ T cells did not correlate with enhanced tumour protection. The expression of IL-7Rα on $OVA_{257-264}$ specific $CD8^+$ T cells (Figure 34) occurred predominantly within lymphoid compartments as did CD62L expression (Figure 35) and was similar between MS-OVA and LM-OVA vaccinated mice (except IL-7Rα expression in the blood). Therefore, the differences in memory $CD8^+$ T cell phenotypes observed in the blood did not correlate with any differences in the spleen and lymph nodes. Rather it is likely that other factors are at play to limit the effectiveness of anti-tumour $OVA_{257-264}$ specific $CD8^+$ T cells.

Additional factors associated with LM-OVA infection that could positively affect $CD8^+$ T cell activity include upregulation of IL-21 [309], IL-12 or IL-23 [310]. Whether these attributes aided sustained tumour protection in LM-OVA versus MS-OVA treated mice requires further study.

5.3-06 Timing of priming and boosting in cancer immunotherapy

In initial studies, priming and boosting with MS-OVA was done on day 3 and day 8 after tumour challenge. I surmised that the timing of the MS-OVA booster vaccination may have been too early to propagate large numbers of $OVA_{257-264}$ specific $CD8^+$ T cells. Indeed, an *in vivo* cytotoxic assay confirmed that in the absence of tumour, a second dose of MS-OVA at an early time-point (5 days after priming) reduced the maintenance of $CD8^+$ T cell cytotoxicity, whereas delaying the second dose to a later time-point (21 days later) maintained cytotoxicity at ~100 % killing even up to 23 days after the booster dose (Figure 37). Thus, I first rationalized that delaying the boosting in tumour bearing animals may rescue loss of $CD8^+$ T cell cytotoxicity.

Therefore, the timing of the booster vaccination was delayed from 5 to 21 days post primary vaccination. However, tumour bearing mice exhibited a drop in *in vivo* cytolytic activity with an early or late boost of MS-OVA. Similarly, tumour protection was not enhanced in late versus early boosted mice. Delaying a booster vaccination in a tumour bearing mouse by 2 weeks could fail because tumour burden is much too large to control at this late stage, therefore maximizing the $CD8^+$ T cell response early on has clear advantages, reinforcing the need to design better prime and boost regimes. An alternate strategy to be explored involves the use of small exposures to antigen during priming. The exposure to small amounts of antigen with DNA-protein vaccines or antigen coated microspheres,

generates a low level priming phase which can be rapidly expanded with an early boost [52,53]. It was suggested that the acquisition of cell surface inhibitor molecules (PD-1, CTLA-4 and Lag-3) during activation might lessen the boost-ability of potent $CD8^+$ T cell responses. The aforementioned vaccines prime a $CD8^+$ T cell response that maintain an IL-7Rα^{high} or $CD62L^{high}$, PD-1^{low}, CTLA-4^{low} and Lag-3^{low} phenotype and are responsive to early boosting. Thus, future work focusing on reducing the priming dose, and monitoring the phenotype of primed $CD8^+$ T cells could augment improved anti-tumour $CD8^+$ T cell responses by archaeosomes.

5.3-07 Maximum threshold of vaccine-induced $CD8^+$ T cell immunity

A central challenge for vaccinologists is to create a $CD8^+$ T cell response with maximal potency. By utilizing archaeosomes, I queried whether the $CD8^+$ T cell numbers may be continually increased with repeated dose vaccines. MS-OVA is a unique delivery system that elicits no known anti-lipid immune responses and is capable of homologously boosting $CD8^+$ T cell responses substantially more than a second injection of LM-OVA, a potent primary $CD8^+$ T cell inducer [203]. Therefore, in a prophylactic model, I repeatedly vaccinated mice with MS-OVA to induce a maximal frequency of $OVA_{257-264}$ specific $CD8^+$ T cells and compared the responses with multiple LM-OVA doses.

Priming and boosting with LM-OVA (at 21 day intervals) expanded $OVA_{257-264}$ specific $CD8^+$ T cell responses to ~15 % of all circulating $CD8^+$ T cells (Figure 39). Comparatively, priming and boosting with MS-OVA expanded circulating $OVA_{257-264}$ specific $CD8^+$ T cells frequency to ~30 %, 7 days post the 3rd vaccination. Notably, a 4th and 5th vaccination did not further increase T cell responses past ~30 %. The factors that limit continuous T cell expansion may include T cell suppressive mechanisms such as PD-1

expression and T_{reg} activation as is reported for chronic antigen exposure. Alternately, there may be a maximum quantitative threshold of $CD8^+$ T cell activation as they compete for interactions with APCs and cytokine growth factors for proliferation. Another possibility is that later vaccinations were introduced too early; after each immunization the length of time it takes to regain CD62L expression increases (Figure 40); T cells with a decreased level of cell surface CD62L have decreased proliferative potential than their counterparts. Therefore, delaying the booster shot could allow for the generation of T cells with a greater proliferative potential, further expanding the $OVA_{257-264}$ specific $CD8^+$ T cell frequency.

In order to address this, the booster shots were staggered in a second study. After confirmation of the upregulation of CD62L on $OVA_{257-264}$ specific $CD8^+$ T cells, vaccinations were given at day 0, 29 and 89 (Figure 42). Antigen specific $CD8^+$ cell frequencies were detectable at a similar frequency of 30 %, 7 days post the 3rd vaccination. Notably at 10 days post the 3rd vaccination, the frequency was at 40-60 %. Overall, delaying the 3rd MS-OVA vaccination did not further increase the frequency of $OVA_{257-264}$ specific $CD8^+$ T cells. It is possible that a maximum threshold for $CD8^+$ T cell activation is an evolutionary host adaptation that ensures tissue homeostasis and readiness to respond to multiple pathogens at all times.

5.3-08 Multiple dose vaccines and CD62L expression on $CD8^+$ T cells

In addition to generating a higher number of tumour specific $CD8^+$ T cells, the memory phenotype is thought to be important for the overall anti-tumour immune response. Previously, I have shown that when memory $OVA_{257-264}$ specific $CD8^+$ T cell frequencies are similar and CD62L expression is low or their ligand is absent, long lasting tumour protection is impaired. At late time-points (>200 days) after a single dose of MS-OVA or LM-OVA, a

low frequency of $OVA_{257-264}$ specific $CD8^+$ T cells remain (~0.1 %) and they are predominantly $CD62L^{high}$. Conversely, multiple doses of MS-OVA or LM-OVA induce higher frequencies of $OVA_{257-264}$ specific $CD8^+$ T cells that are predominantly $CD62L^{low}$. Nevertheless, vaccinated mice receiving single or multiple vaccine doses were equally protected (significantly greater than control) when tumour challenge occurred 323 days post initial vaccination. This highlights the potency of 0.1 % circulating $OVA_{257-264}$ specific $CD8^+$ T_{CM} cells (Figure 41). While protection was equal between mice vaccinated once, twice or three times, both groups succumbed to tumour challenge ultimately. This suggests that aging of the mice could have been a confounding factor that lessened T cell responses as older mice are known to have increased numbers of T_{regs} and myeloid suppressor cells [123,311–314]. Nevertheless, a single vaccination with LM-OVA or MS-OVA was capable of providing protection from tumour at this late challenge date, similar to what was achieved with multiple vaccinations that yield a higher frequency of circulating $OVA_{257-264}$ specific $CD8^+$ T cells. This reinforces the idea that even a low frequency of tumour reactive $CD8^+$ T cells of the T_{CM} phenotype can provide protection from tumour. In a separate experiment, mice were vaccinated with MS-OVA at staggered intervals and tumour challenge was introduced much earlier at 216 days post initial vaccination. Again, a single vaccination was capable of mediating long term protection with 1 out of 4 mice completely free of tumour up to 150 days post challenge (Figure 43). Staggering the 3rd dose of MS-OVA vaccination regime did not induce a substantially greater frequency of $OVA_{257-264}$ specific $CD8^+$ T cells, however it facilitated maintenance of a greater proportion of $CD62L^{high}$ (~45 %), T_{CM} cells. This may explain why in this early tumour challenge scenario triply vaccinated mice were protected substantially longer than mice receiving one or two vaccinations. Notably, even though greater proportions of $CD62L^{high}$ $OVA_{257-264}$ specific $CD8^+$ T cells were found with

doubly vaccinated mice (80 %), the frequency of $OVA_{257-264}$ specific $CD8^+$ T cells was 3 times less. Overall, neither a high frequency of $OVA_{257-264}$ specific $CD8^+$ T cells nor a high proportion of T_{CM} cells could solely confer prolonged tumour protection, suggesting a balanced quantity and quality of anti-tumour $CD8^+$ T cells may be optimum for long-term prophylactic immunity.

5.3-09 $CD8^+$ T cell frequency after tumour challenge

Attributing $CD62L^{high}$ $OVA_{257-264}$ specific $CD8^+$ T cells with a greater capacity to provide longer lasting tumour protection relates to their lymphoid migratory properties and proliferative potential when re-confronted with antigen in the context of tumour. Typically, a $CD62L^{high}$ $OVA_{257-264}$ specific $CD8^+$ T cell will reside in lymphoid compartments, interact with its cognate antigen on an APC and proliferate to generate effectors to circulate and combat the tumour. As such, it might be expected that a successful anti-tumour immune response will result in a high frequency of circulating $OVA_{257-264}$ specific $CD8^+$ T cells after tumour challenge. Upon tumour challenge of MS-OVA vaccinated mice, the proliferation of $OVA_{257-264}$ specific $CD8^+$ T cells does occur, however higher frequencies are reached in mice that eventually succumb to tumour burden (Figure 44). Large antigen depots associated with tumour growth could account for the continued $CD8^+$ T cell proliferation. However, in this scenario the timing of activation of $CD8^+$ T cells may be critical. If a large tumour burden drives increased T_E frequencies, it might be too late for tumour elimination. Additionally, tumour evasive properties are probably fine-tuned to be activated in the wake of a profound T_E response which may limit cytolytic functions. An interesting observation I made was that mice that survived tumour challenge did not regain a $CD62L^{high}$ phenotype of $CD8^+$ T cells in the blood faster than mice that succumbed to tumour burden. Overall,

these studies highlight the complexity of a two-way cross-regulation between host immunity and a rapidly growing tumour.

5.3-10 Archaeosomes and other particulate vaccine delivery systems

Archaeosomes are capable of inducing anti-tumour $CD8^+$ T cell responses even in the presence of tumour, however their usefulness in combating a tumour in both a prophylactic and therapeutic setting are confounded by tumour induced immune evasive mechanisms. This is the case for most anti-tumour therapies and is why combinatorial approaches must be employed to simultaneously enhance functionality of vaccine induced $CD8^+$ T cells while inhibiting regulatory mechanisms. A key advantage of archaeosomes is their ability to self-adjuvant vaccine responses. Indeed, many other particulate vaccines such as conventional liposomes, polymeric microspheres, nano-beads, virus-like particles, saponin-immunostimulating complexes (ISCOMS), niosomes and proteosomes [315–318] require extraneous PAMP additives to adjuvant T cell responses.

While live vaccines derived from viral or bacterial vectors have thus far been the best choice for the induction of $CD8^+$ T cell responses, particulate vaccines can offer many advantages. Firstly, attenuated live vectors can potentially revert to a more virulent phenotype while particulate vectors such as archaeosomes inertly facilitate long-term memory. Secondly, particulate archaeosomes are not associated with overt inflammation that can lead to the attenuation or deletion of T cells [203]. Liposomes have also been used with anchored targeting molecules directing them towards tumour sites to enhance or for drug delivery [319,320].

The combination of drug therapy with $CD8^+$ T cell vaccines can have a synergistic affect when the immunogenicity of tumours can be enhanced. Administration of a

chemotherapeutic drug 5-aza-2-deoxycitidine increases tumour MHC-class I expression as well as some tumour antigens, enhancing survival of tumour bearing mice [321,322]. Therefore, co-administration of chemotherapeutic treatments such as 5-aza-2-deoxycitidine with a tumour vaccine has the potential to expose tumour antigens for T cell recognition thus aiding tumour regression. Other combinatorial anti-tumour therapies have been attempted by combining the pro-inflammatory GM-CSF with dendritic cell therapy, which is accredited as the first successful FDA approved therapeutic cancer vaccine, Sipuleucel-T [219,220]. GM-CSF has also been combined with IL-2, IL-15 or IL-21 [321,322] and vaccinia virus [323] to enhance tumour therapy. Since previous studies have shown that liposomes can enhance bioavailability of entrapped cytokines [324,325], the encapsulation of GM-CSF within archaeosomes with tumour antigen may be a promising approach that requires further investigation.

5.3-11 Concluding Remarks:

MS-OVA constitutes a unique $CD8^+$ T cell stimulating vaccine that can be used in homologous prime boost vaccinations to trigger a high frequency of antigen specific effector $CD8^+$ T cells with a long lived memory phase. While MS-OVA vaccination has great potential to induce tumour ablative immune responses, it can be limited by immunosuppressive events such as the upregulation of PD-1 or actions of T_{regs}. Further investigation into the factors that limit potent cytotoxic $CD8^+$ T cells from combating tumour, such as the expression of FasL or Lag-3, and employing strategies to block them may be the logical next step for optimizing archaeosome-based cancer immunotherapy. My studies also highlight that repeated vaccination may not provide benefit in cancer immunotherapy due to the overall limitation in the frequency of $CD8^+$ T cells that can be

evoked, the phenotypic proportions and modulation of other immune regulatory pathways [53,81,129,294].

6.0 CONCLUSION:

Overall, my studies reveal the importance of evoking the appropriate phenotype of $CD8^+$ T cells and not immediate functionality. Thus, when designing $CD8^+$ T cell inducing vaccinations against cancer, one must consider the memory $CD8^+$ T cell phenotype and strive to induce large numbers of a predominant T_{CM} phenotype. Fast proliferation and lymphoid migratory properties of memory $CD8^+$ T cells correlate strongly with tumour protection whereas immediate cytotoxicity may not be sufficient. Additionally, therapeutic $CD8^+$ T cell treatments against cancer require strategies for removing the regulatory road-blocks of immune activation; suppressors of $CD8^+$ T cell cytotoxicity. Inducing large numbers of TILs alone does not confer superior tumour protection due to the actions of suppressive mechanisms like PD-1 engagement or the actions of T_{regs}. The overall findings of my thesis with regards to $CD8^+$ T cell quality following vaccination or treatment with LM-OVA, ST-OVA and MS-OVA are summarized in Figure 45.

Advances in $CD8^+$ T cell priming regimens shed light on the quality of T cell priming. For example, use of a low antigen dose with a DNA adjuvant decreases PD-1 expression and induces early T_{CM} formation.[53] Therefore, further investigation into alternate methods of T cell priming such as the use of BCG vectors or vaccinating with a decreased amount of entrapped OVA antigen in archaeosomes may allow for a sustained long-term anti-tumour response. Recently, $CD8^+$ T cell immunotherapy for cancer treatment has distinctly shifted focus towards removing mediators of T cell suppression. For example, generalized lymphodepletion prior to adoptive T cell transfer significantly lengthened tumour protection [216,326,327]. The isolation of TILs, conditioning *ex vivo*, and delivery back to

the patient have conferred substantial anti-tumour responses in clinical trials [216,326,327]. However, TILs are not found in all tumours, and not all tumours are accessible for removal and culturing; therefore alternate methods of generating tumour reactive T cells must be explored. This thesis highlights the potential of vaccine induced anti-tumour $CD8^+$ T cells and I think that vaccines in combination with lymphodepletion or immunosuppression blockers may have the potential to act synergistically to induce tumour regression and minimize the interference of immunosuppressive mechanisms.

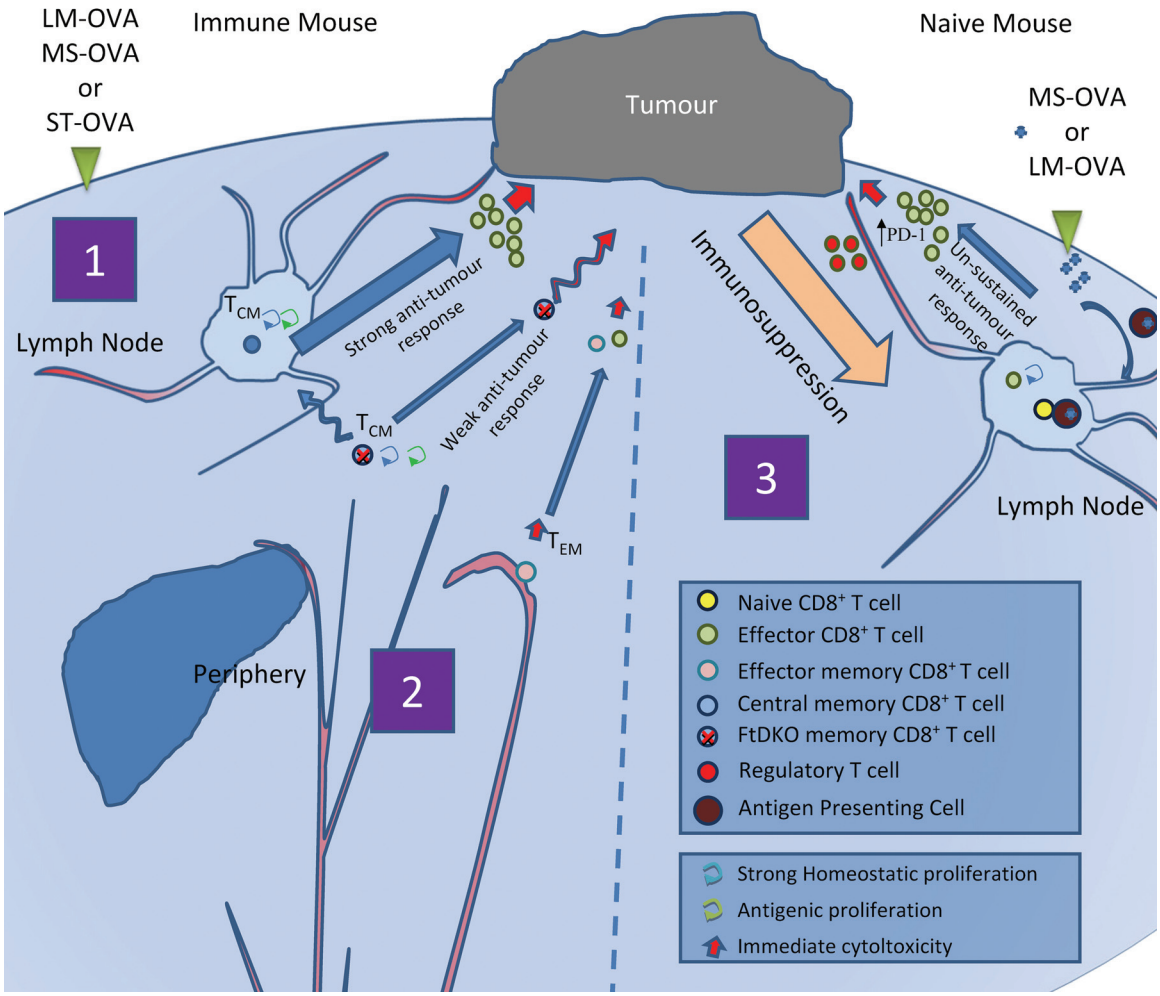

FIGURE 45: Properties of vaccine induced immunity to cancer
This figure describes the factors that limit successful vaccination against tumour (*Left*) and treatment of tumour (*Right*) using LM-OVA, ST-OVA or MS-OVA.

1. The generation of CD62L^{high} IL-7Rα^{high} CD8$^+$ T cell (T_{CM}) cells by LM-OVA or MS-OVA vaccination correlated with long lasting anti-tumour immunity.
2. The generation of T_{EM} cells by ST-OVA vaccination correlated with short lived anti-tumour immunity.
3. Treatment of tumour with MS-OVA induced a high frequency of anti-tumour CD8$^+$ T cells that initially reduced tumour burden, but tumour returned. Immunosuppressive mechanisms such as CD8$^+$ T cell PD-1 upregulation and T_{reg} suppression were observed.

Adoptively transferred T_{CM} conferred longer lasting tumour protection compared to T_{EM}. Importantly, T_{CM} are attributed with having a better ability to proliferate homeostatically as well as in response to tumour antigen and are found within lymphoid organs while T_{EM} are predominantly found in the periphery. The vaccination of selectin ligand deficient mice (FtDKO mice) with LM-OVA did not confer a similar level of tumour protection compared to wild type. This indicated that selectin-ligand engagements of T_{CM} might have functional importance for anti-tumour immunity. Interestingly, anti-tumour $CD8^+$ T cells in FtDKO mice were unable to be maintained within lymph nodes, and were found to have a decreased presence in the tumour indicating a role of selectin ligand interactions in the extravasation or maintenance of tumour specific $CD8^+$ T cells in these locations.

One vaccination of MS-OVA induces a small frequency of $OVA_{257-264}$ specific $CD8^+$ T cells (0.2 %) of the T_{CM} phenotype and is capable of mediating significant tumour protection compared to control even a year after vaccination. This highlights the potency and longevity of the T_{CM} response in combating tumour.

While repeated MS-OVA vaccinations after tumour significantly increased the frequency of tumour specific $CD8^+$ T cells, it did not correlate to longer lasting tumour protection compared to one MS-OVA vaccination. The expression of PD-1 was found to be upregulated on tumour infiltrating tumour-specific $CD8^+$ T cells and could explain the lack of tumour protection and cytotoxicity of $CD8^+$ T cells in tumour bearing mice. Additionally, the depletion of CD25 (found on T_{regs}) prior to tumour challenge and MS-OVA treatment increased the median survival from 31 to 40 days indicating that T_{regs} might play a role to suppress tumour reactive $CD8^+$ T cells during MS-OVA treatment.

References:

1. Murphy, K., Travers, P. & Walport, M.*Immunobiology: The Immune System in Health and Disease. 7th Edition.* 13. Chapter 1-8 (2008).
2. Murphy, K., Travers, P. & Walport, M.*Immunobiology: The Immune System in Health and Disease. 7th Edition.* 83. Chapter 2-23 (2008).
3. Murphy, K., Travers, P. & Walport, M.*Immunobiology: The Immune System in Health and Disease. 7th Edition.* 5. Chapter 1-2. (2008).
4. Murphy, K., Travers, P. & Walport, M.*Immunobiology: The Immune System in Health and Disease. 7th Edition.* 23-27. Chapter 1-17. (2008).
5. Kew, O.M., Sutter, R.W., de Gourville, E.M., Dowdle, W.R. & Pallansch, M.A. Vaccine-derived polioviruses and the endgame strategy for global polio eradication. *Annu. Rev. Microbiol* **59**, 587-635 (2005).
6. Burton, D.R. Antibodies, viruses and vaccines. *Nat. Rev. Immunol* **2**, 706-713 (2002).
7. Zinkernagel, R.M. Maternal antibodies, childhood infections, and autoimmune diseases. *N. Engl. J. Med* **345**, 1331-1335 (2001).
8. Murphy, K., Travers, P. & Walport, M.*Immunobiology: The Immune System in Health and Disease. 7th Edition.* 135-137. Chapter 3-18. (2008).
9. Taniguchi, M., Tashiro, T., Dashtsoodol, N., Hongo, N. & Watarai, H. The specialized iNKT cell system recognizes glycolipid antigens and bridges the innate and acquired immune systems with potential applications for cancer therapy. *Int. Immunol* **22**, 1-6 (2010).
10. Naito, Y. *et al.* CD8+ T cells infiltrated within cancer cell nests as a prognostic factor in human colorectal cancer. *Cancer Res* **58**, 3491-3494 (1998).
11. Klebanoff, C.A., Gattinoni, L. & Restifo, N.P. CD8+ T-cell memory in tumor immunology and immunotherapy. *Immunol. Rev* **211**, 214-224 (2006).
12. Mestas, J. & Hughes, C.C.W. Of Mice and Not Men: Differences between Mouse and Human Immunology. *The Journal of Immunology* **172**, 2731 -2738 (2004).
13. Murphy, K., Travers, P. & Walport, M. *Immunobiology: The Immune System in Health and Disease. 7th Edition.* (Garland Science: New York., 2008).
14. Murphy, K., Travers, P. & Walport, M.*Immunobiology: The Immune System in Health and Disease. 7th Edition.* 339-340. Chapter 8-9. (2008).
15. Murphy, K., Travers, P. & Walport, M.*Immunobiology: The Immune System in Health and Disease. 7th Edition.* 342. Figure 8.16. (2008).
16. Aderem, A. & Ulevitch, R.J. Toll-like receptors in the induction of the innate immune response. *Nature* **406**, 782-787 (2000).
17. Creagh, E.M. & O'Neill, L.A.J. TLRs, NLRs and RLRs: a trinity of pathogen sensors that co-operate in innate immunity. *Trends in Immunology* **27**, 352-357 (2006).
18. Martinon, F. & Tschopp, J. NLRs join TLRs as innate sensors of pathogens. *Trends Immunol* **26**, 447-454 (2005).
19. Seth, R.B., Sun, L. & Chen, Z.J. Antiviral innate immunity pathways. *Cell Res* **16**, 141-147 (2006).
20. Murphy, K., Travers, P. & Walport, M.*Immunobiology: The Immune System in Health and Disease. 7th Edition.* 132. Chapter 3-16. (2008).
21. Murphy, K., Travers, P. & Walport, M.*Immunobiology: The Immune System in Health and Disease. 7th Edition.* 323-377. Chapter 8. (2008).

22. Murphy, K., Travers, P. & Walport, M.*Immunobiology: The Immune System in Health and Disease. 7th Edition.* 129. Chapter 3-14. (2008).
23. Murphy, K., Travers, P. & Walport, M.*Immunobiology: The Immune System in Health and Disease. 7th Edition.* 190-192. Chapter 5-7. (2008).
24. Murphy, K., Travers, P. & Walport, M.*Immunobiology: The Immune System in Health and Disease. 7th Edition.* 347. Figure 8.23 (2008).
25. Murphy, K., Travers, P. & Walport, M.*Immunobiology: The Immune System in Health and Disease. 7th Edition.* 447. Figure 10.22. (2008).
26. Jung, T.M., Gallatin, W.M., Weissman, I.L. & Dailey, M.O. Down-regulation of homing receptors after T cell activation. *J. Immunol* **141**, 4110-4117 (1988).
27. Bierer, B.E. & Burakoff, S.J. T cell adhesion molecules. *FASEB J* **2**, 2584-2590 (1988).
28. Ley, K. & Kansas, G.S. Selectins in T-cell recruitment to non-lymphoid tissues and sites of inflammation. *Nat. Rev. Immunol* **4**, 325-335 (2004).
29. Schoenberger, S.P., Toes, R.E., van der Voort, E.I., Offringa, R. & Melief, C.J. T-cell help for cytotoxic T lymphocytes is mediated by CD40-CD40L interactions. *Nature* **393**, 480-483 (1998).
30. Bennett, S.R. *et al.* Help for cytotoxic-T-cell responses is mediated by CD40 signalling. *Nature* **393**, 478-480 (1998).
31. Ridge, J.P., Di Rosa, F. & Matzinger, P. A conditioned dendritic cell can be a temporal bridge between a CD4+ T-helper and a T-killer cell. *Nature* **393**, 474-478 (1998).
32. Bourgeois, C., Rocha, B. & Tanchot, C. A role for CD40 expression on CD8+ T cells in the generation of CD8+ T cell memory. *Science* **297**, 2060-2063 (2002).
33. Janssen, E.M. *et al.* CD4+ T cells are required for secondary expansion and memory in CD8+ T lymphocytes. *Nature* **421**, 852-856 (2003).
34. Sun, J.C., Williams, M.A. & Bevan, M.J. CD4+ T cells are required for the maintenance, not programming, of memory CD8+ T cells after acute infection. *Nat. Immunol* **5**, 927-933 (2004).
35. Sun, J.C. & Bevan, M.J. Defective CD8 T cell memory following acute infection without CD4 T cell help. *Science* **300**, 339-342 (2003).
36. Shedlock, D.J. & Shen, H. Requirement for CD4 T cell help in generating functional CD8 T cell memory. *Science* **300**, 337-339 (2003).
37. Belz, G.T., Wodarz, D., Diaz, G., Nowak, M.A. & Doherty, P.C. Compromised influenza virus-specific CD8(+)-T-cell memory in CD4(+)-T-cell-deficient mice. *J. Virol* **76**, 12388-12393 (2002).
38. Sad, S. & Krishnan, L. Maintenance and attrition of T-cell memory. *Crit. Rev. Immunol* **23**, 129-147 (2003).
39. Lodolce, J.P. *et al.* IL-15 receptor maintains lymphoid homeostasis by supporting lymphocyte homing and proliferation. *Immunity* **9**, 669-676 (1998).
40. Kennedy, M.K. *et al.* Reversible defects in natural killer and memory CD8 T cell lineages in interleukin 15-deficient mice. *J. Exp. Med* **191**, 771-780 (2000).
41. Judge, A.D., Zhang, X., Fujii, H., Surh, C.D. & Sprent, J. Interleukin 15 controls both proliferation and survival of a subset of memory-phenotype CD8(+) T cells. *J. Exp. Med* **196**, 935-946 (2002).
42. Sallusto, F., Lenig, D., Förster, R., Lipp, M. & Lanzavecchia, A. Two subsets of memory T lymphocytes with distinct homing potentials and effector functions. *Nature* **401**, 708-712 (1999).

43. Arbonés, M.L. *et al.* Lymphocyte homing and leukocyte rolling and migration are impaired in L-selectin-deficient mice. *Immunity* **1**, 247-260 (1994).
44. Wherry, E.J. *et al.* Lineage relationship and protective immunity of memory CD8 T cell subsets. *Nat. Immunol* **4**, 225-234 (2003).
45. Weninger, W., Crowley, M.A., Manjunath, N. & von Andrian, U.H. Migratory properties of naive, effector, and memory CD8(+) T cells. *J. Exp. Med* **194**, 953-966 (2001).
46. Hikono, H. *et al.* Activation phenotype, rather than central- or effector-memory phenotype, predicts the recall efficacy of memory CD8+ T cells. *J. Exp. Med* **204**, 1625-1636 (2007).
47. Campbell, D.J., Kim, C.H. & Butcher, E.C. Chemokines in the systemic organization of immunity. *Immunol. Rev* **195**, 58-71 (2003).
48. Bachmann, M.F., Wolint, P., Schwarz, K. & Oxenius, A. Recall proliferation potential of memory CD8+ T cells and antiviral protection. *J. Immunol* **175**, 4677-4685 (2005).
49. Klebanoff, C.A. *et al.* Central memory self/tumor-reactive CD8+ T cells confer superior antitumor immunity compared with effector memory T cells. *Proc. Natl. Acad. Sci. U.S.A* **102**, 9571-9576 (2005).
50. Opferman, J.T., Ober, B.T. & Ashton-Rickardt, P.G. Linear differentiation of cytotoxic effectors into memory T lymphocytes. *Science* **283**, 1745-1748 (1999).
51. Jacob, J. & Baltimore, D. Modelling T-cell memory by genetic marking of memory T cells in vivo. *Nature* **399**, 593-597 (1999).
52. Pham, N.-L.L. *et al.* Exploiting cross-priming to generate protective CD8 T-cell immunity rapidly. *Proc. Natl. Acad. Sci. U.S.A* **107**, 12198-12203 (2010).
53. Bot, A., Qiu, Z., Wong, R., Obrocea, M. & Smith, K.A. Programmed cell death-1 (PD-1) at the heart of heterologous prime-boost vaccines and regulation of CD8+ T cell immunity. *J Transl Med* **8**, 132-132
54. Arens, R. & Schoenberger, S.P. Plasticity in programming of effector and memory CD8 T-cell formation. *Immunol. Rev* **235**, 190-205 (2010).
55. van Faassen, H. *et al.* Reducing the stimulation of CD8+ T cells during infection with intracellular bacteria promotes differentiation primarily into a central (CD62LhighCD44high) subset. *J. Immunol* **174**, 5341-5350 (2005).
56. Hinrichs, C.S. *et al.* Human effector CD8+ T cells derived from naive rather than memory subsets possess superior traits for adoptive immunotherapy. *Blood* **117**, 808-814 (2010).
57. Speiser, D.E. *et al.* Rapid and strong human CD8+ T cell responses to vaccination with peptide, IFA, and CpG oligodeoxynucleotide 7909. *J. Clin. Invest* **115**, 739-746 (2005).
58. Zanetti, M., Castiglioni, P. & Ingulli, E. Principles of memory CD8 T-cells generation in relation to protective immunity. *Adv. Exp. Med. Biol* **684**, 108-125 (2010).
59. Yang, S. *et al.* In vitro generated anti-tumor T lymphocytes exhibit distinct subsets mimicking in vivo antigen-experienced cells. *Cancer Immunol Immunother* **60**, 739-749 (2011).
60. June, C.H. Adoptive T cell therapy for cancer in the clinic. *J. Clin. Invest* **117**, 1466-1476 (2007).
61. Springer, T.A. Traffic signals for lymphocyte recirculation and leukocyte emigration: the multistep paradigm. *Cell* **76**, 301-314 (1994).
62. Patel, K.D., Cuvelier, S.L. & Wiehler, S. Selectins: critical mediators of leukocyte recruitment. *Semin. Immunol* **14**, 73-81 (2002).

63. Easton, E.W., Schiphorst, W.E., van Drunen, E., van der Schoot, C.E. & van den Eijnden, D.H. Human myeloid alpha 3-fucosyltransferase is involved in the expression of the sialyl-Lewis(x) determinant, a ligand for E- and P-selectin. *Blood* **81**, 2978-2986 (1993).
64. Hwang, S.T. *et al.* GlyCAM-1, a physiologic ligand for L-selectin, activates beta 2 integrins on naive peripheral lymphocytes. *J. Exp. Med* **184**, 1343-1348 (1996).
65. Barkhausen, T., Krettek, C. & van Griensven, M. L-selectin: adhesion, signalling and its importance in pathologic posttraumatic endotoxemia and non-septic inflammation. *Exp. Toxicol. Pathol* **57**, 39-52 (2005).
66. Malý, P. *et al.* The alpha(1,3)fucosyltransferase Fuc-TVII controls leukocyte trafficking through an essential role in L-, E-, and P-selectin ligand biosynthesis. *Cell* **86**, 643-653 (1996).
67. Harp, J.R., Gilchrist, M.A. & Onami, T.M. Memory T cells are enriched in lymph nodes of selectin-ligand-deficient mice. *J. Immunol* **185**, 5751-5761 (2010).
68. Harp, J.R. & Onami, T.M. Naïve T cells re-distribute to the lungs of selectin ligand deficient mice. *PLoS ONE* **5**, e10973 (2010).
69. Wirth, T.C., Badovinac, V.P., Zhao, L., Dailey, M.O. & Harty, J.T. Differentiation of central memory CD8 T cells is independent of CD62L-mediated trafficking to lymph nodes. *J. Immunol* **182**, 6195-6206 (2009).
70. Murphy, K., Travers, P. & Walport, M.*Immunobiology: The Immune System in Health and Disease. 7th Edition.* 365-367. Chapter 8-28. (2008).
71. Rousalova, I. & Krepela, E. Granzyme B-induced apoptosis in cancer cells and its regulation (review). *Int. J. Oncol* **37**, 1361-1378 (2010).
72. Janeway, C., Travers, P. & Walport, M.*Immunobiology: The Immune System in Health and Disease. 5th Edition* Section 8-42. (2001).
73. Adrain, C., Murphy, B.M. & Martin, S.J. Molecular ordering of the caspase activation cascade initiated by the cytotoxic T lymphocyte/natural killer (CTL/NK) protease granzyme B. *J. Biol. Chem* **280**, 4663-4673 (2005).
74. Waterhouse, N.J., Sedelies, K.A. & Trapani, J.A. Role of Bid-induced mitochondrial outer membrane permeabilization in granzyme B-induced apoptosis. *Immunol. Cell Biol* **84**, 72-78 (2006).
75. Han, J. *et al.* Deregulation of mitochondrial membrane potential by mitochondrial insertion of granzyme B and direct Hax-1 cleavage. *J. Biol. Chem* **285**, 22461-22472 (2010).
76. Peter, M.E. & Krammer, P.H. The CD95(APO-1/Fas) DISC and beyond. *Cell Death Differ* **10**, 26-35 (2003).
77. Janeway, C., Travers, P. & Walport, M. *Immunobiology: The Immune System in Health and Disease. 5th Edition. Appendix II. CD Antigens.* (Garland Science: New York, 2001).
78. Griffith, T.S., Brunner, T., Fletcher, S.M., Green, D.R. & Ferguson, T.A. Fas ligand-induced apoptosis as a mechanism of immune privilege. *Science* **270**, 1189-1192 (1995).
79. Bellgrau, D. *et al.* A role for CD95 ligand in preventing graft rejection. *Nature* **377**, 630-632 (1995).
80. Chiou, S.-H., Sheu, B.-C., Chang, W.-C., Huang, S.-C. & Hong-Nerng, H. Current concepts of tumor-infiltrating lymphocytes in human malignancies. *J. Reprod. Immunol* **67**, 35-50 (2005).

81. Ryan, A.E., Shanahan, F., O'Connell, J. & Houston, A.M. Addressing the "Fas counterattack" controversy: blocking fas ligand expression suppresses tumor immune evasion of colon cancer in vivo. *Cancer Res* **65**, 9817-9823 (2005).
82. Bennett, M.W. *et al.* The Fas counterattack in vivo: apoptotic depletion of tumor-infiltrating lymphocytes associated with Fas ligand expression by human esophageal carcinoma. *J. Immunol* **160**, 5669-5675 (1998).
83. Sad, S., Kägi, D. & Mosmann, T.R. Perforin and Fas killing by CD8+ T cells limits their cytokine synthesis and proliferation. *J. Exp. Med* **184**, 1543-1547 (1996).
84. Pappas, P.G. Immunotherapy for invasive fungal infections: from bench to bedside. *Drug Resist. Updat* **7**, 3-10 (2004).
85. Schroder, K., Sweet, M.J. & Hume, D.A. Signal integration between IFNgamma and TLR signalling pathways in macrophages. *Immunobiology* **211**, 511-524 (2006).
86. Hu, X., Chakravarty, S.D. & Ivashkiv, L.B. Regulation of interferon and Toll-like receptor signaling during macrophage activation by opposing feedforward and feedback inhibition mechanisms. *Immunol. Rev* **226**, 41-56 (2008).
87. Murphy, K., Travers, P. & Walport, M.*Immunobiology: The Immune System in Health and Disease. 7th Edition.* 522-523. Chapter 12-17. (2008).
88. Sinha, P., Clements, V.K., Miller, S. & Ostrand-Rosenberg, S. Tumor immunity: a balancing act between T cell activation, macrophage activation and tumor-induced immune suppression. *Cancer Immunol. Immunother* **54**, 1137-1142 (2005).
89. Chawla-Sarkar, M. *et al.* Apoptosis and interferons: role of interferon-stimulated genes as mediators of apoptosis. *Apoptosis* **8**, 237-249 (2003).
90. Saha, B., Jyothi Prasanna, S., Chandrasekar, B. & Nandi, D. Gene modulation and immunoregulatory roles of interferon gamma. *Cytokine* **50**, 1-14 (2010).
91. Murphy, K., Travers, P. & Walport, M.*Immunobiology: The Immune System in Health and Disease. 7th Edition.* 90-92. Chapter 2-27. (2008).
92. Drutskaya, M.S., Efimov, G.A., Kruglov, A.A., Kuprash, D.V. & Nedospasov, S.A. Tumor necrosis factor, lymphotoxin and cancer. *IUBMB Life* **62**, 283-289 (2010).
93. Sethi, G., Sung, B., Kunnumakkara, A.B. & Aggarwal, B.B. Targeting TNF for Treatment of Cancer and Autoimmunity. *Adv. Exp. Med. Biol* **647**, 37-51 (2009).
94. Schmidt, K.J., Büning, J., Jankowiak, C., Lehnert, H. & Fellermann, K. Crohn's targeted therapy: myth or real goal? *Curr Drug Discov Technol* **6**, 290-298 (2009).
95. Nam, J. & Emery, P. Aspects of TNF inhibitor therapy in rheumatoid arthritis. *Mod Rheumatol* **20**, 325-330 (2010).
96. Lejeune, F.J., Rüegg, C. & Liénard, D. Clinical applications of TNF-alpha in cancer. *Curr. Opin. Immunol* **10**, 573-580 (1998).
97. Chen, X. *et al.* Cutting edge: expression of TNFR2 defines a maximally suppressive subset of mouse CD4+CD25+FoxP3+ T regulatory cells: applicability to tumor-infiltrating T regulatory cells. *J. Immunol* **180**, 6467-6471 (2008).
98. Murphy, K., Travers, P. & Walport, M.*Immunobiology: The Immune System in Health and Disease. 7th Edition.* 600-601. Chapter 14-1. (2008).
99. Daniel, C., Nolting, J. & von Boehmer, H. Mechanisms of self-nonself discrimination and possible clinical relevance. *Immunotherapy* **1**, 631-644 (2009).
100. Shimizu, J., Yamazaki, S. & Sakaguchi, S. Induction of tumor immunity by removing CD25+CD4+ T cells: a common basis between tumor immunity and autoimmunity. *J. Immunol* **163**, 5211-5218 (1999).

101. Onizuka, S. *et al.* Tumor rejection by in vivo administration of anti-CD25 (interleukin-2 receptor alpha) monoclonal antibody. *Cancer Res* **59**, 3128-3133 (1999).
102. Sutmuller, R.P. *et al.* Synergism of cytotoxic T lymphocyte-associated antigen 4 blockade and depletion of CD25(+) regulatory T cells in antitumor therapy reveals alternative pathways for suppression of autoreactive cytotoxic T lymphocyte responses. *J. Exp. Med* **194**, 823-832 (2001).
103. Jones, E. *et al.* Depletion of CD25+ regulatory cells results in suppression of melanoma growth and induction of autoreactivity in mice. *Cancer Immun* **2**, 1 (2002).
104. Krishnan, L., Deschatelets, L., Stark, F.C., Gurnani, K. & Sprott, G.D. Archaeosome adjuvant overcomes tolerance to tumor-associated melanoma antigens inducing protective CD8 T cell responses. *Clin. Dev. Immunol* **2010**, 578432 (2010).
105. Prins, R.M. *et al.* Central nervous system tumor immunity generated by a recombinant listeria monocytogenes vaccine targeting tyrosinase related protein-2 and real-time imaging of intracranial tumor burden. *Neurosurgery* **58**, 169-178; discussion 169-178 (2006).
106. Shahabi, V., Maciag, P.C., Rivera, S. & Wallecha, A. Live, attenuated strains of Listeria and Salmonella as vaccine vectors in cancer treatment. *Bioeng Bugs* **1**, 235-239 (2010).
107. William B Coley II Contribution to the Knowledge of Sarcoma. *Ann Surg* **14**, 199-220 (1891).
108. Dock, G. The influence of complicating diseases upon leukemia. *Am J Med Sci* **127**, 563-592 (1904).
109. PELNER, L., FOWLER, G.A. & NAUTS, H.C. Effects of concurrent infections and their toxins on the course of leukemia. *Acta Med. Scand. Suppl* **338**, 1-47 (1958).
110. Kelly, E. & Russell, S.J. History of Oncolytic Viruses: Genesis to Genetic Engineering. *Mol Ther* **15**, 651-659 (2007).
111. Janeway, C., Travers, P. & Walport, M. *Immunobiology: The Immune System in Health and Disease. 5th Edition. Chapter 13-31*. (Garland Science: New York, 2001).
112. Nishikawa, H. & Sakaguchi, S. Regulatory T cells in tumor immunity. *Int. J. Cancer* **127**, 759-767 (2010).
113. Chapon, M. *et al.* Progressive Upregulation of PD-1 in Primary and Metastatic Melanomas Associated with Blunted TCR Signaling in Infiltrating T Lymphocytes. *J Invest Dermatol* (2011).doi:10.1038/jid.2011.30
114. Weber, J. Immune checkpoint proteins: a new therapeutic paradigm for cancer--preclinical background: CTLA-4 and PD-1 blockade. *Semin. Oncol* **37**, 430-439 (2010).
115. Blank, C., Gajewski, T.F. & Mackensen, A. Interaction of PD-L1 on tumor cells with PD-1 on tumor-specific T cells as a mechanism of immune evasion: implications for tumor immunotherapy. *Cancer Immunol. Immunother* **54**, 307-314 (2005).
116. Fontenot, J.D., Gavin, M.A. & Rudensky, A.Y. Foxp3 programs the development and function of CD4+CD25+ regulatory T cells. *Nat. Immunol* **4**, 330-336 (2003).
117. Teng, M.W.L. *et al.* Conditional regulatory T-cell depletion releases adaptive immunity preventing carcinogenesis and suppressing established tumor growth. *Cancer Res* **70**, 7800-7809 (2010).
118. Ishida, M. *et al.* Differential expression of PD-L1 and PD-L2, ligands for an inhibitory receptor PD-1, in the cells of lymphohematopoietic tissues. *Immunol. Lett* **84**, 57-62 (2002).

119. Vignali, D.A.A., Collison, L.W. & Workman, C.J. How regulatory T cells work. *Nat Rev Immunol* **8**, 523-532 (2008).
120. Solinas, G., Germano, G., Mantovani, A. & Allavena, P. Tumor-associated macrophages (TAM) as major players of the cancer-related inflammation. *J. Leukoc. Biol* **86**, 1065-1073 (2009).
121. Pollard, J.W. Macrophages define the invasive microenvironment in breast cancer. *J. Leukoc. Biol* **84**, 623-630 (2008).
122. Condeelis, J. & Pollard, J.W. Macrophages: obligate partners for tumor cell migration, invasion, and metastasis. *Cell* **124**, 263-266 (2006).
123. Ostrand-Rosenberg, S. Myeloid-derived suppressor cells: more mechanisms for inhibiting antitumor immunity. *Cancer Immunol. Immunother* **59**, 1593-1600 (2010).
124. Bannai, S. Transport of cystine and cysteine in mammalian cells. *Biochim. Biophys. Acta* **779**, 289-306 (1984).
125. Hanson, E.M., Clements, V.K., Sinha, P., Ilkovitch, D. & Ostrand-Rosenberg, S. Myeloid-derived suppressor cells down-regulate L-selectin expression on CD4+ and CD8+ T cells. *J. Immunol* **183**, 937-944 (2009).
126. Huang, B. *et al.* Gr-1+CD115+ immature myeloid suppressor cells mediate the development of tumor-induced T regulatory cells and T-cell anergy in tumor-bearing host. *Cancer Res* **66**, 1123-1131 (2006).
127. Serafini, P., Mgebroff, S., Noonan, K. & Borrello, I. Myeloid-derived suppressor cells promote cross-tolerance in B-cell lymphoma by expanding regulatory T cells. *Cancer Res* **68**, 5439-5449 (2008).
128. Blackburn, S.D. *et al.* Coregulation of CD8+ T cell exhaustion by multiple inhibitory receptors during chronic viral infection. *Nat. Immunol.* **10**, 29-37 (2009).
129. Sierro, S., Romero, P. & Speiser, D.E. The CD4-like molecule LAG-3, biology and therapeutic applications. *Expert Opin. Ther. Targets* **15**, 91-101 (2011).
130. Callahan, M.K., Wolchok, J.D. & Allison, J.P. Anti-CTLA-4 antibody therapy: immune monitoring during clinical development of a novel immunotherapy. *Semin. Oncol* **37**, 473-484 (2010).
131. Berger, R. *et al.* Phase I safety and pharmacokinetic study of CT-011, a humanized antibody interacting with PD-1, in patients with advanced hematologic malignancies. *Clin. Cancer Res* **14**, 3044-3051 (2008).
132. Sakuishi, K., Jayaraman, P., Behar, S.M., Anderson, A.C. & Kuchroo, V.K. Emerging Tim-3 functions in antimicrobial and tumor immunity. *Trends Immunol.* **32**, 345-349 (2011).
133. Walunas, T.L. *et al.* CTLA-4 can function as a negative regulator of T cell activation. *Immunity* **1**, 405-413 (1994).
134. Sheppard, K.-A. *et al.* PD-1 inhibits T-cell receptor induced phosphorylation of the ZAP70/CD3zeta signalosome and downstream signaling to PKCtheta. *FEBS Lett* **574**, 37-41 (2004).
135. Grabie, N. *et al.* Endothelial Programmed Death-1 Ligand 1 (PD-L1) Regulates CD8+ T-Cell-Mediated Injury in the Heart. *Circulation* **116**, 2062-2071 (2007).
136. Liang, S.C. *et al.* Regulation of PD-1, PD-L1, and PD-L2 expression during normal and autoimmune responses. *Eur. J. Immunol* **33**, 2706-2716 (2003).
137. Petroff, M.G. *et al.* B7 family molecules are favorably positioned at the human maternal-fetal interface. *Biol. Reprod* **68**, 1496-1504 (2003).

138. Greenwald, R.J., Freeman, G.J. & Sharpe, A.H. The B7 family revisited. *Annu. Rev. Immunol* **23**, 515-548 (2005).
139. Yamazaki, T. *et al.* Expression of programmed death 1 ligands by murine T cells and APC. *J. Immunol* **169**, 5538-5545 (2002).
140. Brahmer, J.R. *et al.* Phase I study of single-agent anti-programmed death-1 (MDX-1106) in refractory solid tumors: safety, clinical activity, pharmacodynamics, and immunologic correlates. *J. Clin. Oncol* **28**, 3167-3175 (2010).
141. Luu, R.A. *et al.* Delayed expansion and contraction of CD8+ T cell response during infection with virulent Salmonella typhimurium. *J. Immunol* **177**, 1516-1525 (2006).
142. Albaghdadi, H., Robinson, N., Finlay, B., Krishnan, L. & Sad, S. Selectively reduced intracellular proliferation of Salmonella enterica serovar typhimurium within APCs limits antigen presentation and development of a rapid CD8 T cell response. *J. Immunol* **183**, 3778-3787 (2009).
143. Murphy, K., Travers, P. & Walport, M.*Immunobiology: The Immune System in Health and Disease. 7th Edition.* 349. Figure 8.25. (2008).
144. Bonifaz, L. *et al.* Efficient targeting of protein antigen to the dendritic cell receptor DEC-205 in the steady state leads to antigen presentation on major histocompatibility complex class I products and peripheral CD8+ T cell tolerance. *J. Exp. Med* **196**, 1627-1638 (2002).
145. van Broekhoven, C.L., Parish, C.R., Demangel, C., Britton, W.J. & Altin, J.G. Targeting dendritic cells with antigen-containing liposomes: a highly effective procedure for induction of antitumor immunity and for tumor immunotherapy. *Cancer Res* **64**, 4357-4365 (2004).
146. Mostböck, S., Vidal, S., Schlom, J. & Sabzevari, H. Enhanced levels of costimulation lead to reduced effector/memory CD8+ T cell functionality. *J. Immunol* **179**, 3524-3534 (2007).
147. Gunn, G.R. *et al.* Two Listeria monocytogenes vaccine vectors that express different molecular forms of human papilloma virus-16 (HPV-16) E7 induce qualitatively different T cell immunity that correlates with their ability to induce regression of established tumors immortalized by HPV-16. *Journal of Immunology* **167**, 6471-6479 (2001).
148. Zhu, X. *et al.* Tumor antigen delivered by Salmonella III secretion protein fused with heat shock protein 70 induces protection and eradication against murine melanoma. *Cancer Sci* **101**, 2621-2628 (2010).
149. Overwijk, W.W. *et al.* Vaccination with a recombinant vaccinia virus encoding a "self" antigen induces autoimmune vitiligo and tumor cell destruction in mice: requirement for CD4(+) T lymphocytes. *Proc. Natl. Acad. Sci. U.S.A* **96**, 2982-2987 (1999).
150. Rosenberg, S.A. *et al.* Recombinant fowlpox viruses encoding the anchor-modified gp100 melanoma antigen can generate antitumor immune responses in patients with metastatic melanoma. *Clin. Cancer Res* **9**, 2973-2980 (2003).
151. Liu, M.A. Immunologic basis of vaccine vectors. *Immunity* **33**, 504-515 (2010).
152. Quetglas, J.I. *et al.* Alphavirus vectors for cancer therapy. *Blood* **117**(6) 1888-98 (2011).
153. Näslund, T.I. *et al.* Comparative prime-boost vaccinations using Semliki Forest virus, adenovirus, and ALVAC vectors demonstrate differences in the generation of a protective central memory CTL response against the P815 tumor. *J. Immunol* **178**, 6761-6769 (2007).

154. Paterson, Y., Guirnalda, P.D. & Wood, L.M. Listeria and Salmonella bacterial vectors of tumor-associated antigens for cancer immunotherapy. *Semin. Immunol* **22**, 183-189 (2010).
155. Tangney, M. & Gahan, C.G.M. Listeria monocytogenes as a vector for anti-cancer therapies. *Curr Gene Ther* **10**, 46-55 (2010).
156. Fensterle, J. *et al.* Cancer immunotherapy based on recombinant Salmonella enterica serovar Typhimurium aroA strains secreting prostate-specific antigen and cholera toxin subunit B. *Cancer Gene Ther* **15**, 85-93 (2008).
157. Dudani, R. *et al.* Multiple mechanisms compensate to enhance tumor-protective CD8(+) T cell response in the long-term despite poor CD8(+) T cell priming initially: comparison between an acute versus a chronic intracellular bacterium expressing a model antigen. *J. Immunol* **168**, 5737-5745 (2002).
158. Gahan, M.E., Webster, D.E., Wesselingh, S.L., Strugnell, R.A. & Yang, J. Bacterial antigen expression is an important component in inducing an immune response to orally administered Salmonella-delivered DNA vaccines. *PLoS ONE* **4**, e6062 (2009).
159. Ambrosch, F. *et al.* Immunogenicity and protectivity of a new liposomal hepatitis A vaccine. *Vaccine* **15**, 1209-1213 (1997).
160. Steers, N.J., Peachman, K.K., McClain, S., Alving, C.R. & Rao, M. Liposome-encapsulated HIV-1 Gag p24 containing lipid A induces effector CD4+ T-cells, memory CD8+ T-cells, and pro-inflammatory cytokines. *Vaccine* **27**, 6939-6949 (2009).
161. Hamzah, J. *et al.* Targeted liposomal delivery of TLR9 ligands activates spontaneous antitumor immunity in an autochthonous cancer model. *J. Immunol* **183**, 1091-1098 (2009).
162. Kim, D., Jung, J., Lee, Y. & Kwon, H.-J. Novel immunostimulatory phosphodiester oligodeoxynucleotides with CpT sequences instead of CpG motifs. *Mol. Immunol* **48**, 1494-1504 (2011).
163. Krishnan, L., Sad, S., Patel, G.B. & Sprott, G.D. Archaeosomes induce long-term CD8+ cytotoxic T cell response to entrapped soluble protein by the exogenous cytosolic pathway, in the absence of CD4+ T cell help. *J. Immunol* **165**, 5177-5185 (2000).
164. Krishnan, L., Dicaire, C.J., Patel, G.B. & Sprott, G.D. Archaeosome vaccine adjuvants induce strong humoral, cell-mediated, and memory responses: comparison to conventional liposomes and alum. *Infect. Immun* **68**, 54-63 (2000).
165. Krishnan, L. *et al.* Rapid clonal expansion and prolonged maintenance of memory CD8+ T cells of the effector (CD44highCD62Llow) and central (CD44highCD62Lhigh) phenotype by an archaeosome adjuvant independent of TLR2. *J. Immunol* **178**, 2396-2406 (2007).
166. Krishnan, L., Sad, S., Patel, G.B. & Sprott, G.D. Archaeosomes induce enhanced cytotoxic T lymphocyte responses to entrapped soluble protein in the absence of interleukin 12 and protect against tumor challenge. *Cancer Res* **63**, 2526-2534 (2003).
167. Gurnani, K., Kennedy, J., Sad, S., Sprott, G.D. & Krishnan, L. Phosphatidylserine receptor-mediated recognition of archaeosome adjuvant promotes endocytosis and MHC class I cross-presentation of the entrapped antigen by phagosome-to-cytosol transport and classical processing. *J. Immunol* **173**, 566-578 (2004).
168. Sad, S. *et al.* Pathogen proliferation governs the magnitude but compromises the function of CD8 T cells. *J. Immunol* **180**, 5853-5861 (2008).

169. Konjufca, V. & Miller, M.J. Imaging Listeria monocytogenes infection in vivo. *Curr. Top. Microbiol. Immunol* **334**, 199-226 (2009).
170. Hamon, M., Bierne, H. & Cossart, P. Listeria monocytogenes: a multifaceted model. *Nat. Rev. Microbiol* **4**, 423-434 (2006).
171. Crimmins, G.T. *et al.* Listeria monocytogenes 6-Phosphogluconolactonase mutants induce increased activation of a host cytosolic surveillance pathway. *Infect. Immun* **77**, 3014-3022 (2009).
172. Lecuit, M., Ohayon, H., Braun, L., Mengaud, J. & Cossart, P. Internalin of Listeria monocytogenes with an intact leucine-rich repeat region is sufficient to promote internalization. *Infect. Immun* **65**, 5309-5319 (1997).
173. Swanson, J.A. & Baer, S.C. Phagocytosis by zippers and triggers. *Trends Cell Biol* **5**, 89-93 (1995).
174. Bishop, D.K. & Hinrichs, D.J. Adoptive transfer of immunity to Listeria monocytogenes. The influence of in vitro stimulation on lymphocyte subset requirements. *J. Immunol* **139**, 2005-2009 (1987).
175. Lara-Tejero, M. & Pamer, E.G. T cell responses to Listeria monocytogenes. *Curr. Opin. Microbiol* **7**, 45-50 (2004).
176. van Faassen, H., Dudani, R., Krishnan, L. & Sad, S. Prolonged Antigen Presentation, APC-, and CD8+ T Cell Turnover during Mycobacterial Infection: Comparison with Listeria monocytogenes. *The Journal of Immunology* **172**, 3491 -3500 (2004).
177. Hussain, S.F. & Paterson, Y. What is needed for effective antitumor immunotherapy? Lessons learned using Listeria monocytogenes as a live vector for HPV-associated tumors. *Cancer Immunol. Immunother* **54**, 577-586 (2005).
178. Wood, L.M., Guirnalda, P.D., Seavey, M.M. & Paterson, Y. Cancer immunotherapy using Listeria monocytogenes and listerial virulence factors. *Immunologic Research* **42**, 233-245 (2008).
179. O'Ryan, M., Prado, V. & Pickering, L.K. A millennium update on pediatric diarrheal illness in the developing world. *Semin Pediatr Infect Dis* **16**, 125-136 (2005).
180. Chimalizeni, Y., Kawaza, K. & Molyneux, E. The epidemiology and management of non typhoidal salmonella infections. *Adv. Exp. Med. Biol* **659**, 33-46 (2010).
181. Valdez, Y., Ferreira, R.B.R. & Finlay, B.B. Molecular mechanisms of Salmonella virulence and host resistance. *Curr. Top. Microbiol. Immunol* **337**, 93-127 (2009).
182. Sekirov, I. *et al.* Salmonella SPI-1-mediated neutrophil recruitment during enteric colitis is associated with reduction and alteration in intestinal microbiota. *Gut Microbes* **1**, 30-41 (2010).
183. Vidal, S.M., Pinner, E., Lepage, P., Gauthier, S. & Gros, P. Natural resistance to intracellular infections: Nramp1 encodes a membrane phosphoglycoprotein absent in macrophages from susceptible (Nramp1 D169) mouse strains. *J. Immunol* **157**, 3559-3568 (1996).
184. Arpaia, N. *et al.* TLR Signaling Is Required for Salmonella typhimurium Virulence. *Cell* **144**, 675-688 (2011).
185. Patel, J.C. & Galán, J.E. Manipulation of the host actin cytoskeleton by Salmonella--all in the name of entry. *Curr. Opin. Microbiol* **8**, 10-15 (2005).
186. Finlay, B.B., Ruschkowski, S. & Dedhar, S. Cytoskeletal rearrangements accompanying salmonella entry into epithelial cells. *J. Cell. Sci* **99 (Pt 2)**, 283-296 (1991).

187. Garcia-del Portillo, F. & Finlay, B.B. Salmonella invasion of nonphagocytic cells induces formation of macropinosomes in the host cell. *Infect. Immun* **62**, 4641-4645 (1994).
188. Aiastui, A., Pucciarelli, M.G. & García-del Portillo, F. Salmonella enterica Serovar Typhimurium Invades Fibroblasts by Multiple Routes Differing from the Entry into Epithelial Cells. *Infect Immun* **78**, 2700-2713 (2010).
189. Fass, E. & Groisman, E.A. Control of Salmonella pathogenicity island-2 gene expression. *Curr Opin Microbiol* **12**, 199-204 (2009).
190. Abrahams, G.L. & Hensel, M. Manipulating cellular transport and immune responses: dynamic interactions between intracellular Salmonella enterica and its host cells. *Cell. Microbiol* **8**, 728-737 (2006).
191. Santos, R.L. & Bäumler, A.J. Cell tropism of Salmonella enterica. *Int. J. Med. Microbiol* **294**, 225-233 (2004).
192. Lee, C.-H., Wu, C.-L., Tai, Y.-S. & Shiau, A.-L. Systemic administration of attenuated Salmonella choleraesuis in combination with cisplatin for cancer therapy. *Mol. Ther* **11**, 707-716 (2005).
193. Bermudes, D., Zheng, L.-mou & King, I.C. Live bacteria as anticancer agents and tumor-selective protein delivery vectors. *Curr Opin Drug Discov Devel* **5**, 194-199 (2002).
194. Jain, K.K. Use of bacteria as anticancer agents. *Expert Opin Biol Ther* **1**, 291-300 (2001).
195. Wall, D.M., Srikanth, C.V. & McCormick, B.A. Targeting tumors with salmonella Typhimurium- potential for therapy. *Oncotarget* **1**, 721-728 (2010).
196. al-Ramadi, B.K. *et al.* Potent anti-tumor activity of systemically-administered IL2-expressing Salmonella correlates with decreased angiogenesis and enhanced tumor apoptosis. *Clin. Immunol* **130**, 89-97 (2009).
197. Yang, N., Li, S.-H., Lü, Y.-Z., Chen, L.-S. & Ren, D.-M. Attenuated Salmonella typhimurium carrying shRNA-expressing vectors elicit RNA interference in murine bladder tumors. *Acta Pharmacol. Sin* **32**, 368-374 (2011).
198. Roider, E. *et al.* Invasion and destruction of a murine fibrosarcoma by Salmonella-induced effector CD8 T cells as a therapeutic intervention against cancer. *Cancer Immunol. Immunother* **60**, 371-380 (2011).
199. Kates, M. The phytanyl ether-linked polar lipids and isoprenoid neutral lipids of extremely halophilic bacteria. *Prog Chem Fats Other Lipids* **15**, 301-342 (1978).
200. Sprott, G.D. *et al.* Archaeosomes varying in lipid composition differ in receptor-mediated endocytosis and differentially adjuvant immune responses to entrapped antigen. *Archaea* **1**, 151-164 (2003).
201. Sprott, G.D. *et al.* A structural comparison of the total polar lipids from the human archaea Methanobrevibacter smithii and Methanosphaera stadtmanae and its relevance to the adjuvant activities of their liposomes. *Biochim. Biophys. Acta* **1440**, 275-288 (1999).
202. Sprott, G.D., Tolson, D.L. & Patel, G.B. Archaeosomes as novel antigen delivery systems. *FEMS Microbiol. Lett* **154**, 17-22 (1997).
203. Krishnan, L. & Sprott, G.D. Archaeosome adjuvants: Immunological capabilities and mechanism(s) of action. *Vaccine* **26**, 2043-2055 (2008).

204. Scanlan, P.D., Shanahan, F. & Marchesi, J.R. Human methanogen diversity and incidence in healthy and diseased colonic groups using mcrA gene analysis. *BMC Microbiol* **8**, 79 (2008).
205. Hamm, C., Petrella, T. & Verma, S. Biochemotherapy for the treatment of metastatic malignant melanoma: A systematic review. *Cancer Treat. Rev.* **34**, 145-156 (2008).
206. Wasif, N., Bagaria, S.P., Ray, P. & Morton, D.L. Does metastasectomy improve survival in patients with stage IV melanoma? a cancer registry analysis of outcomes. *J Surg Oncol* **104**, 111-115 (2011).
207. McKay, J.D. & Deacon, A. Isolated melanoma metastasis to stomach with possible regressed primary lesion: the importance of pursuing solitary melanoma metastases. *N. Z. Med. J* **123**, 78-79 (2010).
208. Crosby, T., Fish, R., Coles, B. & Mason, M.D. Systemic treatments for metastatic cutaneous melanoma. *Cochrane Database Syst Rev* CD001215 (2000).
209. Valenzano Menada, M. *et al.* Spontaneous regression of transplacental metastases from maternal melanoma in a newborn: case report and review of the literature. *Melanoma Res* **20**, 443-449 (2010).
210. Ribas, A. Anti-CTLA4 Antibody Clinical Trials in Melanoma. *Update Cancer Ther* **2**, 133-139 (2007).
211. Cerottini, J.C., von Fliedner, V. & Boon, T. Recognition of tumor-associated antigens by T lymphocytes: from basic concepts to new approaches. *Ann. Oncol* **3**, 11-16 (1992).
212. Yoshikawa, T. *et al.* Vaccine efficacy of fusogenic liposomes containing tumor cell-lysate against murine B16BL6 melanoma. *Biological and Pharmaceutical Bulletin* **29**, 100-104 (2006).
213. Klebanoff, C.A., Acquavella, N., Yu, Z. & Restifo, N.P. Therapeutic cancer vaccines: are we there yet? *Immunol. Rev* **239**, 27-44 (2011).
214. Webster, W.S. *et al.* Targeting molecular and cellular inhibitory mechanisms for improvement of antitumor memory responses reactivated by tumor cell vaccine. *J. Immunol* **179**, 2860-2869 (2007).
215. Rosenberg, S.A. & Dudley, M.E. Adoptive cell therapy for the treatment of patients with metastatic melanoma. *Current Opinion in Immunology* **21**, 233-240 (2009).
216. Gattinoni, L. *et al.* Removal of homeostatic cytokine sinks by lymphodepletion enhances the efficacy of adoptively transferred tumor-specific CD8+ T cells. *J. Exp. Med* **202**, 907-912 (2005).
217. Singh, P., Yam, M., Russell, P.J. & Khatri, A. Molecular and traditional chemotherapy: A united front against prostate cancer. *Cancer Letters* **293**, 1-14 (2010).
218. McNeel, D. & Olson, B. Sipuleucel-T: immunotherapy for advanced prostate cancer. *OAJU* **2011**, 49-60 (2011).
219. Cheever, M.A. & Higano, C. PROVENGE (Sipuleucel-T) in Prostate Cancer: The First FDA Approved Therapeutic Cancer Vaccine. *Clin Cancer Res* **17**, 3520-6 (2011).
220. Carballido, E. & Fishman, M. Sipuleucel-T: Prototype for development of anti-tumor vaccines. *Curr Oncol Rep* **13**, 112-119 (2011).
221. McKarney, I. Sipuleucel-T (Provenge): active cellular immunotherapy for advanced prostate cancer. *Issues Emerg Health Technol* 1-4 (2007).
222. Gilboa, E. DC-based cancer vaccines. *J Clin Invest* **117**, 1195-1203 (2007).
223. Gilboa, E. Knocking the SOCS1 off dendritic cells. *Nat. Biotechnol* **22**, 1521-1522 (2004).

224. Perret, R. & Ronchese, F. Memory T cells in cancer immunotherapy: which CD8 T-cell population provides the best protection against tumours? *Tissue Antigens* **72**, 187-194 (2008).
225. Gattinoni, L. *et al.* Acquisition of full effector function in vitro paradoxically impairs the in vivo antitumor efficacy of adoptively transferred CD8+ T cells. *J. Clin. Invest* **115**, 1616-1626 (2005).
226. Medina, E., Guzmán, C.A., Staendner, L.H., Colombo, M.P. & Paglia, P. Salmonella vaccine carrier strains: effective delivery system to trigger anti-tumor immunity by oral route. *Eur. J. Immunol* **29**, 693-699 (1999).
227. Homeister, J.W. *et al.* The alpha(1,3)fucosyltransferases FucT-IV and FucT-VII exert collaborative control over selectin-dependent leukocyte recruitment and lymphocyte homing. *Immunity* **15**, 115-126 (2001).
228. Brown, D.M., Fisher, T.L., Wei, C., Frelinger, J.G. & Lord, E.M. Tumours can act as adjuvants for humoral immunity. *Immunology* **102**, 486-497 (2001).
229. Dudani, R. *et al.* Preexisting inflammation due to Mycobacterium bovis BCG infection differentially modulates T-cell priming against a replicating or nonreplicating immunogen. *Infect. Immun* **70**, 1957-1964 (2002).
230. Choquet, C.G., Patel, G.B., Beveridge, T.J. & Sprott, G.D. Stability of pressure-extruded liposomes made from archaeobacterial ether lipids. *Appl. Microbiol. Biotechnol* **42**, 375-384 (1994).
231. Choquet, C.G., Richards, J.C., Patel, G.B. & Sprott, G.D. Purine and pyrimidine biosynthesis in methanogenic bacteria. *Arch. Microbiol.* **161**, 471-480 (1994).
232. Sprott, G.D., Patel, G.B. & Krishnan, L. Archaeobacterial ether lipid liposomes as vaccine adjuvants. *Meth. Enzymol* **373**, 155-172 (2003).
233. Barber, D.L., Wherry, E.J. & Ahmed, R. Cutting edge: rapid in vivo killing by memory CD8 T cells. *J. Immunol* **171**, 27-31 (2003).
234. Kaech, S.M., Wherry, E.J. & Ahmed, R. Effector and memory T-cell differentiation: implications for vaccine development. *Nat. Rev. Immunol* **2**, 251-262 (2002).
235. Suvas, S. & Rouse, B.T. Treg control of antimicrobial T cell responses. *Curr. Opin. Immunol* **18**, 344-348 (2006).
236. Zou, W. Regulatory T cells, tumour immunity and immunotherapy. *Nat. Rev. Immunol* **6**, 295-307 (2006).
237. Hodi, F.S. & Dranoff, G. The biologic importance of tumor-infiltrating lymphocytes. *J. Cutan. Pathol* **37 Suppl 1**, 48-53 (2010).
238. Tan, J.T. *et al.* Interleukin (IL)-15 and IL-7 Jointly Regulate Homeostatic Proliferation of Memory Phenotype CD8+ Cells but Are Not Required for Memory Phenotype CD4+ Cells. *J Exp Med* **195**, 1523-1532 (2002).
239. Obar, J.J. & Lefrançois, L. Memory CD8+ T cell differentiation. *Ann. N. Y. Acad. Sci* **1183**, 251-266 (2010).
240. Zhang, L. *et al.* Intratumoral T cells, recurrence, and survival in epithelial ovarian cancer. *N. Engl. J. Med* **348**, 203-213 (2003).
241. Anichini, A., Vegetti, C. & Mortarini, R. The paradox of T-cell-mediated antitumor immunity in spite of poor clinical outcome in human melanoma. *Cancer Immunol. Immunother* **53**, 855-864 (2004).
242. Agata, Y. *et al.* Expression of the PD-1 antigen on the surface of stimulated mouse T and B lymphocytes. *Int. Immunol* **8**, 765-772 (1996).

243. Badovinac, V.P. & Harty, J.T. Programming, demarcating, and manipulating CD8+ T-cell memory. *Immunol. Rev* **211**, 67-80 (2006).
244. Castiglioni, P., Gerloni, M. & Zanetti, M. Genetically programmed B lymphocytes are highly efficient in inducing anti-virus protective immunity mediated by central memory CD8 T cells. *Vaccine* **23**, 699-708 (2004).
245. Vaccari, M., Trindade, C.J., Venzon, D., Zanetti, M. & Franchini, G. Vaccine-induced CD8+ central memory T cells in protection from simian AIDS. *J. Immunol* **175**, 3502-3507 (2005).
246. Roberts, A.D., Ely, K.H. & Woodland, D.L. Differential contributions of central and effector memory T cells to recall responses. *J. Exp. Med* **202**, 123-133 (2005).
247. Busch, D.H., Kerksiek, K. & Pamer, E.G. Processing of Listeria monocytogenes antigens and the in vivo T-cell response to bacterial infection. *Immunol. Rev* **172**, 163-169 (1999).
248. Ahmed, R. & Gray, D. Immunological memory and protective immunity: understanding their relation. *Science* **272**, 54-60 (1996).
249. Stark, F.C., Sad, S. & Krishnan, L. Intracellular bacterial vectors that induce CD8(+) T cells with similar cytolytic abilities but disparate memory phenotypes provide contrasting tumor protection. *Cancer Res* **69**, 4327-4334 (2009).
250. Klebanoff, C.A. *et al.* IL-15 enhances the in vivo antitumor activity of tumor-reactive CD8+ T cells. *Proc. Natl. Acad. Sci. U.S.A* **101**, 1969-1974 (2004).
251. Marzo, A.L. *et al.* Initial T cell frequency dictates memory CD8+ T cell lineage commitment. *Nat. Immunol* **6**, 793-799 (2005).
252. Rolle, C.E., Carrio, R. & Malek, T.R. Modeling the CD8+ T effector to memory transition in adoptive T-cell antitumor immunotherapy. *Cancer Res* **68**, 2984-2992 (2008).
253. Zajac, A.J. *et al.* Viral immune evasion due to persistence of activated T cells without effector function. *J. Exp. Med* **188**, 2205-2213 (1998).
254. Fuller, M.J., Khanolkar, A., Tebo, A.E. & Zajac, A.J. Maintenance, Loss, and Resurgence of T Cell Responses during Acute, Protracted, and Chronic Viral Infections. *Journal of Immunology* **172**, 4204-4214 (2004).
255. Zhou, S., Ou, R., Huang, L., Price, G.E. & Moskophidis, D. Differential tissue-specific regulation of antiviral CD8+ T-cell immune responses during chronic viral infection. *J. Virol* **78**, 3578-3600 (2004).
256. Unsoeld, H., Krautwald, S., Voehringer, D., Kunzendorf, U. & Pircher, H. Cutting edge: CCR7+ and CCR7- memory T cells do not differ in immediate effector cell function. *J. Immunol* **169**, 638-641 (2002).
257. Yajima, T. *et al.* A novel role of IL-15 in early activation of memory CD8+ CTL after reinfection. *J. Immunol* **174**, 3590-3597 (2005).
258. Schluns, K.S. & Lefrançois, L. Cytokine control of memory T-cell development and survival. *Nat. Rev. Immunol* **3**, 269-279 (2003).
259. Johanns, T.M., Ertelt, J.M., Rowe, J.H. & Way, S.S. Regulatory T cell suppressive potency dictates the balance between bacterial proliferation and clearance during persistent Salmonella infection. *PLoS Pathog* **6**, (2010).
260. Belkaid, Y. Regulatory T cells and infection: a dangerous necessity. *Nat. Rev. Immunol* **7**, 875-888 (2007).
261. Belkaid, Y. & Tarbell, K. Regulatory T cells in the control of host-microorganism interactions (*). *Annu. Rev. Immunol* **27**, 551-589 (2009).

262. Peters, N. & Sacks, D. Immune privilege in sites of chronic infection: Leishmania and regulatory T cells. *Immunol. Rev* **213**, 159-179 (2006).
263. Loeffler, M., Le'Negrate, G., Krajewska, M. & Reed, J.C. Attenuated Salmonella engineered to produce human cytokine LIGHT inhibit tumor growth. *Proc. Natl. Acad. Sci. U.S.A* **104**, 12879-12883 (2007).
264. Zhong, Z. *et al.* Salmonella-host cell interactions, changes in host cell architecture, and destruction of prostate tumor cells with genetically altered Salmonella. *Microsc. Microanal* **13**, 372-383 (2007).
265. Bruhn, K.W., Craft, N., Nguyen, B.D., Yip, J. & Miller, J.F. Characterization of anti-self CD8 T-cell responses stimulated by recombinant Listeria monocytogenes expressing the melanoma antigen TRP-2. *Vaccine* **23**, 4263-4272 (2005).
266. Hamilton, S.E., Badovinac, V.P., Khanolkar, A. & Harty, J.T. Listeriolysin O-deficient Listeria monocytogenes as a vaccine delivery vehicle: antigen-specific CD8 T cell priming and protective immunity. *J. Immunol* **177**, 4012-4020 (2006).
267. Jones, T.R., Shirasugi, N., Adams, A.B., Pearson, T.C. & Larsen, C.P. Intravital microscopy identifies selectins that regulate T cell traffic into allografts. *J. Clin. Invest* **112**, 1714-1723 (2003).
268. Luangsay, S. *et al.* CCR5 mediates specific migration of Toxoplasma gondii-primed CD8 lymphocytes to inflammatory intestinal epithelial cells. *Gastroenterology* **125**, 491-500 (2003).
269. Kershaw, M.H. *et al.* Redirecting migration of T cells to chemokine secreted from tumors by genetic modification with CXCR2. *Hum. Gene Ther* **13**, 1971-1980 (2002).
270. Sasaki, K. *et al.* Stat6 signaling suppresses VLA-4 expression by CD8+ T cells and limits their ability to infiltrate tumor lesions in vivo. *Journal of Immunology* **181**, 104-108 (2008).
271. Cai, Y.H. *et al.* Abrogation of functional selectin-ligand expression reduces migration of pathogenic CD8+ T cells into heart. *J. Immunol* **176**, 6568-6575 (2006).
272. Smithson, G. *et al.* Fuc-TVII is required for T helper 1 and T cytotoxic 1 lymphocyte selectin ligand expression and recruitment in inflammation, and together with Fuc-TIV regulates naive T cell trafficking to lymph nodes. *J. Exp. Med* **194**, 601-614 (2001).
273. Wang, X. *et al.* Engraftment of human central memory-derived effector CD8+ T cells in immunodeficient mice. *Blood* **117**, 1888-98 (2010).
274. Erdmann, I. *et al.* Fucosyltransferase VII-deficient mice with defective E-, P-, and L-selectin ligands show impaired CD4+ and CD8+ T cell migration into the skin, but normal extravasation into visceral organs. *J. Immunol* **168**, 2139-2146 (2002).
275. Spertini, O., Cordey, A.S., Monai, N., Giuffrè, L. & Schapira, M. P-selectin glycoprotein ligand 1 is a ligand for L-selectin on neutrophils, monocytes, and CD34+ hematopoietic progenitor cells. *The Journal of Cell Biology* **135**, 523 -531 (1996).
276. Howard, D.R., Fukuda, M., Fukuda, M.N. & Stanley, P. The GDP-fucose:N-acetylglucosaminide 3-alpha-L-fucosyltransferases of LEC11 and LEC12 Chinese hamster ovary mutants exhibit novel specificities for glycolipid substrates. *J. Biol. Chem* **262**, 16830-16837 (1987).
277. Ehlers, S., Schreiber, T., Dunzendorfer, A., Lowe, J.B. & Hölscher, C. Fucosyltransferase IV and VII-directed selectin ligand function determines long-term survival in experimental tuberculosis. *Immunobiology* **214**, 674-682 (2009).

278. Schuster, K. *et al.* Homeostatic proliferation of naïve CD8+ T cells depends on CD62L/L-selectin-mediated homing to peripheral LN. *Eur. J. Immunol* **39**, 2981-2990 (2009).
279. Stekel, D.J. The simulation of density-dependent effects in the recirculation of T lymphocytes. *Scandinavian Journal of Immunology* **47**, 426-430 (1998).
280. Morgan, R.A. *et al.* Cancer regression in patients after transfer of genetically engineered lymphocytes. *Science* **314**, 126-129 (2006).
281. Zhao, Y. *et al.* Primary Human Lymphocytes Transduced with NY-ESO-1 Antigen-Specific TCR Genes Recognize and Kill Diverse Human Tumor Cell Lines. *J Immunol* **174**, 4415-4423 (2005).
282. Beveridge, T.J., Choquet, C.G., Patel, G.B. & Sprott, G.D. Freeze-fracture planes of methanogen membranes correlate with the content of tetraether lipids. *J. Bacteriol* **175**, 1191-1197 (1993).
283. De Rosa, M., Gambacorta, A. & Gliozzi, A. Structure, biosynthesis, and physicochemical properties of archaebacterial lipids. *Microbiol. Rev* **50**, 70-80 (1986).
284. Krishnan, L. & Dennis Sprott, G. Archaeosomes as self-adjuvanting delivery systems for cancer vaccines. *J Drug Target* **11**, 515-524 (2003).
285. Lu, S. Heterologous prime-boost vaccination. *Curr. Opin. Immunol* **21**, 346-351 (2009).
286. Ishizaki, H. *et al.* Heterologous prime/boost immunization with p53-based vaccines combined with Toll-like receptor stimulation enhances tumor regression. *Journal of Immunotherapy* **33**, 609-617 (2010).
287. Keir, M.E., Freeman, G.J. & Sharpe, A.H. PD-1 regulates self-reactive CD8+ T cell responses to antigen in lymph nodes and tissues. *J. Immunol* **179**, 5064-5070 (2007).
288. Barber, D.L. *et al.* Restoring function in exhausted CD8 T cells during chronic viral infection. *Nature* **439**, 682-687 (2006).
289. Golden-Mason, L. *et al.* Upregulation of PD-1 expression on circulating and intrahepatic hepatitis C virus-specific CD8+ T cells associated with reversible immune dysfunction. *J. Virol* **81**, 9249-9258 (2007).
290. Day, C.L. *et al.* PD-1 expression on HIV-specific T cells is associated with T-cell exhaustion and disease progression. *Nature* **443**, 350-354 (2006).
291. Trautmann, L. *et al.* Upregulation of PD-1 expression on HIV-specific CD8+ T cells leads to reversible immune dysfunction. *Nat. Med* **12**, 1198-1202 (2006).
292. Petrovas, C. *et al.* PD-1 is a regulator of virus-specific CD8+ T cell survival in HIV infection. *J. Exp. Med* **203**, 2281-2292 (2006).
293. Sharpe, A.H., Wherry, E.J., Ahmed, R. & Freeman, G.J. The function of programmed cell death 1 and its ligands in regulating autoimmunity and infection. *Nat. Immunol* **8**, 239-245 (2007).
294. Wong, R.M. *et al.* Programmed death-1 blockade enhances expansion and functional capacity of human melanoma antigen-specific CTLs. *Int. Immunol* **19**, 1223-1234 (2007).
295. Inozume, T. *et al.* Selection of CD8+PD-1+ lymphocytes in fresh human melanomas enriches for tumor-reactive T cells. *J. Immunother* **33**, 956-964 (2010).
296. Borkner, L. *et al.* RNA interference targeting programmed death receptor-1 improves immune functions of tumor-specific T cells. *Cancer Immunol. Immunother* **59**, 1173-1183 (2010).
297. Blank, C. *et al.* Blockade of PD-L1 (B7-H1) augments human tumor-specific T cell responses in vitro. *Int. J. Cancer* **119**, 317-327 (2006).

298. Song, M.-Y., Park, S.-H., Nam, H.J., Choi, D.-H. & Sung, Y.-C. Enhancement of Vaccine-induced Primary and Memory CD8+ T-cell Responses by Soluble PD-1. *J. Immunother* **34**, 297-306 (2011).
299. Iwai, Y. *et al.* Involvement of PD-L1 on tumor cells in the escape from host immune system and tumor immunotherapy by PD-L1 blockade. *Proc. Natl. Acad. Sci. U.S.A* **99**, 12293-12297 (2002).
300. Weber, J. Ipilimumab: controversies in its development, utility and autoimmune adverse events. *Cancer Immunology, Immunotherapy* **58**, 823-830 (2009).
301. Di Giacomo, A.M., Biagioli, M. & Maio, M. The emerging toxicity profiles of anti-CTLA-4 antibodies across clinical indications. *Semin. Oncol* **37**, 499-507 (2010).
302. Sakaguchi, S. Regulatory T cells: history and perspective. *Methods Mol. Biol* **707**, 3-17 (2011).
303. Golovina, T.N. & Vonderheide, R.H. Regulatory T cells: overcoming suppression of T-cell immunity. *Cancer J* **16**, 342-347 (2010).
304. Golgher, D., Jones, E., Powrie, F., Elliott, T. & Gallimore, A. Depletion of CD25+ regulatory cells uncovers immune responses to shared murine tumor rejection antigens. *Eur. J. Immunol* **32**, 3267-3275 (2002).
305. Dannull, J. *et al.* Enhancement of vaccine-mediated antitumor immunity in cancer patients after depletion of regulatory T cells. *J. Clin. Invest* **115**, 3623-3633 (2005).
306. Jacobs, J.F.M. *et al.* Dendritic cell vaccination in combination with anti-CD25 monoclonal antibody treatment: a phase I/II study in metastatic melanoma patients. *Clin. Cancer Res* **16**, 5067-5078 (2010).
307. Williams, M.A., Tyznik, A.J. & Bevan, M.J. Interleukin-2 signals during priming are required for secondary expansion of CD8+ memory T cells. *Nature* **441**, 890-893 (2006).
308. Patel, G.B. & Chen, W. Archaeosome immunostimulatory vaccine delivery system. *Curr Drug Deliv* **2**, 407-421 (2005).
309. Novy, P., Huang, X., Leonard, W.J. & Yang, Y. Intrinsic IL-21 Signaling Is Critical for CD8 T Cell Survival and Memory Formation in Response to Vaccinia Viral Infection. *J. Immunol* **186**, 2729-2738 (2011).
310. Henry, C.J. *et al.* The roles of IL-12 and IL-23 in CD8+ T cell-mediated immunity against Listeria monocytogenes: Insights from a DC vaccination model. *Cell. Immunol* **264**, 23-31 (2010).
311. Provinciali, M. Immunosenescence and cancer vaccines. *Cancer Immunol. Immunother* **58**, 1959-1967 (2009).
312. Provinciali, M. & Smorlesi, A. Immunoprevention and immunotherapy of cancer in ageing. *Cancer Immunol. Immunother* **54**, 93-106 (2005).
313. Sharma, S., Dominguez, A.L. & Lustgarten, J. High accumulation of T regulatory cells prevents the activation of immune responses in aged animals. *J. Immunol* **177**, 8348-8355 (2006).
314. Gregg, R. *et al.* The number of human peripheral blood CD4+ CD25high regulatory T cells increases with age. *Clin. Exp. Immunol* **140**, 540-546 (2005).
315. O'Hagan, D.T. & Valiante, N.M. Recent advances in the discovery and delivery of vaccine adjuvants. *Nat Rev Drug Discov* **2**, 727-735 (2003).
316. Alving, C.R. Design and selection of vaccine adjuvants: animal models and human trials. *Vaccine* **20 Suppl 3**, S56-64 (2002).

317. Ben Ahmeida, E.T., Gregoriadis, G., Potter, C.W. & Jennings, R. Immunopotentiation of local and systemic humoral immune responses by ISCOMs, liposomes and FCA: role in protection against influenza A in mice. *Vaccine* **11**, 1302-1309 (1993).
318. Lowell, G.H. *et al.* Proteosomes, emulsomes, and cholera toxin B improve nasal immunogenicity of human immunodeficiency virus gp160 in mice: induction of serum, intestinal, vaginal, and lung IgA and IgG. *J. Infect. Dis* **175**, 292-301 (1997).
319. Iyer, A.K. *et al.* The effect of internalizing human single chain antibody fragment on liposome targeting to epithelioid and sarcomatoid mesothelioma. *Biomaterials* **32**, 2605-2613 (2011).
320. Felnerova, D., Viret, J.-F., Glück, R. & Moser, C. Liposomes and virosomes as delivery systems for antigens, nucleic acids and drugs. *Current Opinion in Biotechnology* **15**, 518-529 (2004).
321. Williams, P. & Galipeau, J. GM-CSF-Based Fusion Cytokines as Ligands for Immune Modulation. *J. Immunol* **186**, 5527-5532 (2011).
322. Williams, P. & Galipeau, J. GMCSF-interleukin fusion cytokines induce novel immune effectors that can serve as biopharmaceuticals for treatment of autoimmunity and cancer. *J. Intern. Med* **269**, 74-84 (2011).
323. Guse, K., Cerullo, V. & Hemminki, A. Oncolytic vaccinia virus for the treatment of cancer. *Expert Opin Biol Ther* **11**, 595-608 (2011).
324. ten Hagen, T.L.M. Liposomal cytokines in the treatment of infectious diseases and cancer. *Meth. Enzymol* **391**, 125-145 (2005).
325. Kedar, E., Palgi, O., Golod, G., Babai, I. & Barenholz, Y. Delivery of cytokines by liposomes. III. Liposome-encapsulated GM-CSF and TNF-alpha show improved pharmacokinetics and biological activity and reduced toxicity in mice. *J. Immunother* **20**, 180-193 (1997).
326. Gattinoni, L., Powell, D.J., Jr, Rosenberg, S.A. & Restifo, N.P. Adoptive immunotherapy for cancer: building on success. *Nat. Rev. Immunol* **6**, 383-393 (2006).
327. Rosenberg, S.A., Restifo, N.P., Yang, J.C., Morgan, R.A. & Dudley, M.E. Adoptive cell transfer: a clinical path to effective cancer immunotherapy. *Nat. Rev. Cancer* **8**, 299-308 (2008).